# IAEA TECDOC SERIES

# Assessment of Post-irradiation Examination Techniques for Advanced Reactor Fuel and Materials

*Report of a Technical Meeting*

**IAEA**
**International Atomic Energy Agency**

# ASSESSMENT OF POST-IRRADIATION EXAMINATION TECHNIQUES FOR ADVANCED REACTOR FUEL AND MATERIALS

The following States are Members of the International Atomic Energy Agency:

| | | |
|---|---|---|
| AFGHANISTAN | GAMBIA | NORWAY |
| ALBANIA | GEORGIA | OMAN |
| ALGERIA | GERMANY | PAKISTAN |
| ANGOLA | GHANA | PALAU |
| ANTIGUA AND BARBUDA | GREECE | PANAMA |
| ARGENTINA | GRENADA | PAPUA NEW GUINEA |
| ARMENIA | GUATEMALA | PARAGUAY |
| AUSTRALIA | GUINEA | PERU |
| AUSTRIA | GUYANA | PHILIPPINES |
| AZERBAIJAN | HAITI | POLAND |
| BAHAMAS | HOLY SEE | PORTUGAL |
| BAHRAIN | HONDURAS | QATAR |
| BANGLADESH | HUNGARY | REPUBLIC OF MOLDOVA |
| BARBADOS | ICELAND | ROMANIA |
| BELARUS | INDIA | RUSSIAN FEDERATION |
| BELGIUM | INDONESIA | RWANDA |
| BELIZE | IRAN, ISLAMIC REPUBLIC OF | SAINT KITTS AND NEVIS |
| BENIN | IRAQ | SAINT LUCIA |
| BOLIVIA, PLURINATIONAL | IRELAND | SAINT VINCENT AND |
| STATE OF | ISRAEL | THE GRENADINES |
| BOSNIA AND HERZEGOVINA | ITALY | SAMOA |
| BOTSWANA | JAMAICA | SAN MARINO |
| BRAZIL | JAPAN | SAUDI ARABIA |
| BRUNEI DARUSSALAM | JORDAN | SENEGAL |
| BULGARIA | KAZAKHSTAN | SERBIA |
| BURKINA FASO | KENYA | SEYCHELLES |
| BURUNDI | KOREA, REPUBLIC OF | SIERRA LEONE |
| CABO VERDE | KUWAIT | SINGAPORE |
| CAMBODIA | KYRGYZSTAN | SLOVAKIA |
| CAMEROON | LAO PEOPLE'S DEMOCRATIC | SLOVENIA |
| CANADA | REPUBLIC | SOUTH AFRICA |
| CENTRAL AFRICAN | LATVIA | SPAIN |
| REPUBLIC | LEBANON | SRI LANKA |
| CHAD | LESOTHO | SUDAN |
| CHILE | LIBERIA | SWEDEN |
| CHINA | LIBYA | SWITZERLAND |
| COLOMBIA | LIECHTENSTEIN | SYRIAN ARAB REPUBLIC |
| COMOROS | LITHUANIA | TAJIKISTAN |
| CONGO | LUXEMBOURG | THAILAND |
| COSTA RICA | MADAGASCAR | TOGO |
| CÔTE D'IVOIRE | MALAWI | TONGA |
| CROATIA | MALAYSIA | TRINIDAD AND TOBAGO |
| CUBA | MALI | TUNISIA |
| CYPRUS | MALTA | TÜRKİYE |
| CZECH REPUBLIC | MARSHALL ISLANDS | TURKMENISTAN |
| DEMOCRATIC REPUBLIC | MAURITANIA | UGANDA |
| OF THE CONGO | MAURITIUS | UKRAINE |
| DENMARK | MEXICO | UNITED ARAB EMIRATES |
| DJIBOUTI | MONACO | UNITED KINGDOM OF |
| DOMINICA | MONGOLIA | GREAT BRITAIN AND |
| DOMINICAN REPUBLIC | MONTENEGRO | NORTHERN IRELAND |
| ECUADOR | MOROCCO | UNITED REPUBLIC OF TANZANIA |
| EGYPT | MOZAMBIQUE | UNITED STATES OF AMERICA |
| EL SALVADOR | MYANMAR | URUGUAY |
| ERITREA | NAMIBIA | UZBEKISTAN |
| ESTONIA | NEPAL | VANUATU |
| ESWATINI | NETHERLANDS | VENEZUELA, BOLIVARIAN |
| ETHIOPIA | NEW ZEALAND | REPUBLIC OF |
| FIJI | NICARAGUA | VIET NAM |
| FINLAND | NIGER | YEMEN |
| FRANCE | NIGERIA | ZAMBIA |
| GABON | NORTH MACEDONIA | ZIMBABWE |

The Agency's Statute was approved on 23 October 1956 by the Conference on the Statute of the IAEA held at United Nations Headquarters, New York; it entered into force on 29 July 1957. The Headquarters of the Agency are situated in Vienna. Its principal objective is "to accelerate and enlarge the contribution of atomic energy to peace, health and prosperity throughout the world".

IAEA-TECDOC-2035

# ASSESSMENT OF POST-IRRADIATION EXAMINATION TECHNIQUES FOR ADVANCED REACTOR FUEL AND MATERIALS

## REPORT OF A TECHNICAL MEETING

INTERNATIONAL ATOMIC ENERGY AGENCY
VIENNA, 2023

# COPYRIGHT NOTICE

# FOREWORD

The development of advanced reactor technologies is rapidly accelerating, spurred by a growing need for secure and reliable low carbon energy sources, to help achieve climate reduction targets and secure baseload energy production sources to meet future electricity demands. To confirm that advanced reactor fuel and materials perform in the reactor core as expected, a post-irradiation examination is conducted to provide the necessary data to assess the performance of an in-reactor fuel or other irradiated material.

Post-irradiation examinations typically utilize a wide array of sample preparation, examination and analysis methods; in most cases, remote handling and shielding is required to protect the worker or sensitive instrumentation from radiation hazards. The data obtained during post-irradiation examinations are supported by prior knowledge of irradiation conditions, fabrication parameters and other relevant information that can be obtained during reactor operation or shortly after discharge. Post-irradiation examinations are thus vital to the development, qualification and continued surveillance of current and next generation reactor fuels and materials. The importance of post-irradiation examinations extends to other applications, including but not limited to providing supporting data for code or model validation and verification, further development of fuel and fuel assemblies to maximize performance, extraction and study of isotopes from spent fuels for health and space applications, and developing short and long term fuel storage and/or reprocessing solutions.

The fairly recent introduction of many advanced reactor designs, including small modular reactors, has accelerated research into new fuel concepts, many of which require qualification through irradiation testing and examination under the expected range of operating conditions. At a Technical Meeting on Advances in Post-Irradiation Examination Techniques for Power Reactor Irradiated Fuels and Innovative Fuels in July 2021, it was recognized that as the development of novel reactor materials and post-irradiation examination techniques grows, resources at hot cell facilities (both equipment and skilled technical staff) may become increasingly strained, leading to potential delays in the production of critical performance data for specific fuel technologies.

This publication explores the use of existing and new post-irradiation examination techniques for the study of next generation fuel types, many of which could also be applied to current generation fuel types. Through the creation of strategic collaboration between two or more nuclear laboratories, technological gaps in examination and analysis methods for specific advanced reactor fuel types of interest can be more clearly identified.

This publication may be used as a reference for the international community involved in post-irradiation examination to gain an understanding of which important performance parameters are typically studied for each fuel type to properly assess their performance, and the relevant post-irradiation examination techniques required for the analyses. This publication includes supplementary files, available on-line, and contains presentations made at the aforementioned technical meeting.

*EDITORIAL NOTE*

# CONTENTS

# 1. INTRODUCTION

## 1.1. BACKGROUND

Post-irradiation examination (PIE) is expected to remain a vital component in the understanding, development, qualification and continued surveillance of advanced reactor fuel and in-core materials. Insight gained during PIE regarding the performance of fuel and materials in the reactor core forms the basis of actions and subsequent path forward to be taken by the fuel community that comprises reactor operators, computer code developers, regulators, fuel designers and fabricators, waste management specialists and other researchers. Therefore, sufficient information needs to be obtained during a typical PIE campaign to ensure adequate data is obtained on the performance parameters of a certain fuel type under a set of known irradiation conditions.

In many cases, PIE is used to assess fuel performance at or near failure thresholds or in postulated accident conditions, helping to validate operational and safety limits on maximum powers and burnups. Other applications of PIE include (but are not limited to): fuel and material surveillance and life extension activities for ageing reactors, the study of harvested structural materials from decommissioned reactors, medical isotope and biological research (and sample preparation), the development of intermediate and high-level waste management, decommissioning and storage solutions, and examination of irradiated materials for space or nuclear forensics applications. In recent years, greater focus has been placed on the safe long-term operation of existing nuclear power plants and the development of new reactor types. The first line of research aims at preventing rise of a metal-water reaction and developing accident tolerant and advanced technology fuels (ATFs). The second research area involves work on the development of small modular reactors (SMR), minor actinide burners and a closed fuel cycle.

A fairly broad array of PIE capabilities is currently utilized for the examination of current-generation fuel and in-core materials, that could be applied to one or more advanced reactor fuel types. Ideally, the PIE techniques and toolsets developed can be applied to multiple fuel types ('fuel technology agnostic'); however, in some cases, unique toolsets, sample preparation techniques or environments may be required (e.g., inert gas atmosphere, cryogenically cooled samples).

Given the growing number of advanced reactor concepts and various fuel types under development, the need for improved PIE techniques to adequately assess the performance parameters of novel fuel and materials has grown. Furthermore, not every nuclear laboratory may have the capability to effectively study every fuel type.

Under these circumstances, a IAEA Technical Meeting (TM) on Advances in Post-Irradiation Examination Techniques for Power-Reactor Irradiated Fuels and Innovative Fuels was virtually held on 21–27 July 2021 (hereafter, called TM 2021). During the TM 2021, meeting participants reviewed current PIE capabilities in Member States and assessed potential gaps to be addressed for the development of advanced reactor fuel types.

## 1.2. OBJECTIVE

Underpinned by the 2010 assessment of PIE techniques for water reactor fuel, which is described in IAEA publications (i.e., TECDOC-1635 [1] and TECDOC-1673 [2]), this publication examines emerging PIE requirements and trends regarding the development of PIE techniques for advanced reactor fuel and materials. It is noted that those PIE techniques

described will not be inclusive for all advanced fuel and reactor types in existence at time of publication, for example silicide, nitride and U-Mo forms.

This publication will support Member States in determining if their PIE capabilities align with PIE requirements for their fuel types of interest for advanced reactor designs, including small modular reactors (SMR).

## 1.3. SCOPE

This publication is intended to describe:

— Current PIE capabilities in Member States, focusing on advancements in PIE capabilities since 2010, based on information provided during TM 2021;
— Desired PIE capabilities and related techniques for advanced reactor fuel types together with identified potential gaps in the PIE capabilities, based on discussions at TM 2021 and follow-up Consultancy Meeting with PIE experts;
— International collaboration – drivers and proposed methods to address the identified gaps.

With respect to desired PIE capabilities for advanced reactor fuel types, typical fuel performance parameters to be assessed are summarized along with the PIE technique/toolset required to obtain the relevant data. Potential gaps in PIE capabilities to support development and deployment of specific fuels and in core materials are identified.

This publication is intended to suggest effective ways to address the identified gaps in PIE capabilities through targeted, fuel technology-specific collaborations between nuclear laboratories and related organizations. Example of collaboration may include the co-development of key capabilities necessary to obtain relevant fuel and core material data and allowing external laboratories easier access to PIE techniques that are unique to another laboratory.

## 1.4. STRUCTURE

The publication describes up-to-date PIE techniques for non-destructive and destructive post-irradiation examinations. The most recent information on PIE capabilities in Member States is described in Section 2. In the subsequent Sections 3 and 4, specific PIE techniques are described with improved features for non-destructive and destructive examination capabilities, respectively. These include examination such as gamma scanning, profilometry, mechanical testing, X-ray diffraction (XRD) and transmission electron microscopy (TEM) that are used for conventional fuel examinations and ATF studies, and can be effectively applied to SMR, minor actinide burner and closed fuel cycle applications.

Computer codes used in fuel design and safety analysis need to be validated to assess the adequacy and applicability of fuel models incorporated in the computer codes, to demonstrate the capabilities and limits of the computer codes, and to determine the prediction accuracy of the computer codes. In Section 5, current PIE capabilities to support such verification and validation of fuel analysis computer codes are assessed.

The fuel performance parameters expected to require assessment during PIE for advanced reactor fuel are summarized in Section 6. Through review of PIE capabilities at individual nuclear laboratories, or in consultation with other nuclear laboratories wishing to collaborate

on PIE of specific fuel types, the technological gaps in PIE capabilities to support the development of advanced reactor fuel are also discussed can be assessed on a case-by-case basis.

Identified gaps in desired PIE capabilities, including the estimated 'technology readiness level (TRL)' for a prescribed examination or analysis method, are important consideration for planning to study and qualify new fuel types. Prioritization methods for the identified gaps are described in Section 7.

In Section 8, the outline of the proposed coordinated research project (CRP) is provided, together with a summarized discussion on other methods proposed for collaboration. Such collaboration may aim at reducing the cost of test data, harmonizing (standardizing) sample preparation and examination processes, and selecting the most appropriate PIE techniques and equipment for PIE. Hence, this publication may be used a reference for hot cell engineers during the development of collaborative PIE work.

In the Annex, a list of presentations provided at TM 2021 is described. These presentation files have been retained as supplementary material and can be retrieved from the publication's individual web page[1].

---

[1] Refer to: www.iaea.org/publications.

# 2. OVERVIEW OF PIE CAPABILITIES IN MEMBER STATES

## 2.1. BACKGROUND

The 2021 Technical Meeting on advanced PIE techniques (TM 2021) saw a number of Member States present an overview of their capabilities (see Annex I for presentations), which are summarized in the following sections. The previous meeting held a decade earlier (in 2010) is also summarized for the benefit of demonstrating advances in PIE capability across Member States, and also drawing out any trends in new and advanced PIE capabilities that are being developed across the world.

## 2.2. PREVIOUS IAEA MEETINGS AND TECDOCS

IAEA publications, TECDOC-1635 [1] and TECDOC-1673 [2] summarize PIE activities in many Member States between 2009 and 2011. In addition, IAEA's PIE database[2] is kept up to date by Member States and summarizes developments and advancements in PIE capability.

It is noted that since the meetings in 2009 and 2011, PIE techniques and the justification for their development have seen some advancement. Whilst the basis for examination may remain the same and ultimately is geared towards fuel and materials safety and characterization at various stages of the fuel cycle (from fabrication and operation to safe disposal), specific capabilities have improved. For example, the advancement of the focused ion beam (FIB) equipment to improve resolution capabilities, digital camera technology for increased resolution and data acquisition, or more frequently applied methodologies during PIE such as laser-based excitation - Raman spectroscopy, laser induced breakdown spectroscopy (LIBS), etc.

Broadly it can be stated that a number of techniques were identified as core capabilities across Member States' laboratories, noting that not all Member States had capability in each area, as this depends heavily on PIE needs and requirements in a Member State. These include:

— Poolside/underwater inspection (including eddy-current (EC) examination);
— Gamma spectroscopy/tomography/ X-ray diffraction (XRD);
— Burnup/isotopic analysis (chemical or non-destructive);
— Fission gas measurements and analyses, and void volume measurement;
— Mechanical testing and refabrication of standardized specimens;
— Microscopy (including metallography) – optical and electron;
— Basic hot cell visual inspection;
— Profilometry.

In addition to using PIE techniques and toolsets normally used for water-cooled reactors (and other existing reactor types such as liquid metal-cooled fast reactors), new reactor design concepts require new special-purpose equipment and new research methods. For example, to study the performance and isotopic inventory of TRISO[3] particles for use in high temperature gas-cooled (HTGR) reactors, high-temperature tests up to 2400°C or higher may be required to analyze fission gas release from fuel particles. Furthermore, it is necessary to study the physical

---

[2]  Refer to: (Post Irradiation Examination Facilities Database (PIE) (iaea.org)).
[3]  Tri-structural isotropic.

and mechanical properties of both gas reactor fuel and components under conditions and temperatures close to operating conditions and at emergency temperatures.

Techniques for non-destructive PIE have not changed significantly over the past decade, other than the quality of image and spectra processing has significantly improved. Greater development has been observed in the area of destructive examinations. More recently, routine tensile tests with irradiated material samples are complemented by new types of testing, such as expansion-due-to-compression tests, or tests with sub-sized samples during micro-mechanical testing, where evaluation of various mechanical characteristics of the materials can be completed. Conventional TEM studies are effectively complemented with the FIB equipment used to prepare samples from irradiated nuclear fuel or structural materials with significant microstructural non-homogeneities. FIB allows for detailed characterization of microstructural features such as hydride precipitates, where orientation and density determine mechanical properties and service life of the cladding or other structural materials.

Advanced PIE in the last decade has seen the addition, increased application or development of some core techniques, such as:

— Computed X-ray tomography;
— Neutron radiography;
— Surface Science – including Raman spectroscopy, LIBS, X-ray photoelectron spectroscopy (XPS);
— Electrochemical testing;
— Thermal properties (e.g., laser flash/thermal conductivity microscope, thermogravimetric analysis (TGA)/differential scanning calorimetry (DSC)/dilatometry);
— Advancements in FIB/ transmission electron microscopy (TEM)/ atom probe tomography (APT)/ secondary ion mass spectrometry (SIMS), including heating and cooling stages;
— Advancements in hydrogen determination analysis;
— Small-scale mechanical testing developments (e.g., small/shear punch, tensile and bending test, micro/nano hardness).

## 2.3. PIE CAPABILITIES DESCRIPTION IN IAEA'S PIE DATABASE

There are various ways to categorize international PIE facilities to demonstrate their capabilities. The following information is used to describe PIE capabilities of facilities in the IAEA PIE database[2],where 54 PIE facilities from 24 Member States are categorized:

— Acceptance criteria for irradiated components (dimensions, total activity limits, activity type);
— Cell characteristics – High active/heavily shielded, medium active, low/trace active;
— Available PIE techniques (geared towards PIE of certain fuel types);
— Storage or conditioning capabilities for waste forms;
— Transport cask acceptance.

In addition to the capabilities of each Member State, it is recognized that many of these countries and laboratories will hold irradiated materials which may be classed as unique and

valuable to the international community. These material archives are discussed future in Section 8.3.4. Note that these will be specific to individual Member States.

There was general consensus during TM 2021 that increased collaboration would be beneficial between two or more nuclear laboratories, affiliated universities, the fuel designer/fabricator and/or SMR and advanced reactor vendors to develop the best available PIE techniques for hot cell use.

# 3. NON-DESTRUCTIVE EXAMINATION CAPABILITIES

The non-destructive examination (NDE) techniques discussed in this section can be applied to both poolside and hot cell PIE.

## 3.1. POOLSIDE INSPECTIONS

Poolside inspections at pressurized heavy water (PHWR) facilities such as CANDU reactors mainly include visual inspections (Fig. 1) and underwater sipping tests. If the root cause of a defect or anomaly cannot be interpreted from poolside inspection, the fuel bundles or removed elements may be extracted and sent to a hot cell facility for further PIE.
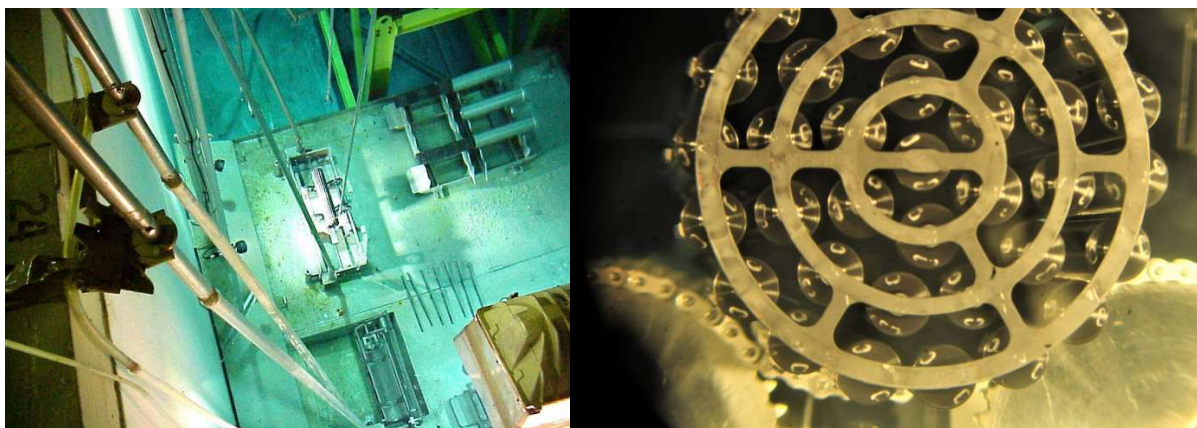


FIG. 1. Poolside inspection of PHWR (CANDU) fuel bundles (courtesy of Canadian Nuclear Laboratories (CNL) and Ontario Power Generation (OPG))

The poolside PIE techniques for LWR fuel typically include visual inspection for visible defects and abnormalities, eddy current measurement for oxide thickness and defects, and rod growth measurement. The poolside inspection at Advanced Gas-Cooled Reactors in UK is described below as an example, which in principle is similar with the poolside PIE at water-cooled reactor sites (e.g., see [3] for example of the poolside inspection in light water reactors (LWRs) and PHWRs).

At UK Advanced Gas Reactor (AGR) sites, visual inspection of the fuel rods is performed within the pond of the reactor and transferred to storage ponds at Sellafield for various poolside PIEs. A survey is carried out to look for any damage that may be present on the fuel rod components and the extent of carbonaceous deposits inhibiting heat transfer [4,5] on the fuel clad surface. Radiation-hardened cameras are lowered by crane into the fuel assemblies in the cooling pond and powered using remote computer control systems. The primary containment (fuel can) condition and other components with the fuel rod can be assessed directly. Data is generated primarily via visual inspection methods, although in-pond sampling has also been utilized. Visual inspection will typically consider the following on UK AGR fuel:

— Visible damage to the fuel rod cladding and graphite sleeve, along its length and around its diameter;
— Visible and measurable length changes or dimensional changes in the fuel rod itself [6];
— Extent and estimation of carbonaceous surface deposit types on the fuel cladding.

With poolside visual inspection, unlike hot cell-based PIE, the fuel can be examined soon after removal from the reactor, yielding a large quantity of information in a timely manner.

Figure 2 illustrates the poolside inspection at an AGR, UK.
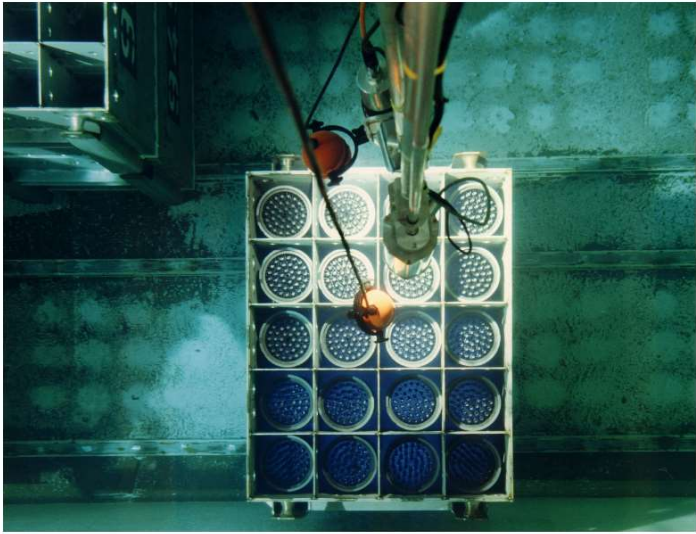


*FIG. 2. Poolside inspection at AGR (courtesy of National Nuclear Laboratory (NNL))*

Figure 3 illustrates the poolside inspection at Advanced Test Reactor (ATR), Idaho Nuclear Laboratory (INL).



*FIG. 3. Poolside inspection at ATR canal (courtesy of INL)*

## 3.2. ULTRASONIC TEST

The inspection equipment comprises ultrasonic scanning for defect characterization and dimensional measurements. Ultrasonic test (UT) techniques use mechanical pressure waves with higher frequencies than audible waves. The two main characteristics of the ultrasonic signal (coating delamination and minimal coating thickness) can be estimated using two

different methods. A target is penetrated by ultrasonic waves coming from a piezoelectric UT emitter. The qualities of the target can then be determined by measuring the signal that is received by a piezoelectric transducer. The impedance of the medium, as well as the wave's capacity to be reflected, scattered, or absorbed as it passes through material of varied densities, all affect how quickly ultrasonic waves travel through various media. A piezoelectric transducer picks up an ultrasonic wave after it has passed through its target and been reflected or attenuated. As a result, the transducer experiences a brief deformation that causes a voltage change equal to the strength of the reflected or attenuated ultrasonic wave. The relative strength of the reflected or attenuated ultrasonic signal can then be calculated by displaying the data after this voltage change has been measured. Because ultrasonic waves may travel more easily through a liquid than a gas, such as air, the ultrasonic scan tests are carried out underwater with the transducer and experimental fuel (plate or pin) completely submerged in a dedicated water tank.

Advanced Test Reactor (ATR) canal-based UT scanners with specialized construction are used to perform in-canal UT. The UT inspection and evaluation systems are remotely controlled and have radiation-tolerant detectors. The ATR canal is a perfect location for these kinds of scans because UT scans are carried out in enclosed water tanks. This technique (using a fuel plate as an example), which functions similarly to min-clad thickness UT scans, employs a piezoelectric transducer to transmit ultrasonic waves in pulse echo mode and then detect boundary reflections from the interface between the outer fuel plate edge and the surrounding canal water. This allows the use of transducer to measure the distance to the fuel plate edge. The fuel plate's surface profile can be visualized using a mapped image created by the UT scanner technology by combining the beam signals from the raster scan. Taking plate fuel as an example, the original thickness of the fuel plate and the thickness of the plate at intermittent intervals of irradiation can be compared using a mapped picture of the fuel profile, enabling for the identification of small changes in plate thickness and the monitoring of fuel swelling.

The application of UT dimensional analysis for fuel rods has been shown in various research initiatives [7–9], despite the fact that it is currently only applicable to plates. Typically, a specific rod housing assembly that deploys a piezoelectric film is made, and with the right calibration, the UT configuration used for flat plates is modified. Once a standardized housing assembly and calibration technique are created, the UT technique can be used for a variety of fuel rod designs. For example, in an effort to improve defect detection in CANDU fuel elements during NDE, UT has shown promising results in detecting flaws as small as 10μm [10,11] (as illustrated by Fig. 4). The technique has also shown success in revealing anomalies at the weld closure (endcap) regions.
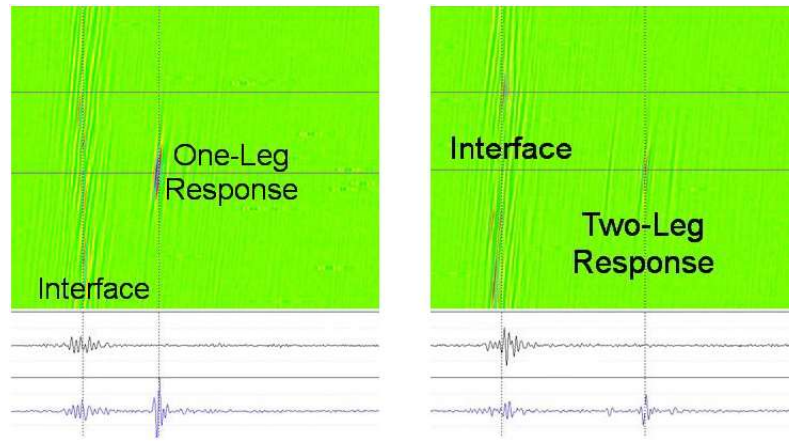
(a)
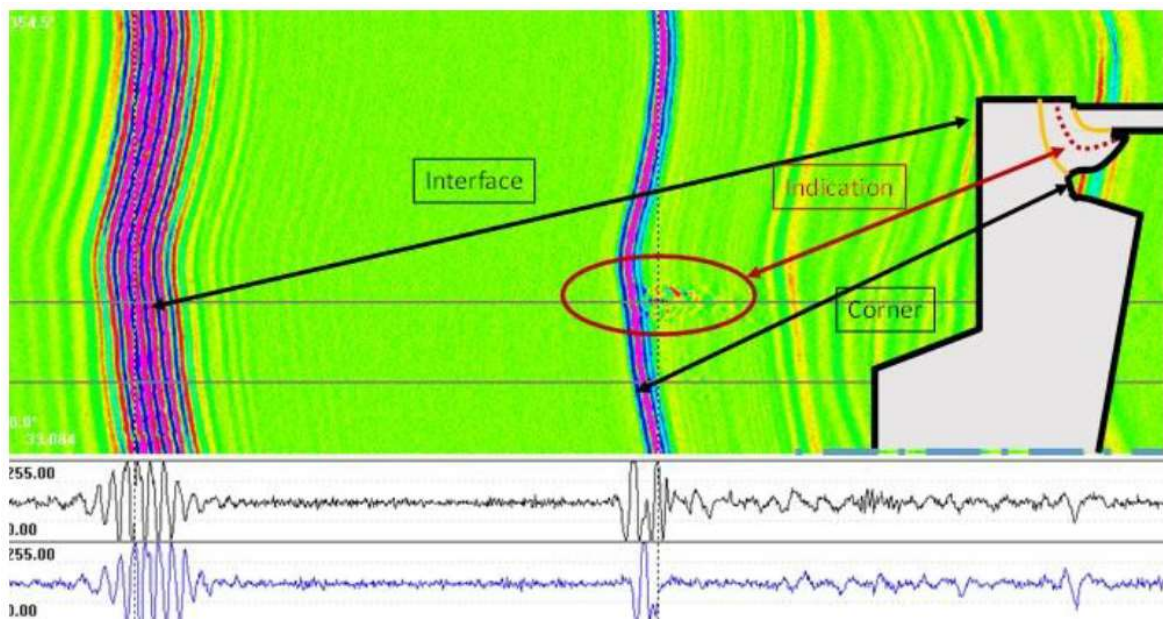


(b)

*FIG. 4. Axial shear responses (a) from a 10 μm flaw and (b) from the endcap of the CANDU fuel element (courtesy of CNL)*

Also, a variety of NDE approaches have recently been made available to support various accident tolerant fuel (ATF) experiments, thanks to the conceptualization and implementation of the ATR NDE System (ANDES). The poolside PIE offered by ANDES would supplement the present hot-cell-based PIE with multifunctional NDE for many specimen types. In order to better understand and analyze new nuclear fuels and materials, it is now possible to collect irradiation data that may be utilized to establish continuous-performance correlations rather than cumulative data. Underwater gamma spectroscopy, remote specimen handling, high-resolution visual inspection, computed gamma tomography, and underwater laser metrology are some of these ANDES functions. If deployed, ANDES would offer PIE capabilities that would be advantageous to ATR both operationally and in terms of experiment programming. Measurement of irradiation swelling, fuel rod breaking, hydride cracking, and expedited comparison of cladding topologies are made possible.

## 3.3. EDDY CURRENT

Eddy current (EC) testing can be used to assess the cladding on nuclear fuel rods, pinpoint discontinuities that emerge during reactor operation or during PIE and identify them. This capability is applicable for poolside PIE and hot cell PIE. High frequency EC testing has recently demonstrated [12–14] the capability of characterizing ceramics and composite-based materials, such as identifying individual fibre layers, local fibre density distributions, inclusions of air (pores) or impurities (depending on the included material), and cracks.

The EC measurement equipment can be placed on the surface of the fuel plates or fuel rods. The thickness of nonconductive coatings on nonferrous metal surfaces can be measured. This is accomplished by using a method that generates an alternating magnetic field at the probe's surface using a wire coil carrying a high frequency alternating current. The oscillating magnetic field created by the probe will cause eddy currents to occur when it is brought close to a conductive surface. The properties of the substrate and the distance between the probe and the substrate (the coating thickness) affect the magnitude of the eddy currents. The magnitude of the currents is measured by the probe and converted into an equivalent thickness. Controls are available on a Kollmorgan periscope to aim the objective (i.e., point the line of view), choose between three magnifications, and focus the image. Special planar optics, which keep the whole surface of a flat object (oriented normal to the optical axis of the system) in focus at the film plane, have been used to replace the periscope's standard (spherical) optics.

The ASTM standard, ASTM-E376-11 [15], can be used to guide eddy current testing.

## 3.4. VISUAL AND DIMENSIONAL INSPECTIONS

Both capabilities are applicable for poolside and hot cell PIE. In this section hot cell techniques are discussed.

To execute the visual inspection at known azimuthal orientations for a fuel rod, a specialized holder needs to be developed to hold the fuel rod with the ability to rotate. On the back of the holder, a ruler has been added for length reference (Fig.5 [16]). At the Hot Fuel Examination Facility (HFEF) at INL, the instrument has built-in halogen modelling lamps for viewing and photography as well as commercial photographic strobe lights that are only utilized for photography. The full rodlet length can be captured digitally in photos that show the rodlets. The rodlets can be visually inspected from a variety of azimuthal angles. Dimensional changes, macroscopic cracking, the presence of scratches, and irregularities on the surface can all be noted. Similar tooling is utilized at CNL for detailed low-magnification visual examinations (Fig. 6). The low-magnification microscope includes recently-upgraded USB-2 and USB-3 cameras, and also utilizes specialized element (and separate bundle) rotators [10].

A profilometer can be used to do dimensional inspections. Along the rodlets, measurements of the outside diameter can be taken at various angles and in small (0.5 mm) increments (Fig. 5). With a 2μm accuracy, diameter measurements may be taken, and radial strain of the cladding along the axial direction can be determined. The prospect of modifying the tool to add fuel rod bending characterization is also possible.
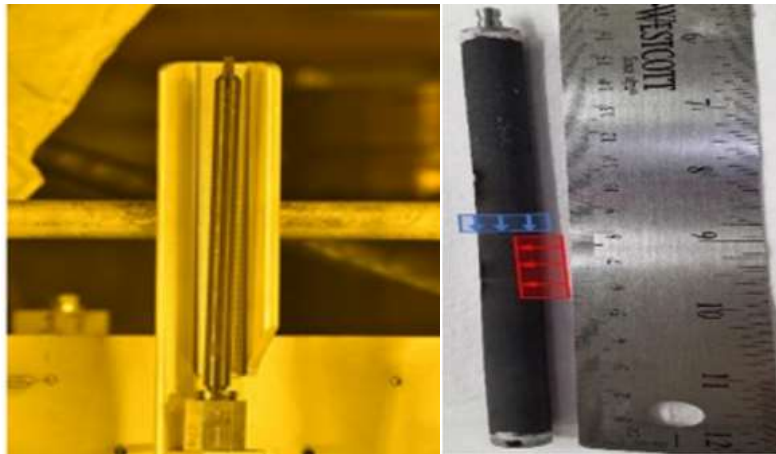
(a)
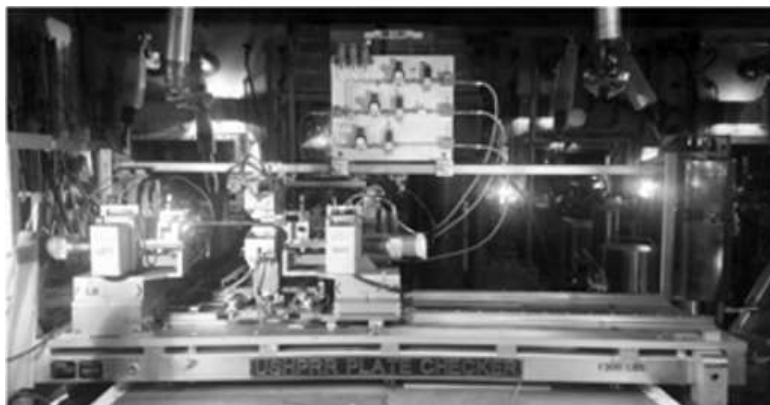


(b)

*FIG. 5. (a) A rodlet being visually inspected in specially designed holder and (b) HFEF Plate checker and (courtesy of INL)*

## 3.5. PROFILOMETRY

A continuous contact profilometer can be used to measure the axial and spiral diameter (surface) profiles of fuel plates and fuel rods. The element is moved vertically through sapphire-tipped probes and into contact with horizontally opposed linear transducers. The element is kept upright in relation to the transducers by guide rollers positioned above and below. Two magnetic transducers that are horizontally opposed and are linked to contact probes with sapphire tips measure the diameter. A digital position readout system generates linear locations and displacements, which are then recorded on a data acquisition system. The measurement error for diametral measurements using contact profilometry is about ±0.0005 cm (0.0002 in.) [17].

Laser profilometry has also been demonstrated for use in hot cells (for example, at Argonne National Laboratory (ANL)), where diameters in the range from 2.5 to 25 mm can be measured with an accuracy of ±0.0025 mm [18].
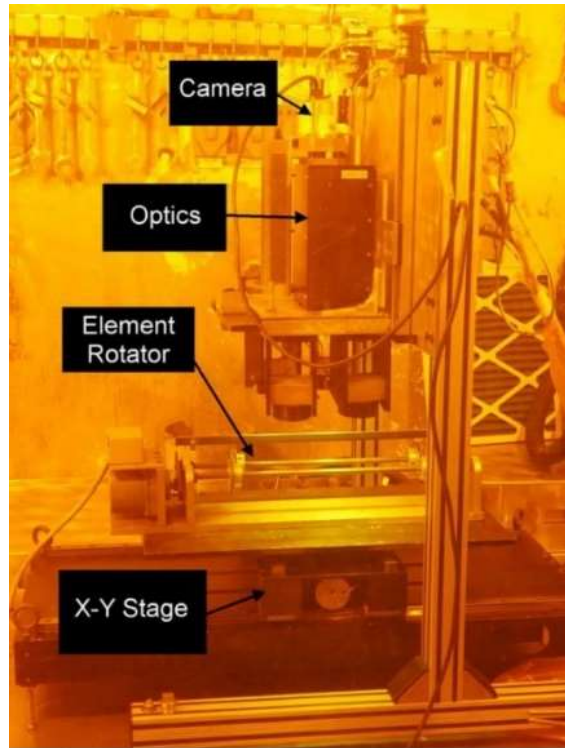
*FIG. 6. Low magnification microscope for NDE visual examinations (courtesy of CNL)*

## 3.6. DENSITY MEASUREMENT

Understanding radiation-induced dimensional changes for fuel and cladding and subsequent deformation of the cladding in accident scenarios requires a thorough understanding of the post-irradiation and post-transient density characterization. The Archimedes based methods and pycnometry are two generic approaches for density measurements. The Archimedes method is to immerse samples in liquid while pycnometry is to immerse samples in gas to determine the volume of the samples, and the density can be calculated as the ratio of mass to volume.

## 3.7. GAMMA SPECTROMETRY

Axial gamma spectrometry can reveal the most discernible fission products ($^{144}Ce$, $^{95}Zr$, $^{154}Eu$, $^{106}Ru$, among others). The axial burnup profile of the rodlets can be calculated using the activity ratio, where the burnup was scaled from the value discovered using analytical chemistry tests. The gamma scanner can be used to scan larger components like test loops, reactor parts, and fuel elements. Using gross gamma scans, the amount of activity present along the component's length or width can be determined; an example of a gross gamma scan on a CANDU fuel rod is shown in Fig. 7. The peaks at each end of the scan indicate the element was subject to end-flux peaking effects. The $^{137}Cs$ dips along the length reveal the pellet-pellet dish gap regions.

To ascertain the isotopic distribution of activity along a component's length or width, isotopic gamma scans can be utilized. The most discernible fission products are shown by axial gamma spectrometry ($^{144}Ce$, $^{154}Eu$, $^{106}Ru$, among others [16]). When the burnup is scaled from the value acquired from analytical chemistry measurements, the activity ratio gained can be utilized to compute the axial burnup profile of the rodlets.
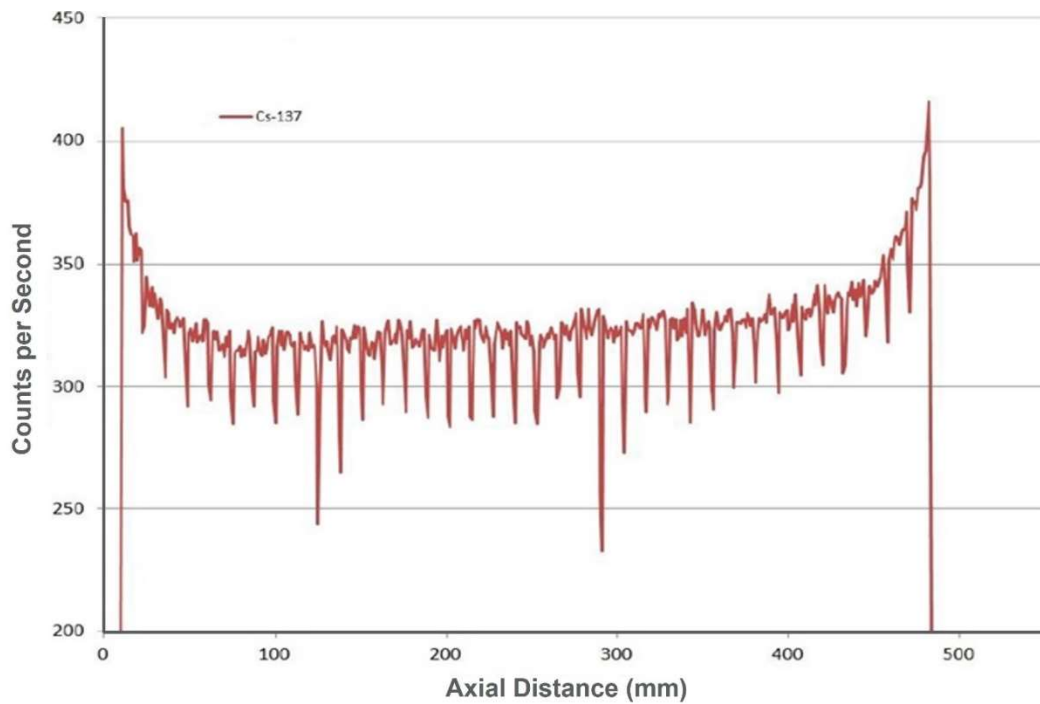
*FIG. 7. Example of gross gamma scan of a CANDU fuel rod (Courtesy of CNL)*

The Precision Gamma Scanner (PGS) at HFEF at INL [16] is used for gamma ray spectroscopy. The collimator, stage, and detector are the three main elements of the PGS. With a rectangular aperture that can be adjusted from 0.254 cm to 0.00254 cm in height and 2.2225 cm in width, the collimator enters the HFEF cell wall. The PGS uses a custom control-software interface that controls both the collection of gamma-ray spectra and the movement of the sample in the hot cell. It is possible to switch the collimator's orientation from horizontal to vertical. The sample can be rotated around its central axis on the stage and can be moved in the plane confronting the collimator in front of the sample. The detector is a high purity germanium detector with Compton suppression, and its control system moves the stage and collimator as well as starts the scans. The distribution of fission and activation-product activity in fuel elements or capsules is measured by this apparatus, which offers important insights into how reactor operation and storage impact components. These measurements can yield information on the power profiles of reactor fuels as well as relative fuel burnup. Position and dimensions of internal structures within fuel assemblies, as well as the structural activation profile of core components Interest-generating isotopes' relative abundance in fuel and breached elements.

## 3.8. NEUTRON RADIOGRAPHY

Neutron radiography is a non-destructive imaging technique that can be used to confirm fuel behaviours such as fuel pellet separations, fuel central-void creation, pellet cracking, evidence of fuel melting, dimensional measurements, and material integrity under normal and extreme situations. Neutron radiography was also used for detecting water (hydrogen/deuterium) ingress in CANDU fuel elements (i.e. defects). Neutron radiography has been routinely applied to ceramic fuels and has been applied to metallic U-Pu-Zr and U-Zr fuels to obtain dimensional information, including data on the axial growth of the fuel. In addition, large defects and density changes in the fuel can be revealed by neutron radiography.

14

The Neutron Radiography Reactor (NRAD), which is housed in HFEF's basement at INL, can be used for neutron radiography as an example. The 250 kW TRIGA NRAD reactor has two beam lines and two independent radiography stations. The NRAD beam tubes were created for the analysis of fuel components in order to pinpoint regions of interest, such as where the fuel needs to be disassembled, the presence of cracking (example shown in Fig.8 [16]), density changes, and possibly hydrides in the cladding. The NRAD neutron beam is positioned below the floor, and specimens are put into a radiograph holder that is lowered into the beam. The holders place the specimen for radiography in the best possible position without adding too much scatter.

Irradiated fuel is serviced by the east beam line, which is located underneath the hot cell's main floor. The radiography fixture comprises a scale marked with Gd paint that generates a calibrated scale for calculating the size of the irradiated fuel as neutrons flow through the fuel specimen and reveal various activation foils. Both a dysprosium (Dy) foil for thermal neutron radiography and a Cd-covered indium (In) foil for epithermal neutron radiography can be used to obtain neutron radiography images of the pins from a variety of angles. Although specimen thickness and fuel enrichment are constrained, the dysprosium foils utilized for thermal neutron radiography of low-enriched fuels and thin structural materials show good detail. The indium foils are employed for epithermal neutron radiography of thicker structural materials and highly enriched fuels. These can be used for thicker specimens and more highly enriched fuel, but they do not display as much specimen detail. Both foils are frequently employed to obtain information on the fuel's external and interior structures. For specific purposes, other techniques like Polaroid and track-etch radiography are available. The rodlets were put in a collet to fix the radial location, which fixed the rotations.

Figure 8 displays examples of ATF Rodlet neutron radiography (part (a)). The information on individual pellet breaking, cracking at the interface in individual pellets, and composite cracking are notable aspects from neutron radiography.

## 3.9. 3D X-RAY IMAGING

X-ray computed tomography (XCT), commonly known as three-dimensional (3D) X-ray imaging, is a data-rich characterization technique that can offer spatial information about the surface and subsurface without causing damage. Rotation of the source or detector or both is used to capture absorption-contrast radiographs of a sample (i.e., gantry systems) As a result of sample rotation, several hundred to several thousand X-radiographs are often acquired. The radiographs are computationally rebuilt to create a 3D dataset (i.e., tomogram) that can be utilized for finite element analysis, image quantification, and sample/part examination of flaws. This method's spatial resolution range is broad and can change depending on the X-ray source used (such as micro- or nano-focus tube sources, synchrotron sources, linear accelerators, etc.).

With 3D X-ray microscopy, which commonly uses a micro-focus X-ray source and objective lens/charge coupled device (CCD) camera combination to reach finer resolutions than what is possible with most classic X-ray tomographic imaging systems, sub-micrometre resolution can be achieved. The X-ray microscope housed at the Irradiated Materials Characterization Laboratory (IMCL) of INL shown in Fig. 9 can non-destructively image a variety of fuel and structural materials over four orders of magnitude in length scales ($10^1 - 10^{-2}$ cm). The device uses two different sorts of detectors: a flat panel and an objective lens, and it employs several magnification techniques.
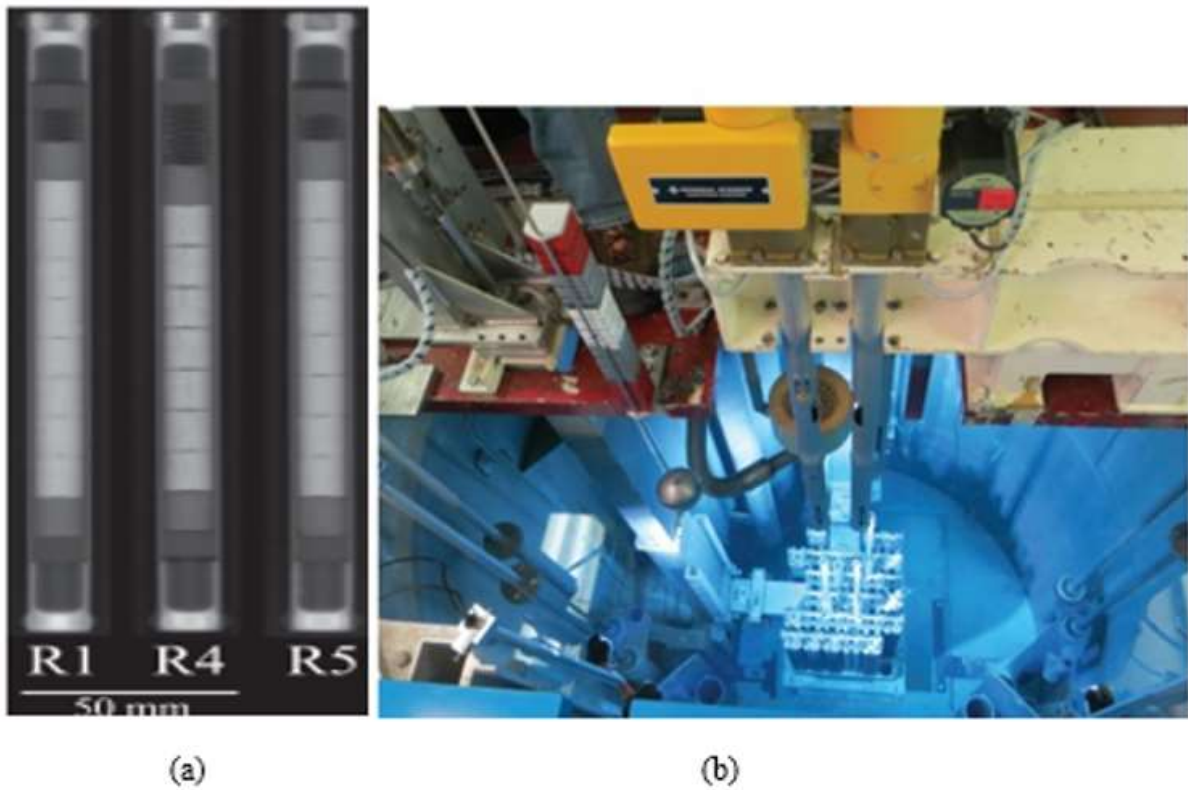
*FIG. 8. (a) Example of neutron radiography and (b) NRAD reactor (courtesy of INL)*



*FIG. 9. ZEISS Xradia 520 Versa X-ray microscope located at INL (courtesy of INL)*

Using image processing methods on 3D X-ray pictures, defect characterization and analysis can be automated. The method finds the materials, uses picture segmentation to label the voids/cracks, and then employs global thresholding to find the vacancies. The technique

16

allowed for the detection of exterior and subsurface cracks that are invisible to the naked eye, highlighting the usefulness of X-ray tomographic imaging for post-irradiation studies.

## 3.10. NEUTRON AND X-RAY DIFFRACTION

Neutron diffraction is a potent tool for characterizing nuclear materials. The lattice information, atomic locations, and stress state of a bulk material can be obtained by neutron diffraction. There are several nuclear facilities in the world that can perform neutron diffraction and scattering studies, such as the Spallation Neutron Source (SNS)[4] and the High Flux Isotope Reactor (HFIR) in the Oak Ridge National Laboratory (ORNL)[5], Los Alamos Neutron Science Center (LANSCE) at the Los Alamos National Laboratory[6], and the Swiss Spallation Neutron Source at PSI in Switzerland[7], etc. It is noted, however, that any neutron scattering source requires special permission and equipment to handle irradiated materials, especially fuels.

X-ray diffraction (XRD) offers quick, dependable, and precise materials analysis solutions. Step size, increment, and run time can all be customized to the materials undergoing examination. For phase identification, line profiling, crystal structure, texture, defect density, stacking faults, crystallite size, and micro-strain, XRD scans can be carried out at various temperature intervals. There are several synchrotron facilities in the world that can perform a variety of studies using the synchrotron X-ray source, such as the Advanced Photon Source (APS) at ANL[8], the National Synchrotron Light Source II at Brookhaven National Laboratory (BNL)[9], the Advanced Light Source at Lawrence Berkeley National Laboratory[10], and the Swiss Light Source at PSI[11].

## 3.11. SUMMARY OF NDE TECHNIQUES

Table 1 provides a summary of NDE PIE techniques with intended applications.

TABLE 1. SUMMARY OF PIE CAPABILITIES: NON-DESTRUCTIVE EXAMINATION

| PIE Technique | Application |
|---|---|
| Visual Inspections | For visible surface defect and abnormalities identification. |
| Dimensional Inspection | For dimensional change measurement, such as rod growth and bowing. |
| Neutron Radiography | Provides critical information on the presence of cracking, density changes, and hydrides in the cladding, Supplements X-ray tomography. |
| Gamma Spectrometry | Fission products and burn up analysis, rod integrity and defects, rough dimensional measurements such as fuel-clad gap. Power effects such as power gradients-based Cs distribution. |
| Eddy current | Oxide or coating thickness, surface defects. |
| Profilometry | Provide dimensional as well as surface roughness details (contact or laser). |

---

[4]  Refer to: https://neutrons.ornl.gov/sns.
[5]  Refer to: https://neutrons.ornl.gov/hfir.
[6]  Refer to: https://lansce.lanl.gov.
[7]  Refer to: https://www.psi.ch.
[8]  Refer to: https://www.aps.anl.gov.
[9]  Refer to: https://www.bnl.gov.
[10]  Refer to: https://als.lbl.gov.
[11]  Refer to: https://www.psi.ch.

TABLE 1. SUMMARY OF PIE CAPABILITIES: NON-DESTRUCTIVE EXAMINATION (CONT.)

| PIE Technique | Application |
|---|---|
| Density measurement | Irradiation induced dimensional changes, voids and porosity determination. |
| Neutron diffraction | Microstructural information and the lattice characteristics, atomic locations, phase composition, and stress state of a bulk material. |
| X-ray imaging | High resolution 3D imaging with sophisticated data analysis available. Detailed information on defects in 3D. |
| X-ray diffraction | Provides phase composition and a variation of analysis such as strain/stress characterization. |

# 4. HOT CELL DESTRUCTIVE EXAMINATION

## 4.1. METALLURGY AND CERAMOGRAPHY BY OPTICAL MICROSCOPE

Characterization of the fuel particle size and shape, porosity, phase, fuel-cladding interaction, cladding oxide thickness, and hydride distribution can be done using optical microscopy. For additional examination, optical microscope data is captured using digital cameras that are integrated with the metallograph and the microhardness tester.

## 4.2. MICROHARDNESS

The microhardness tester applies varies loads weighing to areas of interest for both Vickers and Knoop hardness data that can be linked to mechanical properties. Figure 10 illustrates the microhardness tester[12].



*FIG. 10. Illustration of microhardness tester*

## 4.3. TENSILE TESTING

A load frame in a hot cell can be used to perform tensile testing. The ASTM high force capacity load cell and adaptable fixturing enable tensile testing of a variety of standard (and nonstandard) specimens as well as other tests that call for the controlled application of tensile or compressive force, like bending tests or flexure tests. High-temperature testing is possible with heating capability such as using high temperature furnace. Tests on the tension of a ring hoop (bottom) are used to identify plasticity behaviour in a circumferential direction for fuel cladding, as shown in Fig. 11. Additionally, the subsize mechanical testing can be performed for irradiated samples, as shown in Fig. 12.

---

[12]     Refer to: **Error! Hyperlink reference not valid.**
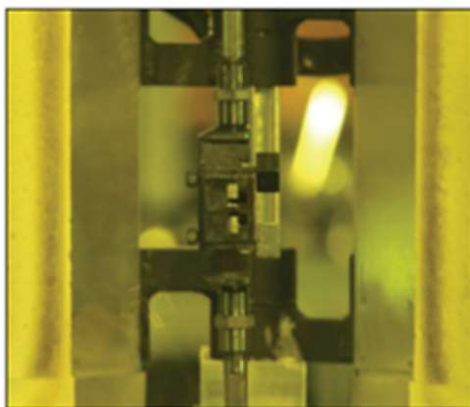
*FIG. 11. Example of mechanical testing of cladding – test specimens in a mechanical testing load frame in HFEF hot cell (courtesy of INL)*



*FIG. 12. The actual subsize specimen fixture and the subsize specimen (courtesy of INL)*

Non-contact optical metrology methods with digital image correlation (DIC) computation capabilities can be added as shown in Fig. 13, where two-dimensional (2D) DIC capability was established. The specimen is covered in speckling. Despite the high contrast of the applied speckle pattern, a sizable fraction of the speckles is typically too large for the small specimen

geometries. Generally speaking, airbrushing, stamping, or powders improve the quality of the speckle pattern. An opensource 2D DIC program called NCORR can be used to examine the camera data that has been acquired. The user was able to remove regions with weak speckle patterns by using the software's ability to frame the region of interest as a polygon for DIC computations. A long-distance lens and camera system has been developed to enable strain measurements in the hot cell.
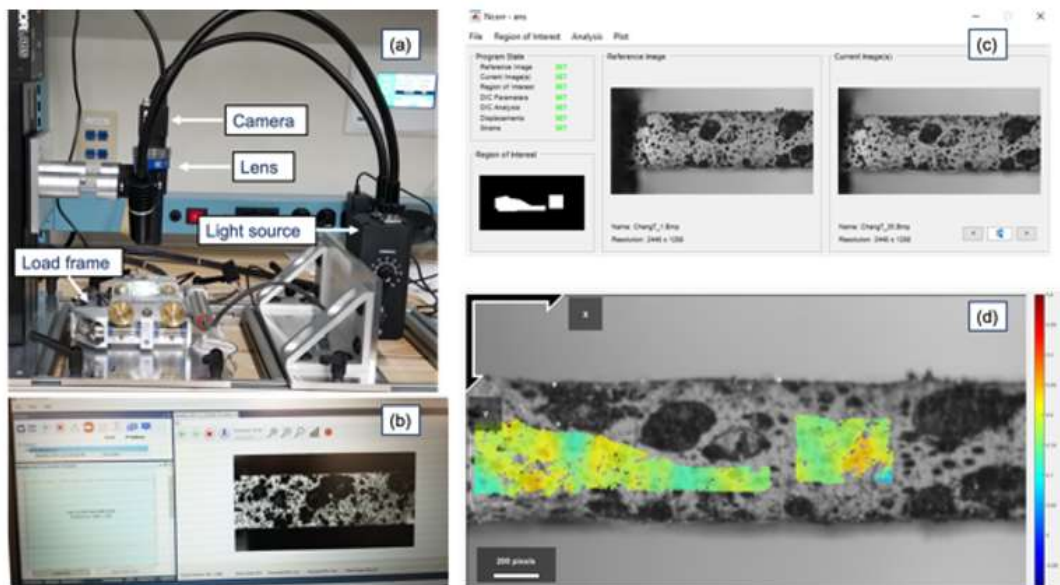


*FIG. 13. (a) Optical metrology setup, (b) speckle pattern data acquisition, (c) 2D speckle pattern images for DIC analysis, (d) 2D distribution of mechanical strain on the specimen surface (courtesy of INL)*

## 4.4. EXPANSION DUE TO COMPRESSION FOR CLADDING TUBE

In order to evaluate the mechanical response under strain-driven loading and investigate the mechanical response of the cladding under pellet-cladding mechanical interaction conditions during reactivity-initiated accident conditions, the expansion-due-to-compression (EDC) test can be developed for cladding test.

Figure 14 depicts the EDC's operating principle. The insert, which could be made of polyurethane, aluminium, or another soft metal, is compressed as the upper platen descends. The inner surface of the cladding sample experiences strain as a result of the insert's lateral expansion and compression.

## 4.5. IN-SITU TENSILE AND HOOP TESTING-X RAY MICROSCOPY

The X-ray microscopy (XRM) and the Deben mechanical test stage are both compatible with the EDC technique, as shown in Fig.15. This feature allows for the collection of precise volumetric strain data during mechanical testing of cladding tubes as well as the observation of crack microstructure. This capacity is ideal for modern high-temperature nuclear reactors that use composite materials for structural or fuel cladding purposes. This technique typically applies to subsized specimens.
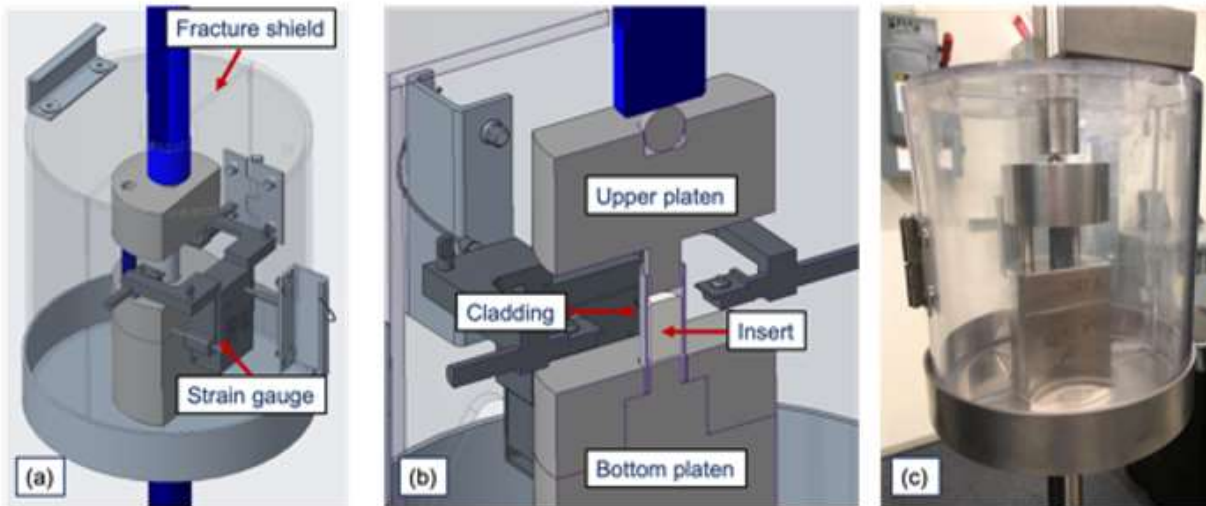
*FIG. 14. (a) Expansion-due-to-compression (EDC) test fixtures and fracture shield, (b) cross-sectional view of the EDC setup showing the orientation of specimen and insert with respect to the upper and bottom platens, (c) actual setup (courtesy of INL)*
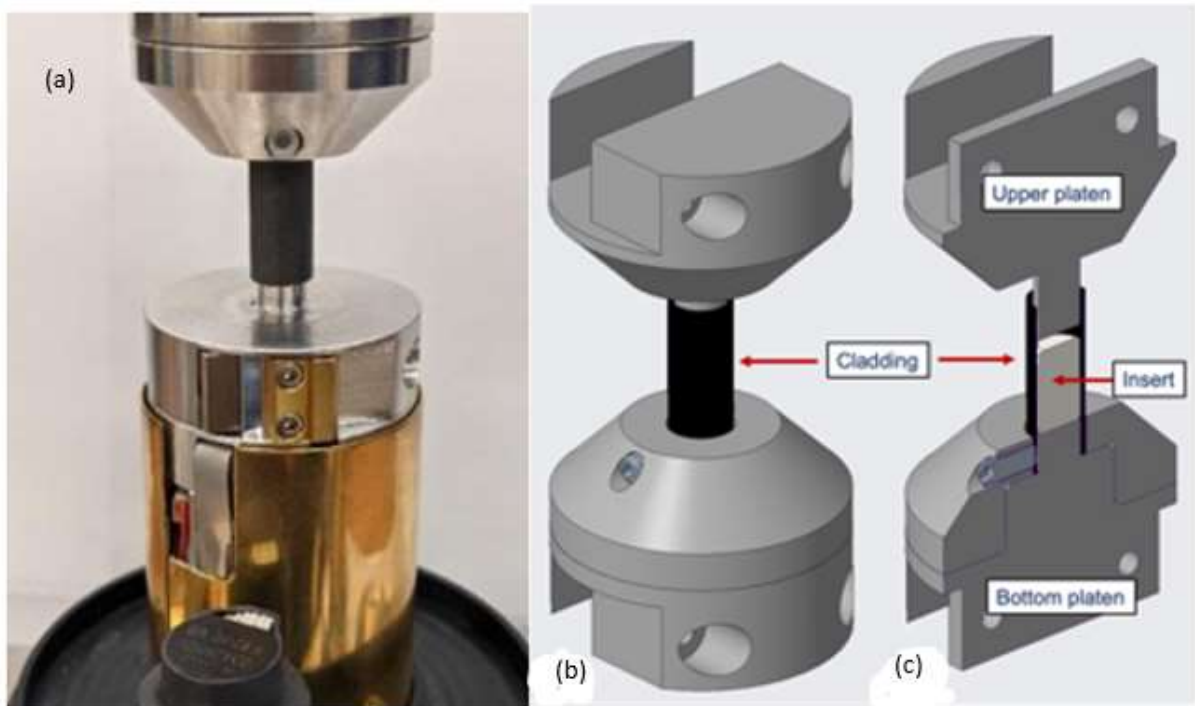


*FIG. 15. (a) EDC setup for IMCL's XRM, with (b) schematic configuration of the sample setup and (c) the cross-sectional view of the same setup (courtesy of INL)*

22

## 4.6. CLADDING BURST TESTING

The ability of cladding tubes to withstand burst-creep-fatigue is importance for cladding performance evaluation. A burst test system uses three Swagelok fittings attached to the test sample to the pressure testing apparatus. The capability to perform burst and stress-relaxation testing on heated, defueled irradiated cladding specimens has been recently demonstrated at CNL. On each end, the fittings enclose of the cladding test sample, leaving a test portion exposed. The entire test section, including the end fittings, is contained inside a chamber that is linked to an inert gas bottle in order to produce an oxygen-free atmosphere and reach high temperatures. Inside an Instron load frame is where the furnace and environmental chamber are located. The gas pressure lines are attached to a bulkhead beneath the furnace/environmental chamber. To perform 'limited' burst tests, Swagelok fittings and piping attached to the top of the sample can be extended out to the top of the furnace or environmental chamber and fastened to the Instron load cell. Booster pumps are connected to allow for the pressurization of the test specimen at varies pressures ranges from 200 psi (1.379 MPa) to 20 000 psi (137.9 MPa).

Figure 16 shows a burst test capability at INL, with Zircaloy-4 shown as an example. This technique can be used for cladding creep and fatigue tests as well.
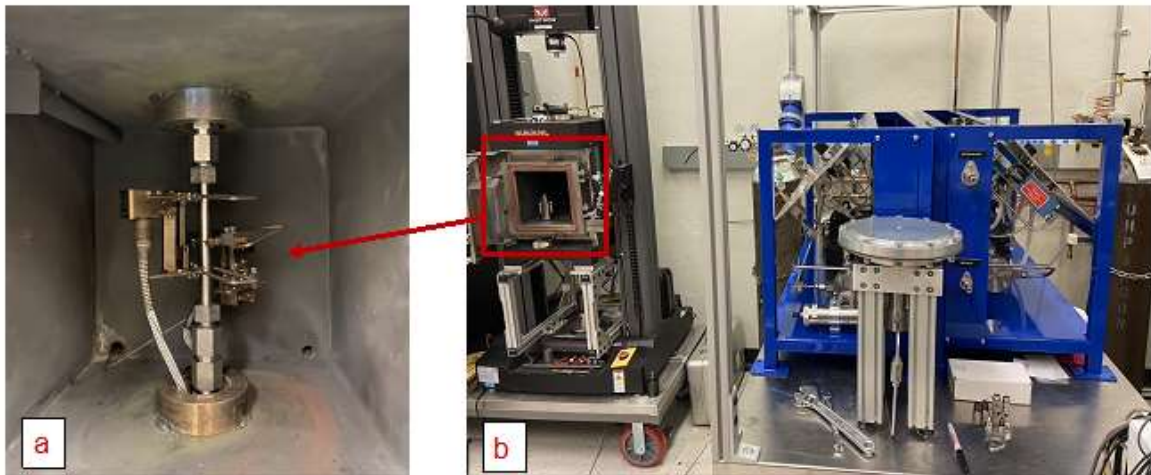


FIG. 16. (a) Actual specimen setup with extensometers in the furnace, (b) cladding burst test (courtesy of INL)

## 4.7. MICROMECHANICAL TESTING

Small scale mechanical testing (SSMT) is a method that could speed up the process of developing better nuclear fuels while also cutting costs and time required for PIE. The materials science community has been working on scaling mechanical testing in the micro- and nanoscale range, and it has now become a broad discipline that can assess a variety of mechanical characteristics of materials, including but not limited to Young's modulus, hardness, and elongation.

Because the specimens are so small, it is possible to target microstructural elements like precipitates that could have an impact on the specimens' overall strength. Targeting specific microstructural elements will allow for more in-depth analyses of how each element influences the overall strength of the fuel plates. Another benefit of the specimens' tiny size is that it makes

it possible to manufacture numerous specimens from very modest amounts of material. This is highly advantageous for cladding research since it enables testing to be done outside of protective hot cells, significantly cutting down on time and costs.

An in-situ pico-indenter fitted with a diamond indenter can be used to perform nanoindentation measurements in the FIB/scanning electron microscopy (SEM) apparatus. With irradiated nuclear fuels, using the FIB-based SSMT has the advantage of allowing for the independent evaluation of a variety of sample locations while limiting dose to the worker. The Plasma FIB process made it possible to reduce the volume of material sufficiently that the radiation emission was reduced to the point that the sample could be loaded into the nano-indenter by hand.

In-situ micro-tensile testing can also be performed using the same Pico-indenter with a push-to-pull device. The SEM beam is utilized during the testing of the micro-tensile bars to capture photographs and record movies for post-test analysis.

Figure 17 illustrates nanoindentation and micro-tensile testing for HT9, which is an advanced cladding material for fast reactors. Figure 18 demonstrates In-situ micro-tensile testing of hydrided specimen.
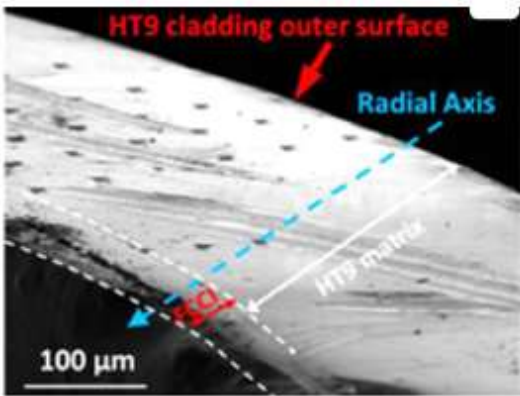


(a)
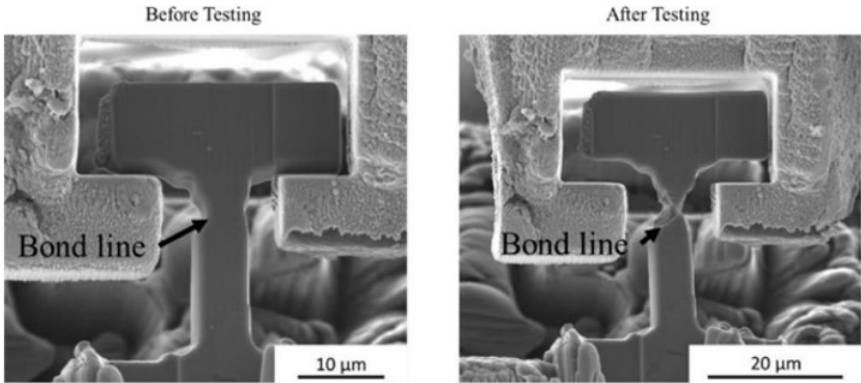


(b)

FIG. 17. Example of (a) nanoindentation and (b) micro-tensile testing done HT9 cladding material (courtesy of INL)
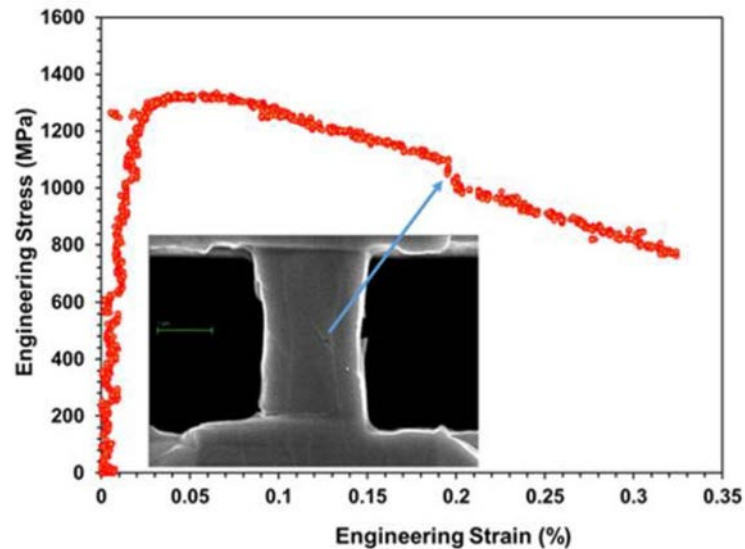
*FIG.18. In-situ micro-tensile testing of hydrided specimen; sample prepared using FIB (Courtesy of CNL)*

## 4.8. PLASMA MASS SPECTROMETRY AND PLASMA ATOMIC-EMISSION SPECTROMETRY

Inductively coupled plasma mass spectrometers are capable of determining major components, impurities, and fission products in fuels. Depending on the building materials used and the radiation exposure history, the majority of fission products between $^{85}$Rb and $^{154}$Sm can often be measured. Two-sigma errors typically range from plus/minus 3–5% in analyses. Compared to Plasma Mass Spectrometry, Plasma Atomic-Emission Spectrometry provides higher detection limit for metallic and non-metallic components from ppm to ppb.

## 4.9. FISSION GAS RELEASE

The Gas Assay, Sample and Recharge (GASR) device located at HFEF at INL and the sweep gas test equipment that was installed at CNL are typical examples of the device to determine fission gas release in fuel rods. This equipment enables the measurement of free volume and pressure as well as the collection of a gas sample for composition analysis.

The GASR system consists of a mechanical pump, gauges, calibrated volumes, a 150-watt Nd-YAG pulsed laser for rod puncturing, shielded optical and gas cell-wall feed-through, and controls. A clamp attached to a neoprene gasket holds the fuel rods in place on the laser. Between the fuel sample and the laser seal head, the gasket creates a seal. A sequence of expansions into the GASR system and backfills into the ruptured fuel rod are used to calculate the void volume. The fuel rod internal gas pressure is derived from the void volume measurement and fission gas puncture pressure measurement. Fission gas composition is analyzed by a gas mass spectrometer to provide krypton (Kr) and xenon (Xe) isotopic and total elemental composition. The rodlet void volume and internal gas pressure uncertainty is ≤ ±5% in the range of 0.03 to 60 litre-atmospheres. Depending on the relative abundance of the analyte, the uncertainty of the isotopic and elemental analysis ranges from 1 to 5%.

## 4.10. CARBON, HYDROGEN, NITROGEN AND SURFER ANALYSIS

A carbon, hydrogen, nitrogen and surfer (CHNS) analyzer can be used to measure the oxygen, nitrogen, and hydrogen content of diverse samples from radioactive and nonradioactive sources. Samples for solid sample analysis often weigh more than 1 gram. Oxygen and nitrogen in a helium carrier gas or oxygen and hydrogen in a nitrogen carrier gas stream can both be measured concurrently in a single analysis.

A thermal conductivity (TC) detector measures hydrogen or nitrogen, while an infrared (IR) detector measures oxygen, which is measured as $CO_2$. On top of the electrode furnace, inside a sample loading mechanism, the solid sample (0.5g) is weighed and put. An electrode furnace is filled with a graphite crucible, which is then heated to a high temperature (about 3000°C) by a low voltage (about 6 VDC) and high current (about 1200A) flowing through it in an inert atmosphere. Entrapped gases from the graphite crucible release because to the high temperature.

The sample is placed in the hot crucible, where it melts and releases oxygen in the form of CO, by reaction with the graphite. The gas stream exits the glovebox through a high-efficiency particulate air (HEPA) filter to remove any radioactive particulates, before entering the analyzer cabinet. To oxidize all CO into $CO_2$, the gas stream is fed into a heated copper-oxide furnace (350°C) or Schultz reagent (ambient temperature). The oxygen concentration is then determined by the sample's $CO_2$ IR absorption using high- and low-range infrared (IR) cells. The remaining $CO_2$ and water are subsequently completely removed from the gas stream using sodium hydroxide and magnesium perchlorate (anhydrone) reagents. The gas stream is then sent through a TC cell to detect thermal conductivity and measure nitrogen or hydrogen.

Similar to CHNS, an alternative but widely used technique is Hot Vacuum Extraction (HVE) with mass spectrometry to determine hydrogen content in metallic cladding such as zircaloy.

## 4.11. TIME-OF-FLIGHT SECONDARY ION MASS SPECTROMETRY (TOF-SIMS)

TOF-SIMS is a surface analysis technique which produces detailed chemical information for a material at nanometre resolution and with a detection limit in ppm. TOF-SIMS is able to scan all atomic masses across a range of 0-10 000 amu, the rastered beam provides maps of any mass of interest on a sub-micron scale, and depth profiles are also produced. Coupled with new generation Plasma FIB such as G4 Hydra, the plasma ion column can be used as the primary beam and the resultant secondary ions are extracted and mass separated. The high-resolution multi-ion column makes it ideal for SIMS analysis and imaging. First, the small spot sizes allow for chemical and isotopic information on the nano scale. Secondly, the ability to use reactive ions such as $O_2$ and $N_2$ provide large useful ion yield enhancements that lower detection limits.

## 4.12. ELECTRON PROBE MICROANALYZER (EPMA)

Electron probe microanalyzer (EPMA) is utilized to assess the chemical composition of solid specimens on a micrometre scale. The EPMA can acquire electron images of specimens just like a secondary ion mass spectrometry (SIMS), however unlike the SIMS, which is designed for image acquisition, the EPMA is designed for the acquisition of quantitative chemical compositional data. If shielded, this instrument can be used to perform elemental chemical analysis of irradiated nuclear materials.

The EPMA (Fig.19) used for irradiated fuel research at INL is shielded to 3Ci of ^{137}Cs and equipped with four wavelength-dispersive spectrometers capable of detecting elements from B to Cm. The chemical spatial scale resolution varies with the material interrogated, but for

uranium-based materials is in the order of 1 $\mu m^3$. Detection limit varies with the element and analysis conditions but is typically in the order of ~100 ppm.

Sample preparation involves mounting the material into a 25 mm metallography mount and polishing to < 1 $\mu m$ finish. The EPMA is used to study such phenomena as elemental redistribution in fuels, diffusion profiles, phase composition, and fuel-cladding chemical interaction. Complex peak overlaps can be deconvoluted in both quantitative spot mode acquisition and X-ray mapping mode using the combination software suite of Probe for EPMA and Probe Image. For example, it is being utilized to research how fission products are distributed in metallic- and tri-structural isotropic (TRISO)-type fuels for advanced reactors.



*FIG. 19. EPMA shown through a leaded glass confinement window at IMCL from INL (courtesy of INL)*

## 4.13. LOCAL ELECTRODE ATOM PROBE (LEAP) TOMOGRAPHY (LEAP/APT)

Atom probe tomography (APT) is a distinctive characterization method for revealing materials that offers three-dimensional chemical and isotopic data at sizes close to the atomic. When appropriately positioned at the tip of a needle-shaped specimen, regions of interest up to 100nm in size can be used to gather such detailed information on a regular basis. Atoms are eliminated off the surface of a specimen with a tip-like form and a radius of curvature less than 100nm during an APT examination using the field evaporation mechanism. Ions are field evaporated, then projected radially onto a position-sensitive detector, where Time-of-flight mass spectrometry (TOF-MS) is used to determine their isotopic and chemical composition.

A mass spectrum, also referred to as a histogram of counts, shows the mass-to-charge ratios of field evaporated ions. For appropriate data interpretation and quantification, intervals or ranges

are supplied within the mass spectrum for certain ionic species. Depending on how the examined materials in APT behaved during their field evaporation, the evaporated ionic species are identified either elemental or molecular. Multiple charge states are more frequently found for a single species. Since the whole spectrum is captured for each pulse, the mass spectrum acquired with APT is unique in that no pre-selection or assumption of elements or isotopes is necessary. Additionally, each atom for any given element can be assumed to have an equal chance of being ionized and detected in APT, thus providing quantitative information from different isotopes of the same element. In the situation when multiple isotopes may be potentially present with the same mass-to-charge ratio, stability of the isotopes needs to be considered to determine for quantification. Figure 20 illustrates a modern APT system LEAP 5000.



FIG. 20. LEAP 5000 APT system

## 4.14. THERMAL DIFFUSIVITY: LASER FLASH METHOD

The laser flash analyzer (LFA) fires a brief pulse at the surface of a thin disk specimen, and analyzes the temperature change on the opposite surface, which enables calculation of the thermal diffusivity. Measurements of radioactive, nonradioactive, and irradiated fuel and structural materials will be made using this equipment. Samples can be in varies solid forms such as cylindrical, disk, or slab shapes with dimensions of 6 to 12mm in diameter and roughly 2mm in length and mass of about100mg. with special holder designs, LFA can be used to measure thermal diffusivity of liquid samples.

If installed in shielded hot cell, the LFA can be used to measure highly-irradiated fuel and materials. Figure 21 shows the LFA installed in a shielded cell at IMCL from INL.

## 4.15. DIFFERENTIAL SCANNING CALORIMETRY (DSC)

The specific heat capacity is determined using the heat flow, time, and subsequent change in sample temperature using the DSC. Temperatures for phase transformations are also calculated using it. Most sample materials will be in solid form, though occasionally there may be powders. Sample sizes typically vary from 10 to 150mg. It gathers data about a sample's thermodynamics. Phase transition temperatures, melting temperatures, heats of formation and

solution, and specific heat capacity are examples of property measurements. For the majority of materials, accuracy can be achieved in the range of 2.5% for specific heat over the temperature range of room temperature (RT) to 1400°C and better than 2.0% for latent heat over the temperature range of RT to 1600°C. DSC can be used in vacuum, oxidizing, reducing, and inert atmospheres. If shielded, DSC system can be used to determine properties for irradiated fuel and structural materials. A schematic of DSC is shown in Fig.22.
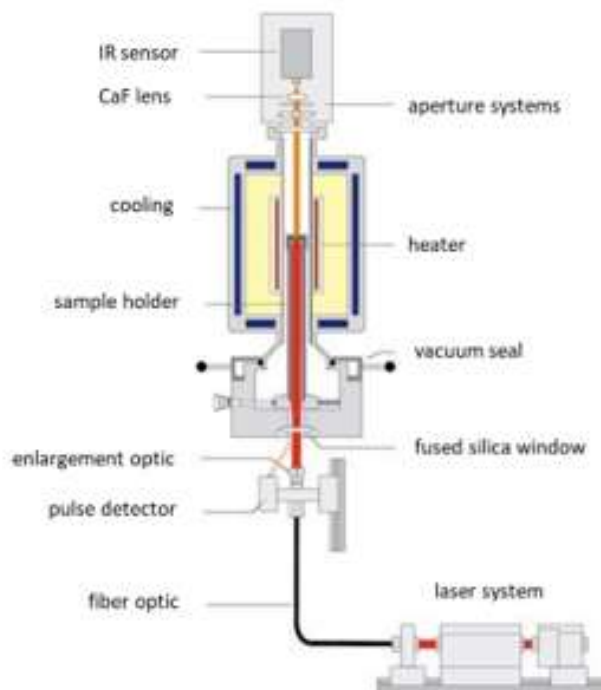


*FIG. 21. LFA in shielded cell at IMCL at INL (courtesy of INL)*
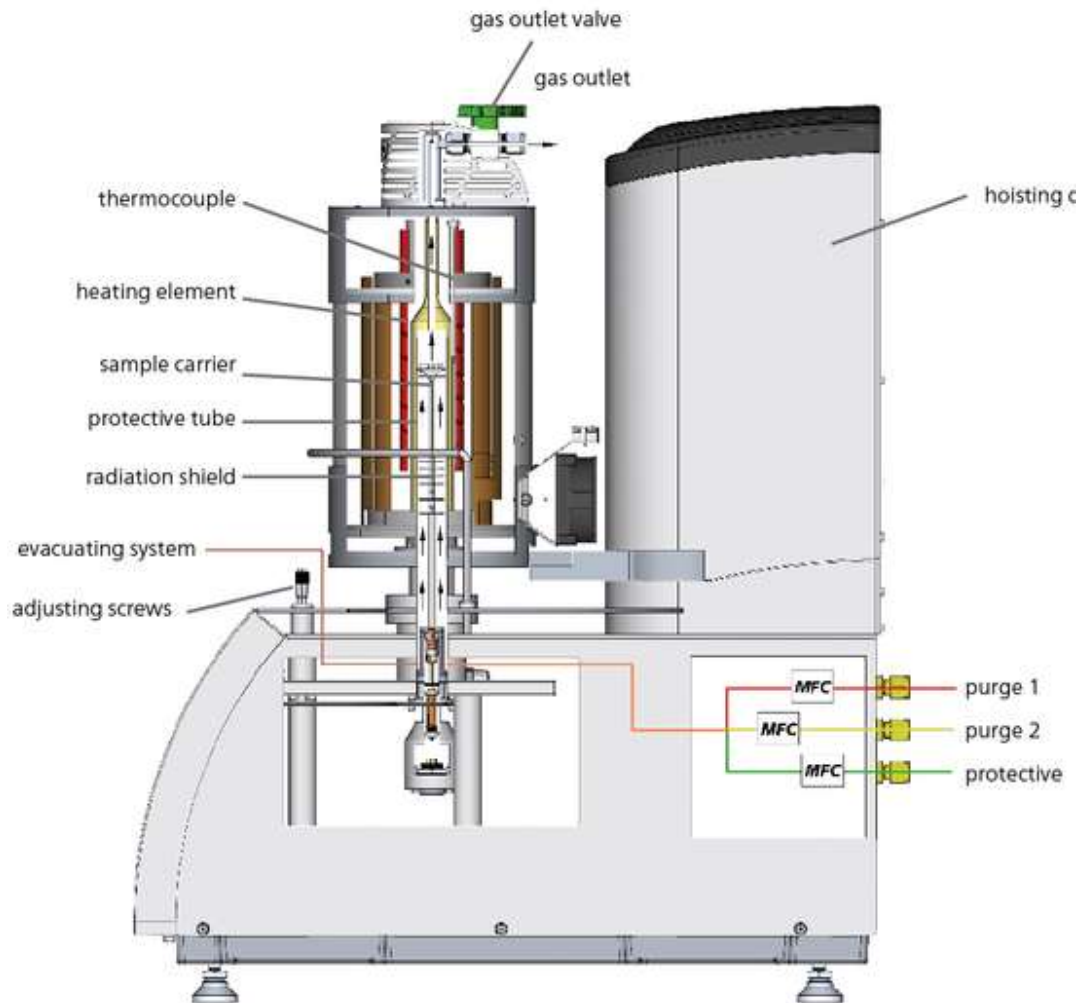
*FIG. 22. Schematic of DSC system*

## 4.16. THERMAL CONDUCTIVITY MICROSCOPE

The thermal conductivity microscope (TCM) system is based on the thermos-reflectance method to aid in the post-irradiated measurement of thermal conductivity. It concurrently measures thermal diffusivity (D) and thermal conductivity (k) using finely focused laser beams. Thermal wave methods can only be used in LFA analysis to determine D values; conductivity requires additional measuring methods to estimate density and heat capacity values. However, the TCM is unique in that it can simultaneously measure both k and D values using a technique called modulated thermos-reflectance.

In this measurement method, samples stimulated by an amplitude modulated continuous-wave laser beam are measured for their temperature field spatial profile. The samples are covered in a thin layer of gold to ensure high optical absorption and to create a second boundary condition that adds an expression containing the thermal conductivity of the substrate. By contrasting a continuum-based model with the measured phase profile of the temperature field, the thermal transport properties are determined. Two lasers are needed to implement this technique: a modulated pump laser to create the oscillating temperature field and a probe laser to detect it. Thermo-reflectivity effect, or the change in reflectivity of the gold sheet with temperature, is what allows for detection. As a result, the temperature modulates the intensity of the probe

beam that is reflected. To achieve a robust thermos-reflective reaction and, thus, a strong thermal wave transduction, the sample is coated with a thin gold coating. The pump beam initially coincides with the probe beam but is then swept to enable temperature field inquiry. As the separation distance and modulation frequency increase, so does the phase shift of the temperature field. The D and k values of the sample substrate are then derived by minimizing the difference between the theoretical and actual phase profiles. Scans are done at various frequencies, typically from 1 to 100kHz.

Figure 23 depicts a schematic and photograph of the TCM system. For reliable measurements using TCM, the sample surfaces need to be polished since rough surfaces might scatter probe light, which significantly lowers the signal-to-noise ratio. Any sample material is assumed to be thermally homogeneous and isotropic over the sampling volume by the current measurement arrangement and models.
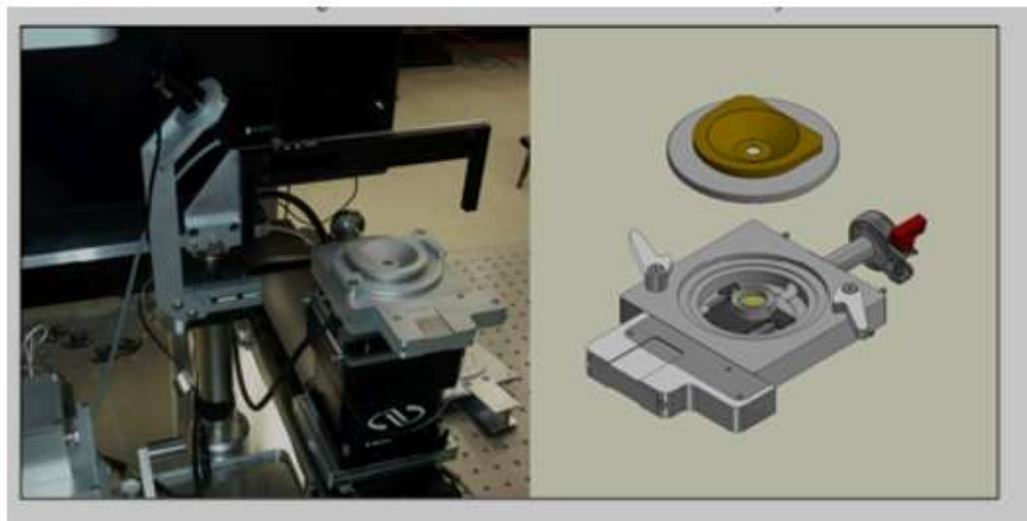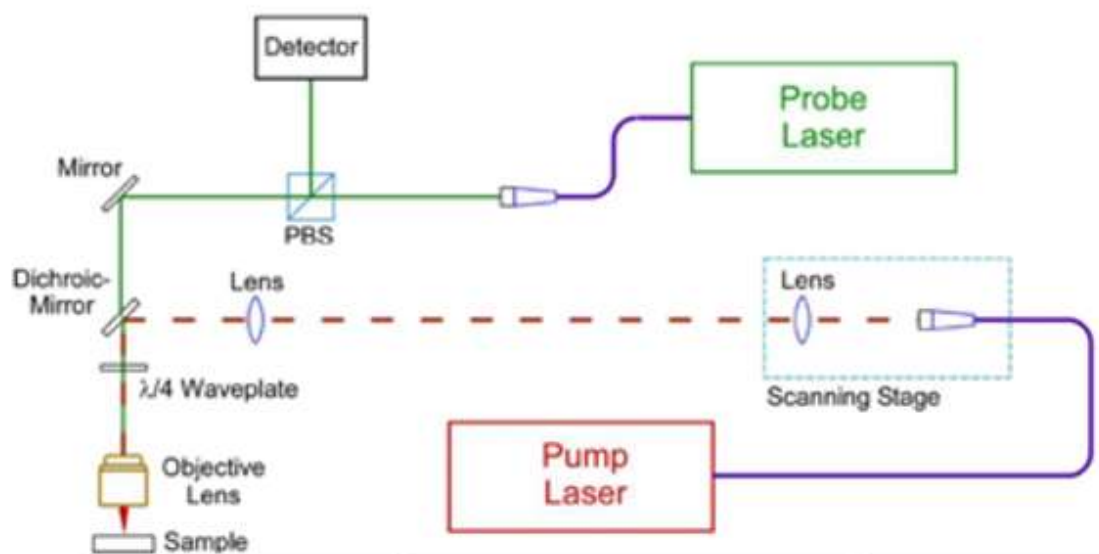


FIG. 23. (top) Schematic and (bottom) photograph of thermal conductivity microscope (courtesy of INL)

## 4.17. POSITRON ANNIHILATION SPECTROSCOPY (PAS)

Radiation induced defects can be measured using positron annihilation spectroscopy (PAS) at the atomistic to nanometre scale. Positrons are sensitive to open volume flaws, like vacancies, voids, and bubbles, in materials. The concentration and type of flaws existing in materials can be determined using a Doppler broadening PAS system that can operate in coincident or singular mode. This device has two positron sources—a $^{22}$Na and a $^{68}$Ge—that make it possible to find flaws in the bulk of materials or even closer to their surfaces.

When they enter the substance, the positrons from the source annihilate with the electrons. Two gamma rays (about 511keV each) are produced as a result of this annihilation, and they are then detected using high purity gamma ray spectrometers. This device was created to perform point measurements or two-dimensional scanning of specimens. The largest specimen size that may be accommodated is 75mm by 150mm, measured in millimetres in both length and width. This is a not a standard or typical PIE technique so requires further development and demonstration of its applications.

## 4.18. SCANNING ELECTRON MICROSCOPY (SEM)

A Schottky-type field emission (T-FE) gun is typically used as the electron source in the high-resolution field emission scanning electron microscope.

SEM is used to characterize microstructure of highly radioactive materials and irradiated nuclear fuels and is of critical importance to capture the microstructural-structure property relationships. Both compositional and topographical imaging modes can be used with backscattered electron imaging. The main analytical capabilities that can be attached to SEM are an electron backscatter diffraction (EBSD) system, an energy dispersive spectroscopy (EDS) detector, and a wavelength dispersive X-ray spectroscopy (WDS) detector for crystal structure and chemical composition characterization.

## 4.19. FOCUSED ION BEAM (FIB)

FIB operates like standard SEM typically equipped with a high-resolution field emission electron column and standard analytical capabilities such as EDS and EBSD, but with at least one ion column such as Ga or Xe (plasma FIB) for added micromachining capabilities. Some newer FIBs like G4 are equipped with multiple ion sources, including O, N, Xe, and Ar. Typical FIB also equips withs gas injector systems for platinum and carbon deposition as well as Omni-probe micromanipulators for in-situ sample lift-out. If shielded, FIB can be used to fabricate large area lift-outs (LALO), TEM, APT, and micromechanical testing samples from irradiated fuel and structural materials. In addition, a cryogenic sample stage can be used to eliminate hydride artifacts introduced during preparation of zirconium alloy fuel cladding samples with the FIB.  Sample preparation of irradiated zirconium cladding using the FIB allows detailed characterization of microstructural features such as hydride precipitates whose density and orientation determine cladding mechanical properties and lifetime. Preparation of samples in the FIB, if not performed at cryogenic temperatures, leads to introduction of hydrogen artefacts that confuse analysis of uptake, precipitation, growth, and reorientation mechanisms.

## 4.20. TRANSMISSION ELECTRON MICROSCOPY (TEM)

Transmission electron microscopy (TEM) is a microscopy technique where a beam of electrons is transmitted through a sample to form an image or diffraction pattern. High end TEM is often equipped with varies analytical capabilities such as EDS and electron energy loss spectroscopy

(EELS) for chemical composition characterization. TEM is often used to achieve high resolution images such as atomic resolution, to identify varies defects in the microstructure, chemical composition and nano-precipitates, elemental mapping, etc. Coupled with EELS, an analysis of electron energy loss during inelastic interaction with materials can yield valuable information for the materials, such as atomic composition, chemical states, bonding energies, valence and conduction band electronic properties, surface characteristics, and element-specific pair distance distribution functions. Varies in-situ testing capabilities can be added, such as heating, cooling and indentation stages.

## 4.21. SUMMARY OF DE TECHNIQUES

Table 2 provides a summary of destructive PIE techniques with intended applications.

TABLE 2. SUMMARY OF PIE CAPABILITIES: DESTRUCTIVE EXAMINATION

| PIE Technique | Application |
| --- | --- |
| Metallurgy and Ceramography by optical microscope | Provides information on microstructure for fuel and cladding, voids, impurities, and crack distribution. |
| Microhardness | Provide information on mechanical properties. |
| Tensile testing | Determine yield strength and ultimate strength, ASTM standards are available. |
| Expansion due to compression for cladding tube | Provides information on cladding burst strength and failure at high strain rates. |
| In-situ Tensile testing Xray Microscopy | Provides information on volumetric flaws such as cracking under loading. |
| Burst/creep/fatigue testing | Determine cladding mechanical properties/behaviour. |
| Micromechanical testing | Help understand heterogeneous micro-mechanical and localized mechanical behaviour that is tied to microstructure and radiation damage. |
| Inductively coupled plasma mass spectrometers | Determine chemical and fission product compositions, impurities. |
| Fission gas release | Determine the amount of fission gases related to rod plenum from fuel pellet. |
| Chemical burnup analysis | Determine the chemical burnup of the fuel-by-fuel dissolution and analysis of $^{139}$La, $^{148}$Nd, or U and Pu isotopes. |
| CHNS analysis | Provide information on carbon and oxygen stoichiometry. |
| SIMS | Provides high resolution details on surface and sub-surface chemistry. |
| EPMA | Quantification of fission products and migration in fuels. |
| LEAP/APT | Three-dimensional chemical and isotopic data at atomic resolution. |
| Laser Flash Analyzer (LFA) | Determine thermal diffusivity for fuel and materials. |
| Differential scanning calorimetry | Provides specific heat capacity of samples, small pieces from cladding specimen. |
| Thermal conductivity microscope | Provides localized thermal conductivity and thermal diffusivity distribution that is tied to microstructure and radiation damage. |
| Positron Annihilation | Provide information on irradiation induced point defects, vacancies and clusters. |
| SEM | Provides details on microstructural damages, grain size, orientation, strain, texture, and surface chemistry. |

TABLE 2. SUMMARY OF PIE CAPABILITIES: DESTRUCTIVE EXAMINATION (CONT.)

| PIE Technique | Application |
|---|---|
| FIB | Prepare TEM and APT samples, Large Area Lift Outs, provides 3D microstructural information such as grain size and orientation, grain boundaries, defects, voids, chemical composition and segregation, etc. |
| TEM | Provides details on internal composition, morphology, crystal structure and orientation, lattice strain, radiation induced defects, precipitates, phase separation and segregation, chemical bonding. |

# 5.  POST-IRRADIATION EXAMINATIONS TO SUPPORT FUEL MODELLING AND CODES' VALIDATION

## 5.1.  BACKGROUND

The use of certain PIE techniques is required to determine various properties of structural and fuel materials that determine operational and economic performance during reactor operation, but it is also used to update of calculation codes used in fuel design and safety analysis. Computer codes used in fuel design and safety analysis need to be validated to assess the adequacy and applicability of fuel models employed in the codes, demonstrate the capabilities and limits of the codes, and to determine code accuracy. The validation of fuel analysis codes and fuel models is mainly performed by comparing their predictions with experimental data that are obtained from irradiated fuels irradiated in power reactors or research reactors.

In cooperation with the Expert Group of Reactor Fuel Performance (EGRFP) of the Organization for Economic Cooperation and Development-Nuclear Energy Agency (OECD-NEA), fuel models and related experimental data for the assessment of water-cooled reactor fuel performance have been identified. The experimental data cover: interim fuel-performance processes (e.g., degradation of thermal mechanical properties due to irradiation in the reactor) and codes' output parameters used for fuel performance assessments (e.g., rod internal pressure).

The list developed by the EGRFP of the OECD-NEA was delivered as a questionnaire to participants of the TM 2021 for a survey of PIE capabilities and whether their PIE facilities can provide these experimental data. The survey results were reviewed during the TM.

In the subsequent sections, the assessment of the survey results is described separately for water reactor fuels and for non-water innovative reactor fuels.

## 5.2.  PIE CAPABILITIES TO SUPPORT FUEL TECHNOLOGY FOR WATER-COOLED REACTORS

Table 3 and Table 4 summarize the assessment results on PIE capabilities to support assessments of water-cooled reactor fuels. Table 3 is to access PIE capabilities for interim fuel-performance processes, and Table 4 summarizes computer codes' output parameters. In both tables, the first two columns describe fuel models and related experimental data, which were identified by the EGRFP of OECD-NEA and sent to TM 2021 participants as a questionnaire, and the third column describes Member States' practice to assess PIE capabilities to provide necessary experimental data.

In general,

— Experimental capabilities to support water reactor fuel technologies (e.g., fuel modelling and fuel analysis codes) are matured with some exceptions on specific interim performance processes e.g., fission gas bubble kinetics;
— There have been few applications of specific PIE measurements on the thermal mechanical properties of irradiated materials;
— Most PIE capabilities are applicable to support ATF concepts except for some revolutionary ATF concepts.

TABLE 3. ASSESSMENT OF PIE CAPABILITIES TO SUPPORT WATER-COOLED
REACTOR FUEL MODELLING AND VALIDATION OF FUEL PERFORMANCE PROCESSES

| Model (performance process) | Related experimental data required for the validation of the fuel model | Member States' practice to provide required experimental data |
|---|---|---|
| Heat transfer within fuel pellets | Fuel centre and surface temperatures | - Fuel temperatures can be measured using instrumented fuel rods. |
| | Fuel thermal conductivity (for thermal conductivity sub-model) | - Fuel thermal conductivity can be determined with the use of laser flash apparatus (LFA). <br> - The LFA has been applied on unirradiated materials, though the plan is to use it for irradiated fuel as well. |
| | Fuel specific heat capacity and/or enthalpy (for heat capacity and/or enthalpy sub-models) | - Fuel specific heat capacity can be determined with the use of LFA. |
| | Fuel density (for density sub-model) | - Fuel density can be measured using the immersion density method and using pyrometry (for geometric and weight measurements). |
| Heat transfer within cladding | Clad inner and outer surface temperatures | - The same technique described for fuel pellets above is applied. |
| | Clad thermal conductivity (for thermal conductivity sub-model) | - The same technique described for fuel pellets above is applied. |
| | Clad specific heat capacity and/or enthalpy (for heat capacity and/or enthalpy sub-models) | - The same technique described for fuel pellets above is applied. |
| | Clad density (for density sub-model) | - The same technique described for fuel pellets above is applied. |
| Heat transfer between fuel and clad | Cladding inner surface temperature and either fuel outer surface temperature or gap heat transfer coefficient | - Gap heat transfer coefficients are deduced from the measured pellet temperatures and cladding or coolant temperatures. |
| | Cladding hardness (for hardness sub-models) | - The cladding hardness can be determined using Reichert Telatom-3 inverted microscope equipped with a Vickers microhardness indenter. <br> - Cladding hardness has been measured on unirradiated material so far although the technique is applicable to irradiated material. |
| | Fuel and cladding emissivity (for emissivity sub-models) | - Currently, emissivity tests are performed on unirradiated cladding material, and never performed neither on irradiated material nor on fuel pellets, which may not be necessary. |

TABLE 3. ASSESSMENT OF PIE CAPABILITIES TO SUPPORT WATER-COOLED
REACTOR FUEL MODELLING AND VALIDATION OF FUEL PERFORMANCE PROCESSES
(CONT.)

| Model (performance process) | Related experimental data required for the validation of the fuel model | Member States' practice to provide required experimental data |
|---|---|---|
| Heat transfer between clad and coolant | Bulk coolant temperature and either cladding outer surface temperature or clad-to-coolant convection heat transfer coefficient | - Heat transfer coefficient can be determined with the outer surface temperature and the bulk temperature and the heat flux.<br>- Thermal conductivities of oxide and crud built on the out surface of the cladding can be measured. (There is no need to account for irradiation effect on these measurements.) |
| Thermal expansion of fuel | Fuel stack diameter, length or volume change during power increase or decrease | - Fuel stack's dimensional change can be measured with use of instrumentation during irradiation, or with use of profilometry at PIE. |
| | Fuel thermal expansion coefficient (for thermal expansion coefficient sub-model) | - Thermal expansion coefficient can be deduced from length and volume changes of the instrumented fuel rod. |
| Thermal expansion of cladding | Cladding diameter, length or volume change during power increase or decrease | - The dimensional changes can be measured using dilatometer. |
| | Clad thermal expansion coefficient (for thermal expansion coefficient sub-model) | - Thermal expansion coefficient can be deduced from measured dimensional changes of the cladding. |
| Fuel creep | Fuel creep rate (for creep rate sub-model) | - Fuel creep rate can be deduced from three- or four-point bending tests or compression tests.<br>- Small scale mechanical testing techniques, such as micro cantilever testing and nanoindentation, to measure the elastic and creep properties of $UO_2$ are being developed in some countries. |
| Cladding creep | Clad creep rate (for creep rate sub-model) | - Use of profilometry. |
| Fuel elasticity | Fuel elastic moduli (for elastic moduli sub-model) | - Fuel elastic modulus can be determined from compression tests.<br>- Small scale mechanical testing techniques, such as micro cantilever testing and nanoindentation, to measure the elastic and creep properties of $UO_2$ are being developed in some countries. |
| Cladding elasticity | Clad elastic moduli (for elastic moduli sub-model) | - Clad elastic modulus can be determined from uniaxial tests.<br>- Expanding plug test method has been developed and applied for PIE in some countries. |
| Cladding plasticity | Effects of temperature and irradiation on clad yield stress (for yield stress sub-model) | - Clad yield stress can be determined by tensile tests. |

TABLE 3. ASSESSMENT OF PIE CAPABILITIES TO SUPPORT WATER-COOLED REACTOR FUEL MODELLING AND VALIDATION OF FUEL PERFORMANCE PROCESSES (CONT.)

| Model (performance process) | Related experimental data required for the validation of the fuel model | Member States' practice to provide required experimental data |
|---|---|---|
| | Clad instantaneous plasticity (for instantaneous plasticity sub-model) | - Clad instantaneous plasticity can be determined by tensile tests. |
| | Clad ultimate tensile stress, failure stress or failure strain (for relevant sub-model) | - Clad ultimate tensile stress can be determined by tensile tests. |
| Cladding fatigue | Number of cycles to failure as a function of amplitude of clad stress variations | - Fatigue tests have been performed on unirradiated cladding specimens by applying a cyclic pressure to the cladding specimen so that the hoop stress as a function of cycle can be determined.<br>- The same test technique can be applied on irradiated cladding specimen. |
| Cladding phase changes | Phase transformation temperature / fraction of material in $\beta$-phase (for material property sub-model) | - Cladding phase transformation temperatures can be determined using XRD. |
| | Oxygen diffusion coefficient in clad (for diffusion coefficient sub-model) | - Using thermogravimetric analysis (TGA), weight changes as a function of time can be determined, and hence oxygen diffusion coefficient can be deduced.<br>- There have been few applications of TGA measurements on irradiated material. |
| Fuel melting | Fuel melting temperature (for melting temperature sub-model) | - Differential scanning calorimeter (DSC) is used to determine the fuel melting temperature.<br>- There have been few applications of DSC measurements on irradiated material. |
| Cladding melting | Clad melting temperature (for melting temperature sub-model) | - DSC is used to determine the clad melting temperature.<br>- There have been few applications of DSC measurements on irradiated material. |
| Cladding hardening | As per cladding creep and cladding plasticity | - Cladding hardening can be determined by applying tensile tests.<br>- There have been a few applications of tensile testing on irradiated cladding. |
| Cladding embrittlement | Ductile-to-brittle transition temperature (for DBTT sub-model) | - Ring compression (RC) tests with heating can be applied to determine the DBTT.<br>- There have been a few applications of RC testing on irradiated cladding. |
| | Hydrogen diffusion coefficient in clad (for diffusion coefficient sub-model) | - Coulometric Titration (CT) measurements can be applied for hydrogen charging and diffusion on cladding.<br>- There have been a few applications of CT measurements on irradiated cladding. |

TABLE 3. ASSESSMENT OF PIE CAPABILITIES TO SUPPORT WATER-COOLED
REACTOR FUEL MODELLING AND VALIDATION OF FUEL PERFORMANCE PROCESSES
(CONT.)

| Model (performance process) | Related experimental data required for the validation of the fuel model | Member States' practice to provide required experimental data |
|---|---|---|
| | Hydride precipitation and dissolution temperatures | - The hydride dissolution temperature of the Zircaloy-4 cladding can be determined by DSC.<br>- There have been a few applications of DSC on irradiated cladding. |
| Cladding axial growth | Elongation of irradiated cladding tubes (either unfuelled or with no pellet-clad mechanical interaction) | - Axial tensile tests can be applied.<br>- There have been few applications of axial tensile testing on irradiated cladding.<br>- Axial tensile tests are not applicable to ceramic cladding that is developed as an ATF concept. |
| Radial power distribution in fuel pellets | Radial concentration profiles of solid fission products, actinides and burnable absorber elements (or their isotopes), in particular Nd, Pu and Gd | - Radial distribution of solid fission product, actinide and burnable absorber elements can be determined using gamma tomography, SEM/EDS/WDS, EPMA, TEM. |
| Fission gas generation | Nuclear data for Xe and Kr isotopic fission yields, decay constants and neutron capture cross-sections | - Fission yield can be determined using mass spectroscopy, decay constant can be determined using gamma spectroscopy and neutron capture cross section can be determined using neutron beam and detectors.<br>- A few PIE facilities have expertise on measuring fission yields and decay constants. |
| Fission gas release (from fuel to rod free volume) | Rod free volume Xe and Kr contents | - Rod puncture and chemical analysis (i.e., mass spectroscopy). |
| | Radial distributions of Xe and Kr concentrations in fuel pellet | - Electron probe microanalyzer (EPMA) has been used to measure the radial distribution of fission gases. |
| | Xe and Kr (volume) diffusion coefficients in fuel pellet (for diffusion coefficients sub-model) | - No information provided. |
| | Partial pressures of Xe and Kr in as-manufactured pores | - Out-of-reactor post irradiation annealing tests can be performed. CNL has capabilities. |
| | Fission fragment range in fuel pellet | - XCT analysis.<br>- A few PIE facilities have performed XCT on irradiated material. |

TABLE 3. ASSESSMENT OF PIE CAPABILITIES TO SUPPORT WATER-COOLED
REACTOR FUEL MODELLING AND VALIDATION OF FUEL PERFORMANCE PROCESSES
(CONT.)

| Model (performance process) | Related experimental data required for the validation of the fuel model | Member States' practice to provide required experimental data |
|---|---|---|
| Helium generation | Nuclear data for He fission yields, $^{16}$O neutron capture cross-section, and decay constants and cross-sections associated with generation and α-decay of the transuranic isotopes (principally $^{238}$Pu, $^{242}$Cm and $^{244}$Cm) | - Can be measured using TGA-MS. |
| Helium release (from fuel to rod free volume) | Rod free volume He content | - No information provided. |
| | Radial distribution of Helium concentration in fuel pellet | - No information provided. |
| | He (volume) diffusion coefficient in fuel pellet (for diffusion coefficient sub-model) | - No information provided. |
| | Partial pressure of He in as-manufactured pores | - No information provided. |
| | Helium solubility in fuel pellet | - No information provided. |
| Fuel densification | Decrease in fuel stack diameter, length or volume (taking into account the effects of fuel swelling and thermal expansion) | - Fuel stack length is measured using gamma scanning. |
| | Decrease in pore size and/or concentration with burnup | - Use of microscopy. |
| Fuel pellet swelling | Increase in fuel stack diameter, length or volume (taking into account the effects of fuel densification, gas bubble swelling and thermal expansion) | - Can be determined during irradiation test and PIE via microscopy. |
| | Nuclear data for elemental fission yields (mechanistic models only) | - Can be determined via isotopic and microscopy PIE. |

TABLE 3. ASSESSMENT OF PIE CAPABILITIES TO SUPPORT WATER-COOLED
REACTOR FUEL MODELLING AND VALIDATION OF FUEL PERFORMANCE PROCESSES
(CONT.)

| Model (performance process) | Related experimental data required for the validation of the fuel model | Member States' practice to provide required experimental data |
|---|---|---|
| | Gibbs free energies of various fission product compounds (mechanistic models only) | - Can be determined via TGA/DSC at PIE. |
| | Destruction rates of fission product compounds due to radiolysis and fission fragments (mechanistic models only) | - No information provided. |
| | Densities of various fission product phases (mechanistic models only) | - No information provided. |
| | Occupation sites of fission product atoms in solution and the associated lattice parameter changes (mechanistic models only) | - Use of XRD. |
| Fuel gas bubble swelling | Increase in fuel stack diameter, length or volume (taking into account the effects of fuel densification, matrix swelling and thermal expansion) | - Can be determined during irradiation test and PIE via microscopy. |
| | Radial distributions of intra-granular bubble concentration, radius and pressure | - Can be determined via microscopy and elemental analysis PIE, i.e., SEM/EDS/WDS/EPMA/APT/TEM/SIMS/EELS. |
| | Morphology, volume, areal density and pressure of grain face bubbles, and their variation across the fuel pellet radius | - Can be determined via microscopy and elemental analysis PIE, i.e., SEM/EDS/WDS/EPMA/APT/TEM/SIMS/EELS. |
| | Morphology, volume, linear density and pressure of grain edge bubbles, and their variation across the fuel radius | - Can be determined via microscopy and elemental analysis PIE, i.e., SEM/EDS/WDS/EPMA/APT/TEM/SIMS/EELS. |

TABLE 3. ASSESSMENT OF PIE CAPABILITIES TO SUPPORT WATER-COOLED REACTOR FUEL MODELLING AND VALIDATION OF FUEL PERFORMANCE PROCESSES (CONT.)

| Model (performance process) | Related experimental data required for the validation of the fuel model | Member States' practice to provide required experimental data |
|---|---|---|
| | Xe and Kr (surface and grain boundary) diffusion coefficients in fuel (for diffusion coefficients sub-model) | - No information provided. |
| | Vacancy (volume, surface and grain boundary) diffusion coefficients in fuel | - No information provided. |
| | Fuel surface energy | - No information provided. |
| | Fuel grain boundary energy | - No information provided. |
| | Dislocation density, and its variation across the fuel radius | - No information provided. |
| Equiaxed grain growth | Mean grain diameters | - Can be determined from images taken using optical microscopy or via microscopy at PIE. |
| Columnar grain growth | Mean grain diameters and aspect ratios | - Grain sizes are determined from images taken, in general, using optical microscopy.<br>- |
| | Mean pore diameters and aspect ratios | - X-ray computed tomography (XCT) can be used. |
| | Pore migration velocities | - No information provided. |
| Fuel restructuring at high burnup | Thicknesses of fully restructured and transition zones | - X-ray computed tomography (XCT) can be used.<br>- A few PIE facilities have applied XCT on irradiated material. |
| | Mean grain diameters and their radial variation | - X-ray computed tomography (XCT) can be used.<br>- A few PIE facilities have applied XCT on irradiated material. |
| | Rim pore concentrations, sizes and pressures and their radial variation | - X-ray computed tomography (XCT) can be used.<br>- A few PIE facilities have applied XCT on irradiated material. |
| | Fission gas release from the high burnup structure (HBS) | - X-ray computed tomography (XCT) can be used.<br>- A few PIE facilities have applied XCT on irradiated material. |
| | Mechanical properties of the HBS | - X-ray computed tomography (XCT) can be used.<br>- A few PIE facilities have applied XCT on irradiated material. |

TABLE 3. ASSESSMENT OF PIE CAPABILITIES TO SUPPORT WATER-COOLED REACTOR FUEL MODELLING AND VALIDATION OF FUEL PERFORMANCE PROCESSES (CONT.)

| Model (performance process) | Related experimental data required for the validation of the fuel model | Member States' practice to provide required experimental data |
|---|---|---|
| Pellet cracking | Images of irradiated fuel (normal operation) | - Determination, via microscopy, particle size analysis such as sieving, and micromechanical tests at PIE. |
| | Fuel fragment size fractions (extensive fragmentation during severe accidents) | - Determination, via microscopy, particle size analysis such as sieving, and micromechanical tests at PIE. |
| | Fuel fracture stress (for fracture stress sub-model) | - Determination, via microscopy, particle size analysis such as sieving, and micromechanical tests at PIE. |
| Fuel fragment relocation | As per heat transfer between fuel and clad (normal operation) | - Hour-glassing and any other strain related deformations of the cladding (caused by cladding interaction with pellet) can be determined using profilometer. |
| | Change in axial distribution of fuel mass, incl. mass of fuel lost through any clad rupture (extensive fragmentation during severe accidents) | - Can be examined using gamma scan. |
| Pellet wheat sheafing | Deformation of non-uniformly heated pellet fragments | - Can be determined separately via heating test or via gamma scanning and metallography. |
| Clad ridging | Deformation of cladding at pellet-pellet interfaces, especially during and after power ramping | - Can be determined via profilometry. |
| Axial extrusion of fuel | Extent of pellet dish filling | - Can be determined via microscopy or gamma scan. |
| Fuel-clad bonding | Images of bonded fuel pellet and clad | - Can be determined via microscopy. |
| | Chemical analysis of bonding layer | - Can be determined via microscopy. |
| | Oxygen diffusion coefficient in fuel pellet (for diffusion coefficient sub-model) | - Can be determined via microscopy. |

TABLE 3. ASSESSMENT OF PIE CAPABILITIES TO SUPPORT WATER-COOLED
REACTOR FUEL MODELLING AND VALIDATION OF FUEL PERFORMANCE PROCESSES
(CONT.)

| Model (performance process) | Related experimental data required for the validation of the fuel model | Member States' practice to provide required experimental data |
|---|---|---|
| Stress-corrosion cracking (SCC) of clad | SCC failure statistics as a function of clad stress, time-at-stress and corrosive species (principally free iodine) concentrations | - Optical microscopy and eddy current are generally applied.<br>- INL has Iodine-assisted SCC cell to perform such work at LWR conditions. |
| Cladding inner wall oxidation | Inner wall oxide thickness | - Via metallography at PIE. |
| Cladding outer wall oxidation | Outer wall oxide thickness | - Via eddy current and metallography at PIE. |

TABLE 4. ASSESSMENT OF PIE CAPABILITIES TO SUPPORT WATER-COOLED
REACTOR FUEL MODELLING AND VALIDATION OF CODES' OUTPUT PARAMETERS

| Model (output parameters) | Related experimental data required for the validation of the fuel model | Member States' practice to provide required experimental data |
|---|---|---|
| Rod pressurization (primarily due to fuel and clad dimensional changes, fission gas and helium release and gas temperature effects) | Rod internal pressure | - Rod puncture is generally applied.<br>- Rod pressure can be measured during irradiation test, which is not applicable to ceramic fuel cladding concept. |
| Fuel elongation (primarily due to fuel thermal expansion, densification and swelling, together with fuel elasticity and creep when there is fuel-clad contact) | Fuel stack length | - Difficult to measure in-cell, do not have ability to measure stack length; images near endcap weld closures/end pellets may indicate potential interaction between endcap and end pellet.<br>- Gamma scanning can be used to determine the fuel stack length though limited with the length of a fuel rod.<br>- Fuel elongation can be measured during irradiation test, which is not applicable to ceramic fuel cladding concept. |
| Clad elongation (primarily due to clad thermal expansion and axial growth, together with clad creep, plasticity and elasticity when there is fuel-clad contact) | Cladding elongation | - Linear variable differential transformer (LVDT) is used for length measurements, which is not applicable to ceramic fuel cladding concept. |

TABLE 4. ASSESSMENT OF PIE CAPABILITIES TO SUPPORT WATER-COOLED REACTOR FUEL MODELLING AND VALIDATION OF CODES' OUTPUT PARAMETERS (CONT.)

| Model (output parameters) | Related experimental data required for the validation of the fuel model | Member States' practice to provide required experimental data |
|---|---|---|
| Fuel radial deformation (primarily due to fuel thermal expansion, densification and swelling, together with fuel elasticity and creep when there is fuel-clad contact) | Fuel pellet outer diameter | - X-ray Computed Tomography (XCT) can be used.<br>- Few XCT analysis has been performed on irradiated material. |
| Clad radial deformation (primarily due to clad thermal expansion and creep, together with clad creep, plasticity and elasticity when there is fuel-clad contact) | Cladding outer diameter | - Profilometer can be used.<br>- Clad radial deformation also can be measured during irradiation test. |
| Fuel-to-coolant heat transfer (primarily due to conduction through pellets, conduction, convection and radiation across the fuel-clad gap, conduction through the clad, and convection between the clad and coolant) | Fuel centreline temperature | - Film heat transfer coefficient can be deduced from measured fuel cladding and coolant temperatures during irradiation test. |
| Fuel volume change (primarily due to fuel thermal expansion, densification, swelling and elasticity) | Fuel density | - Immersion density method at PIE can be applied.<br>- Fuel volume changes can be measured during irradiation tests, which is not applicable to ceramic cladding concept. |
| Rod free volume change (due to fuel and clad dimensional changes) | Rod free volume | - Rod free volume is determined from rod puncture. |

## 5.3. PIE CAPABILITIES TO SUPPORT FUEL TECHNOLOGY FOR NON-WATER-COOLED REACTORS

Similar assessments were conducted on non-water innovative reactor fuels. A metallic fuel, U-(Pu)-Zr fuel/HT9 cladding considered for use in sodium-cooled fast reactors and a liquid fuel for molten salt reactor were selected for consideration in this exercise. The assessments were conducted by answering the same questionnaires contained in Tables 3 and 4. The assessment results are summarized as follows:

— For metallic fuel, U-(Pu)-Zr fuel/HT9 clad
- Overall, PIE capabilities for water-cooled reactor fuels are also applicable to the metallic fuel. Deficient areas identified in PIE capabilities for water-cooled reactor fuels (e.g., burnup dependent degradation of properties, bubble kinetics) are also applied to PIE capabilities for sodium-cooled fast reactor fuels, and thus need to be improved;
- Regardless of such PIE capabilities, available experimental data to support for modelling the interim fuel-performance process of the metallic fuel seem not enough compared to available experimental data for water-cooled reactor fuels;
- Experimental datasets for the validation of codes' output parameters seem reasonable available but still needs to be expanded so as to reduce uncertainty levels.

— For the liquid fuel for molten salt reactors
- The description on required experimental data does not appear to conservatively cover all in-reactor fuel performance processes in MSRs, and thus interim fuel-performance processes need to be clearly understood first;
- PIE capabilities developed mainly for water-cooled reactor fuels do not appear to be wholly applicable to MSR fuels.

The PIE requirements and associated techniques to support advanced reactor fuel types are discussed in depth in Section 6.

# 6. PIE REQUIREMENTS FOR SUPPORTING INNOVATIVE FUEL DEVELOPMENTS

## 6.1. BACKGROUND

The development of PIE techniques for new/innovative fuel designs is essential for the qualification and ongoing surveillance of advanced reactor fuel and in-core materials. During fuel and fuel assembly manufacturing stages it is important to track the behaviour of certain fabrication parameters that may be relevant during PIE. During reactor operation, reactor diagnostic data obtained using a variety of passive or active sampling and analysis methods [19] also provides information useful during PIE. The data is provided to modellers, analysts and fuel designers and reactor operators in order to gain a better understanding into the in-reactor behaviour of a given fuel or material. The specific PIE requirements for a particular fuel or material may play a role in overall fuel assembly or reactor design with respect to the location and number of instrumentation and sampling lines, detectors, probes and other analytical laboratory needs to ensure useful fuel performance data can be obtained during operation. Depending on the reactor and fuel design, underwater handling, disassembly and NDE inspection capabilities for in-reactor fuel and material components may be required at a reactor site, prior to disassembly and shipment of a portion of fuel assembly for further hot cell examinations.

When possible, PIE techniques and toolsets are developed to allow for the study of more than one fuel type, where only minor variations in sample preparation or minor tooling modification required (such as differences in fuel microstructure etchant formulas between ceramic $UO_2$ and thoria fuels). An example of a highly utilized 'technology agnostic' PIE technique is optical microscopy which can be applied to multiple fuel types, although in many circumstances, different sample preparation techniques may be warranted. In some cases, transition from one fuel type to another may be more difficult, such as the case where inert hot cell atmospheres and sample polishing media may be required for examination of certain molten salt fuel types to avoid corrosion/degradation of the examination surface. Regardless of the PIE technique(s) utilized, sample preparation, size, and handling play a key role in the development of PIE techniques and related toolsets and need to be developed in parallel with fuel technology-specific tooling and equipment development.

Similar to conventional fuel types, the scope of PIE work for advanced fuels needs to be tailored to obtain the necessary irradiation data based on a fuel's pre-determined fuel performance parameters and most probable failure mechanisms, to provide a comprehensive assessment of a fuel's in-reactor behaviour.

## 6.2. PIE REQUIREMENTS FOR SUPPORTING THE DEVELOPMENT OF ADVANCED REACTOR FUEL TYPES

The majority of fuel types and in-core materials require examination and analyses before and after operation, and during storage and waste management. Although this section focuses predominantly on PIE of advanced fuel for SMR and similar advanced reactor applications, it is acknowledged that PIE techniques can be applied to the study of radioactive materials for a number of other applications (e.g., isotope extraction, study corium studies, material harvesting and examination for decommissioning and waste management studies, etc.).

Each fuel type can require a different scope of PIE, depending on the fuel design and the overall objectives of PIE.

Presently there exist more than 70 SMR design concepts [20] available worldwide, which can be classified into five general categories (Table 5):

— High-temperature gas-cooled reactor (HTGR);
— Molten salt-cooled reactor (MSR);
— Water-cooled reactor (WCR);
— Liquid metal-cooled fast reactor (LMFR); and
— Micro modular reactor (MMR).

Fuel and cladding materials for reactor fuel types are presented in Table 5, where Canadian SMR fuels are shown as example. Based on the information in Table 5, it is reasonable to assume that each fuel type will have different PIE requirements, and thus different approaches to sample preparation and what PIE techniques to use.

TABLE 5. CURRENT SMR FUEL AND CLADDING TYPES CONSIDERED FOR DEPLOYMENT

| Reactor Type | Examples (taken from Canadian SMRs submitted to the Canadian regulatory body) | | |
| --- | --- | --- | --- |
| | Fuel | Cladding/structural components | Coolant |
| High-temperature gas-cooled reactor (including MMR) | TRISO particles or fully ceramic microencapsulated (FCM) particles; high-assay low enriched uranium (HALEU) or UCO | SiC or graphite | Helium gas |
| Molten salt-cooled reactor | Fuel salt – $UO_2$ fuel with $CrO_2$ dopant; enrichments less than 5 wt.% $^{235}U$ | N/A (fuel dissolved in coolant salt), stainless steel reactor vessel; Alloy HT91 tubing NIMONIC PE-16 (Ni-Fe-Cr-Mo-Al-Ti Alloy); M5 Alloy; | Fluoride salts (KF and NaF) |
| Water-cooled reactor | $UO_2$ pellet; enrichments less than 5 wt.% $^{235}U$<br><br>Metallic uranium; enrichments less than 20 wt.% research reactor dispersion fuels (U-Si, U-$Al_x$, U-Mo) | Zr based alloys or coated cladding; | $H_2O$, $D_2O$ |
| Liquid metal-cooled reactor | U-10%Zr; 13.1 wt.% $^{235}U$ | HT9 stainless steel (12Cr, 1Mo) | Liquid Na |
| | TRISO particles; HALEU fuel | Zirconium hydride | Liquid Na |
| | $UO_2$ pellet; enrichments less than 20 wt.% $^{235}U$ | 12R72 stainless steel with Fe-10Cr-6Al-RE coating | Lead |

## 6.3. TRI-STRUCTURAL ISOTROPIC (TRISO) FUELS

Modern TRISO fuel is an emergent fuel technology considered for deployment in advanced reactor designs. This fuel design has evolved from a microsphere concept with refractory coatings to contain fission products (FPs) during operation in HTGRs, developed during the initial stages of the UK Dragon Project in the 1950s [21]. The earliest version contained only a fuel kernel and a single coated pyrolytic carbon layer intended to protect the kernel during fabrication. Concern regarding the potential fracture of the pyrolytic carbon led to the development of tri-structural isotropic coatings in the 1960s in the UK and the US that included a metallic carbide layer in between pyrolytic carbon layers [22]. In the following decades, extensive studies on the irradiation performance and safety of TRISO fuel were carried out in the US, Japan, UK, Germany and Europe [21, 22]. The performance of German TRISO fuels in the 1980s was considered superior to US TRISO fuels in terms of the release to birth ratio (R/B) of $^{85}$Kr, which is a measure of fission gas released to that generated (a high R/B can indicate either a significant fission gas release from a small number of TRISO particles, or small amounts of fission gas release from many TRISO particles). In 2004, the US launched the Advanced Gas Reactor (AGR) TRISO Fuel Development and Qualification Program to improve the fabrication and performance of TRISO fuels [19]; the fuel fabricated for AGR program was based on modifications from the historic German TRISO fuels [23]; a significant number of irradiation tests and PIE were performed on these fuels.

The 'international consensus' TRISO fuel particle consists of a uranium-based kernel enriched up to <20wt.% $^{235}$U in total U, as either $UO_2$ or UCO (a heterogeneous mixture of uranium oxide and uranium carbide) with a diameter in the range of $350 – 600\mu m$ [24]. The kernel is surrounded by four different coating layers, including (from inside out): a porous pyrolytic carbon buffer layer (about 50% of theoretical density), a dense and highly isotropic inner pyrolytic carbon layer (IPyC), a SiC layer, and an outer pyrolytic carbon layer (OPyC), as illustrated in Fig. 24.
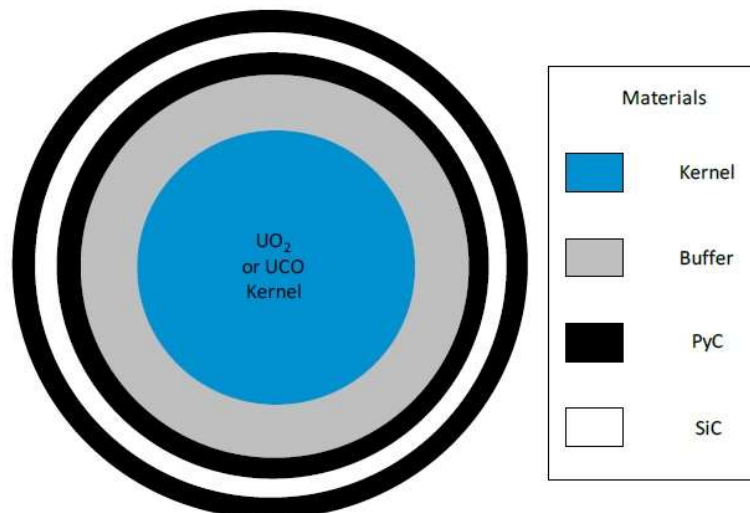


*FIG. 24. International-consensus TRISO particle design*

In addition to retaining fission products (the main function of the TRISO layers), each layer also has a specific function. The first layer (buffer carbon layer) provides a void space for fission gas collection from the kernel and accommodates fuel kernel dimensional changes. The IPyC

layer acts as a seal layer to protect the kernel from the HCl by-product of SiC layer deposition and provides a deposition surface for the SiC layer. The SiC layer provides the main structural strength of the particle and is the primary barrier to the release of non-gaseous fission products not sufficiently retained by pyrolytic carbon or within the kernel itself. Finally, the outer pyrolytic carbon layer (OPyC), with properties similar to the IPyC layer, protects the SiC layer during handling and acts as a surface for bonding to the graphitic fuel matrix. The coating system makes TRISO fuel a robust fuel suited for long-term fuel residency periods.

PIE of TRISO fuels has previously been carried out to assess the performance of fission product retention of the coated layers and to improve understanding of the mechanisms of structural integrity failure. In recent years, comprehensive multi-scale PIE activities on TRISO fuels were carried out in the US, mainly at INL and ORNL in support of advanced fuel development, including assessment of TRISO fuel performance factors associated with:

— Trapping/escape of FPs from TRISO fuel spheres during safety tests;
— Diffusion of non-gaseous FPs into surrounding coating layers;
— Dimensional analysis and damage in TRISO fuel spheres;
— Determining fuel burn-up during irradiation experiments;
— Fission product analyses during safety testing.

Most safety-related testing has been out-of-core or post-irradiation safety tests [25–32]. Out-reactor safety tests are designed to simulate a high-temperature condition during a loss-of-coolant accident and performed by heating irradiated TRISO coated fuel compacts (each compact containing thousands of TRISO particles) to elevated temperatures (1500–1800°C) and monitoring the release of FPs when held at these temperatures. FP analysis of following testing is a common PIE activity [21,22,25–32]. The release of FPs is an indicator of coating layer integrity, where the rapid release of gaseous FPs such as $^{85}$Kr suggest failure of all three coating layers (IPyC/SiC/OPyC). The release of $^{134}$Cs and $^{137}$Cs suggests a defective SiC layer, since the pyrolytic carbon layer does not retain Cs. Some mobile metallic isotopes such as $^{90}$Sr and $^{154}$Eu may be detected even with intact coating layers.

KüFA (from the German Kühlfinger apparatur, i.e., 'cold finger device') is a German safety test facility for spherical fuel elements that commenced operation in the early 1980s [32]. The system consists of a double-walled, water-cooled metal jacketed furnace with tantalum electrical-resistance heating elements (maximum temperature of 1800°C), tantalum hot zone components, and a water-cooled cold finger that holds an exchangeable metal plate to condense fission products during operation. The cold finger can be removed from the facility for gamma spectroscopy or acid leaching and radio-chemical analysis. Fission gasses in the sweep gas circuit are captured in two charcoal cryo-traps, with the second trap providing data on the trapping efficiency of the first trap. The activity in the traps is monitored continuously via NaI detectors during a heating test. The facility is accommodated inside a hot cell.

Two similar safety testing facilities were built in the US as well: the first being the Fuel Accident Condition Simulator (FACS) at INL and the other Core Conduction Cooldown Test Facility (CCCTF) at ORNL. Both facilities have a standard holder that can accommodate a 12.5mm diameter cylindrical fuel compact and has been used to test numerous fuel compacts for AGR-1 and AGR-2 irradiation experiments. The results of the safety tests from AGR-1 and AGR-2 programs are extensively available in the literature [32–35].

The FACS at INL is heated with a graphite resistance element and has a maximum temperature of 2000°C. The samples are held by a tantalum holder inserted from the bottom of the furnace. A Type C (W-Re) thermocouple to monitor fuel temperature is housed within the tantalum tube that supports the sample holder. A tantalum flow tube is used to separate the specimen and the heating element. A water-cooled aluminium cold finger holds a 35mm exchangeable condensation plate. The entire condensate plate exchange operation is automated. A Type J thermocouple is used to monitor the temperature of the cold finger. Helium sweep gas is introduced from the bottom and injected into the hot zone beneath the specimen and flows toward the condensation plate at the end of the cold finger. The helium is then swept from the furnace through particulate and moisture filters and carried to the fission gas monitoring system for analysis of $^{85}$Kr, $^{133}$Xe, or other radioactive noble gases. The gas monitoring system located outside of the hot-cell consists of dual liquid nitrogen-cooled charcoal traps to contain the noble gases. Condensation plates periodically removed from the furnace during operation are gamma counted to quantify gamma-emitting fission products (e.g., $^{137}$Cs, $^{110m}$Ag, $^{154}$Eu, $^{90}$Sr).

The CCCTF at ORNL bears many similarities with FACS in terms of facility design and functionality [36,37]. In addition to condensation plate (FACS) or deposition cup (CCCFT) components, the furnace internal components may also be removed after the completion of safety tests for fission product analysis to assess the collection efficiency of the condensation plate or deposition cup [38].

High temperature testing was also performed in Japan. Fukuda et al. [26] reported heating irradiated TRISO coated fuel up to 2400°C using a furnace installed in a hot-cell. The metallic fission products were collected by a graphite sleeve surrounding the graphite electrode where the fuel particles are situated. The experimental results revealed that the fuel failure began at 2200°C and almost 100% of particles failed at 2400°C.

The FPs can also be monitored during the in-core irradiation testing. Fukuda et al. [26] reported in-pile monitoring of FP gasses ($^{88}$Kr) by measuring the fission gas concentration in the primary loop of the OGL (Oarai Gas Loop) within an in-core gas loop installed JMTR (Japan Material Testing Reactor). In-core measuring of FP gasses can also be done by inserting a gas swept capsule into the fuel zone of JMTR core, which can achieve higher burnups. Collin et al. [29] reported in-pile measuring of released gaseous fission products (Kr and Xenon isotopes) throughout the AGR-3/4 irradiation, using the Fission Product Monitoring System (FPMS) developed at INL. Although in-pile safety tests provided insightful data supporting the design, safety analysis and licensing of HTGRs, they are out of scope PIE activity. A comprehensive review of other in-pile safety tests was summarized by Brown [39].

### 6.3.1. Deconsolidation-leach-burn-leach (DLBL) process

Gaseous FPs and volatile metallic FPs that can escape from fuel compacts during safety tests at elevated temperatures may be collected, monitored and analyzed by the methods mentioned above. However, a fraction of FPs species (such as isotopes of Ag, Pd, Sr, Mo, Ru, and Eu) may be located outside the SiC layer but still retained within the OPyC layer or the graphite matrix of fuel compact. A 'deconsolidation-leach-burn-leach' (DLBL) process is commonly used [26,27,37] to analyze such FPs. DLBL involves a multiple-step chemical actinide and FP extraction process of those retained in the OPyC layer and the graphite matrix. Figure 25 shows the flow chart for the DLBL process. A detailed description of the process was provided by Baldwin et al. [33] and a brief description of the process is provided below.
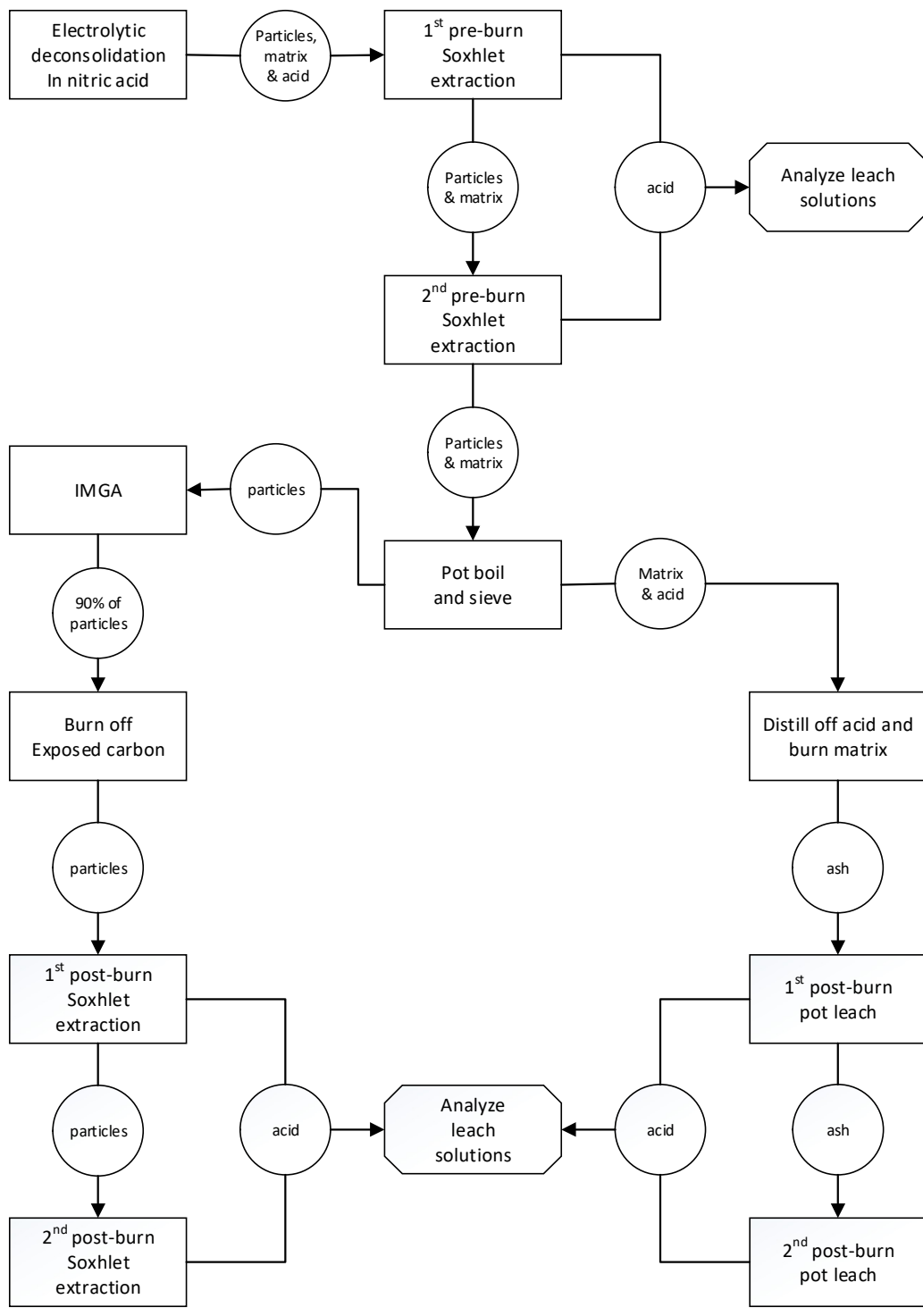
*FIG. 25. Flow Chart for the DLBL extraction process*

There are four main steps involved in the DLBL process.

The first phase (deconsolidation) requires breaking up of the cylindrical fuel compact into small pieces by applying a 0.6A current through the length of the compact with the bottom of the compact submersed in nitric acid. The residue (matrix and particles) of the deconsolidated fuel

compact is collected by a Soxhlet extraction thimble and placed into a Soxhlet extraction apparatus for the second phase of the process (leaching). The residues are leached twice by nitric acid, each for 24 hours. The acid consists of dissolved fission products and actinides that are analyzed via beta/gamma and mass spectrometry. After two pre-burn extractions the particle and the matrix residue are boiled in concentrated nitric acid for another 24 h, the purpose being to further remove the particle layers and any process debris from the fuel particles. The particles are then separated from the acid and matrix by pouring the slurry through a 500-micron mesh sized stainless sieve.

The third phase (burn) is performed separately for the particle and matrix residue prior to burning, the nitric acid is removed from the matrix by distillation. The dried matrix residue is then burnt in a box furnace at 750°C in air for 96h. The ash is collected for the fourth post-burn phase (leach) in boiling concentrated nitric acid (twice, each for 24h). The particles are transferred to an Irradiated Microsphere Gamma Analyzer (IMGA) for further analysis prior to burning. The particles are then burnt and leached in the same manner as the matrix materials. Only the OPyC layer of the particles is burnt. The leach solution is then used for the same analysis as the pre-burn leach solution.

### 6.3.2. Microstructural characterization of TRISO particles

Fission products (FPs) collected and analyzed during the testing and analysis described above provides useful information regarding the integrity of the coating layers of the TRISO particles and overall FP retention performance. However, analysis of FPs that escaped the kernel but are trapped in the buffer, IPyC and SiC layers are not determined, and further insight into the morphology and possible defect mechanisms of the fuel kernels and coating layers is not obtained. Therefore, optical microscopy techniques are utilized to characterize the evolution fuel and coating microstructures and study FP distribution within the SiC, IPyC and buffer layers following irradiations and out-reactor safety tests. Several characterization techniques have been employed to obtain microstructural information, including:

#### 6.3.2.1. Ceramography

Ceramography is a technique involving the preparation, examination, and evaluation of ceramic microstructures. Similar to conventional metallic or ceramic $UO_2$ fuel rods, sample preparation involves fuel compact sectioning, sample mounting, sequential grinding, polishing and/or etching steps. Extra caution needs to be taken to reduce damage or pull-out of TRISO particles or coating layers during sample preparation (i.e., grinding, polishing and/or etching). A detailed description of ceramographic sample preparation was given by Ploger et al. [40]. As shown in Fig.26, the fuel kernel and surrounding coating layers are clearly visible in a well-prepared sample (performed with an optical microscope with a lateral resolution up to 1 μm). This technique is commonly used to investigate such phenomena such as: cracking of the carbon-based matrix, kernel deformation and porosity, buffer layer degradation, SiC layer corrosion, fractures or delamination of the TRISO layers and, and any deleterious interactions between the matrix and OPyC layer [25,32,40–42]. To correlate the irradiated microstructure of TRISO particles and the release of fission products, ceramography can also be performed on epoxy-mounted groups of loose particles obtained after compact deconsolidation and screened by IMGA [43].

#### 6.3.2.2. X-Ray projection radiography/tomography.

The structure inside the irradiated TRISO particles can be non-destructively observed using X-Ray projection radiography or X-Ray tomography: X-Ray radiography provides a projection view of the structure within the 3-dimensional (3D) TRISO particles. By systematically obtaining a series of images taken at different tilting angles, the 3D structure within the irradiated TRISO particle can be computationally reconstructed, a process termed X-Ray tomography. Particles deconsolidated from fuel compacts can be directly used for X-Ray radiography without needing further sample preparation work. The fuel kernel, buffer layer, PyC layers, and SiC all have different densities, thus the kernel and the surrounding layers can be easily differentiated with X-Ray radiography as shown in Fig.26. X-Ray radiography can be performed in the hot-cells or outside the hot-cells using a shielded container [36]. X-Ray radiography has been widely used to detect the morphological change of coating layers and the kernel, such as cracking or fracture of the coating layers [21,28], corrosion of SiC layers [25], protrusion of Kernel [33], de-bonding at the interfaces [44] and porosity in the carbon layers [45]. However, the porosity of the kernel cannot be probed using X-Rays due to negligible transmission of X-Ray through the kernel. X-Ray radiography can also probe fission product accumulation in the SiC layer or the interface of SiC and IPyC [32]. Non-destructive X-Ray 3D tomography also provides guidance on sample sectioning for higher-resolution analysis such as SEM and TEM [25].
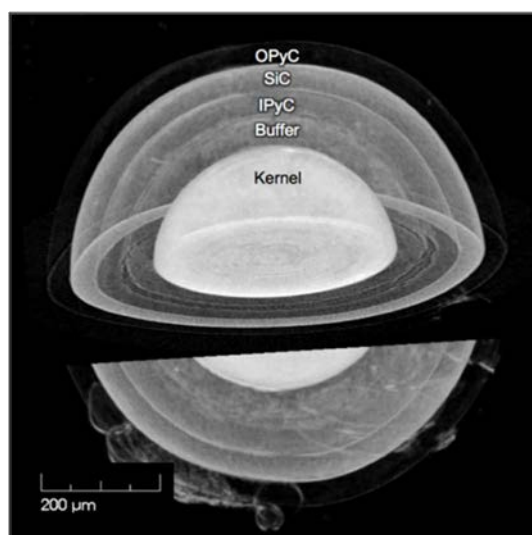


*FIG. 26. X-Ray Tomography of an irradiated TRISO particle (courtesy of INL)*

### 6.3.2.3. Modern scanning electron microscopy (SEM)

This technique has played an important role in recent PIE activities for AGR programs in the US: SEM directs electron beam on the sample surface, generating distinct types of electrons or characteristic X-Rays which can be probed by different types of detectors, providing information pertaining to morphology, phase distribution, elemental segregation, and crystal orientation. SEM provides a lateral resolution up to a few nm. Secondary electron (SE) imaging is sensitive to surface topography and to some extent phase composition, and backscattered electron (BSE) imaging is sensitive to atomic mass. Hence, a combination of SE and BSE have been applied to investigate structural defects (such as micro-cracks, fracture, interface de-bonding, corrosion attack, kernel deformation) and the distribution of fission products diffused outside of the kernel [25,35,36,40]. X-Ray energy dispersive spectroscopy (EDS) was used to determine fission products in the coating layers [25,43,44,46]. Combining with the FIB

technique, FIB-SEM can destructively obtain the 3D structure of the TRISO particles via repeated sequential imaging/milling. Arregui-Mena and co-workers applied this technique to investigate the interface of SiC and PyC layers and map out the 3D network of pores [47]. In addition, electron backscatter diffraction (EBSD) in SEM can map the orientations of the crystalline components of the TRISO particles such as the SiC layer. With the aid of EBSD, the effect of grain boundary characteristics on CO corrosion and fission product transport were investigated [44,48].

*6.3.2.4.    Transmission electron microscopy (TEM)*

This technique offers higher spatial resolution than SEM, down to the atomic scale: TEM examinations have mainly focused on FP particles in the IPyC and SiC layers and the corrosion mechanism specific to the SiC layers. FIB was used to prepare thin lamella from the specific site of interest identified by SEM. TEM examinations on TRISO particles for the AGR-1 program [43,46] indicated that nano-scale Pd-enriched precipitates are preferentially located at the grain boundaries of the SiC layer. EDS results showed U, Pu, Si and Zr are also found in the Pd-rich precipitates. TEM Selected Area Diffraction showed the precipitates have a structure similar as $Upd_2Si_2$. Nano-sized Ag particles without Pd were also identified. Additional TEM work on TRISO particles for the AGR-2 program [44] indicated that O leads the reaction front during CO corrosion of the SiC along the grain boundary. Nano-sized cavities that cannot be observed with other commonly used techniques can be observed with a TEM [49]. Overall, TEM examinations provided a deeper understanding of the fission product transport and the CO corrosion mechanism.

## 6.3.3.  Fuel burnup determination

Fuel burnup is a measure of how much energy is extracted from a nuclear fuel source. It is measured as the fraction of fuel atoms that underwent fission in %FIMA (fissions per initial metal atom). It can be converted to the actual energy released per mass of initial fuel in gigawatt-days/metric ton of heavy metal (GWd/t-HM). Fuel burnup can be determined by considering the release-to-birth (R/B) ratio of certain fission products [27–32,50–52]. Chemically measured isotopic abundances are compared to model-calculated data and normalized to the measured data [53]. Isotopic analysis techniques including gamma spectroscopy and mass spectrometry and online monitoring of released FP gasses are used to determine these isotopic ratios. The coupling of a mass spectrometry method with laser ablation to generate the sample gives greater spatial resolution, allowing for the mapping of burnup and isotopic content down to the sub-millimetre scale. The online monitoring of fission products was performed by continuously sweeping inert gas through the TRISO fuel under irradiation and monitoring the effluent gas using high-purity germanium and sodium iodide (NaI) scintillation detectors [54].

## 6.3.4.  Thermo-mechanical properties

During the development of new reactor fuel and materials, computer codes are used to simulate the behaviour of the fuel and materials under reactor operating conditions. These computer codes incorporate thermo-mechanical properties of the fuel and materials.. Understanding the ability to transfer generated heat and monitor potential dimensional and material changes associated fuel operation are critical to accurate modelling of a fuel's performance and demonstrate safe operation within expected parameters, thus meeting relevant regulatory requirements. While TRISO fuel has been well analyzed, the properties of the structures that contains the fuel kernels such the compaction materials under specific operating conditions for

a given reactor design may require further study. Thermal properties such as thermal conductivity, diffusivity, specific heat capacity and the coefficient of thermal expansion ought to be measured under operating and accident conditions/temperatures. Physical and mechanical properties of the compact, such as density, Young's Modulus, tensile strength, hardness, and Poisson's ratio may require study over the expected range of temperatures and conditions.

### 6.3.5. Summary of PIE techniques for TRISO fuel

Table 6 provides a summary of PIE techniques for TRISO fuel discussed above.

TABLE 6. SUMMARY OF PIE TECHNIQUES USED FOR TRISO FUEL

| Technique | Brief Description | Characteristic or Feature Measured |
|---|---|---|
| High-temperature fission product release monitoring system | A system capable of heating irradiated TRISO particles to accident temperatures (1800°C) and monitoring fission products (gaseous or condensable volatile metallic) released by the fuel particles. | Quantity of gaseous and metallic fission products released – indirect measurement of the condition of coating layers of the TRISO particles. |
| Ceramography by optical microscope | Sectioning and sample preparation of fuel compacts to observe TRISO particle cross-sections under an optical microscope or prepare cross-sections of loose particles of interest. | Characterize the conditions of coating layers and the kernel visually. |
| SEM of fuel compact and TRISO particle cross-sections | Sample preparation of fuel compacts or loose particles to observe TRISO particle cross-sections under the SEM | <ul><li>Structural defects in the coating layers and the kernel (cracks, fracture, corrosion attack, degradation interface de-bonding, deformation) and identify the driving mechanisms if possible.</li><li>Distribution of fission products within SiC and layers inward and the chemical composition of the fission products.</li><li>The porosity of the compact matrix and the coating layers and kernel of the TRISO particle.</li><li>Grain structure of SiC layer and other crystalline components.</li></ul> |
| FIB of TRISO particles | It uses a focused ion beam to sequentially mill and image a sample, which can be used for 3D reconstruction. It can also be used to lift out a lamella and thin it to electron transparent thickness. | <ul><li>3D defect structures of coating laser and kernel.</li><li>3D Porosity of compact matrix and the coating layers and kernel of the TRISO particle.</li><li>Make TEM lamella for further examination.</li></ul> |

TABLE 6. SUMMARY OF PIE TECHNIQUES USED FOR TRISO FUEL (CONT.)

| Technique | Brief Description | Characteristic or Feature Measured |
|---|---|---|
| TEM of TRISO particles | Electron diffraction and nano-scale chemical analysis of FIB lamella lifted out from the region of interest determined under SEM | • Determine the chemical composition and crystal structure of nano-sized fission product.<br>• Examine nano-sized cavities in SiC.<br>• Element segregation at SiC grain boundaries, corrosion front and interface. |
| X-Ray radiography or Computed Tomography (XCT) | Non-destructively create a 2D projection view or 3D view of the internal structure of irradiated individual TRISO particles or fuel compact matrix | • Morphological changes of coating layers and the kernel (cracking, fracture, corrosion, and Kernel protrusion).<br>• Porosity of the fuel compact and the carbon layers of the TRSIO particles (not for SiC layer and fuel kernel).<br>• Fission product within coating layers of TRISO particles.<br>• Guidance for further high-resolution examination (SEM and TEM). |
| Deconsolidation-Leach-Burn-Leach (DLBL) process | Using multi-step chemical processing extract any actinides and fission products retained in the OPyC layer and the graphite matrix using nitric acid. | Combined with beta/gamma spectrometry or mass spectrometry to determine solid fission products retained in OPyC and compact matrix. |
| Gamma spectrometry | Analysis of gaseous or solid samples from Fission Product Release or DLBL Process | To determine fuel burnup, and fission product migration/release. |
| Irradiated-microsphere gamma analyzer (IGMA) | Automatically load and sort TRISO particles based on the recorded gamma spectra | Statistically accurate failure fraction measurements for irradiated TRISO particles and screening the failed particles for further analysis. |
| Mass spectrometry | Analysis of gaseous or solid samples from Fission Product Release or DLBL Process | To determine fuel burnup and fission product migration/release. |
| Laser ablation coupled with mass spectrometry (LA-ICP-MS, LA-TOF-MS) | The use of a laser ablation system to generate very localized samples is coupled with a mass spectrometry system to give isotopic composition with greater spatial resolution and less waste generation than the traditional cut and dissolve method of sample preparation | • Destruction of actinides and minor actinides.<br>• Burnup calculations.<br>• Element distribution maps down to sub-millimetre resolution.<br>• Isotopic composition, including radiometric counting. |
| Laser flash analysis apparatus | Thermal diffusivity from ambient temperature up to 1700°C | Irradiated compact thermal conductivity / diffusivity. |

TABLE 6. SUMMARY OF PIE TECHNIQUES USED FOR TRISO FUEL (CONT.)

| Technique | Brief Description | Characteristic or Feature Measured |
|---|---|---|
| Differential scanning calorimeter (DSC) | The difference in the amount of heat required to increase the temperature of a sample and reference is measured as a function of temperature. | irradiated compact specific heat capacity. |
| In-cell dilatometer | Measure the dimension change as a function of temperature | irradiated compact coefficient of thermal expansion. |
| In-cell pycnometry | Measuring density using gas replacement method | Irradiated compact density, porosity. |
| Immersion density | Immerse the solid in liquid to measure the volume and obtain the density | Irradiated compact density. |
| In-cell tension and compression testing | Mechanical tests for materials strength | Irradiated compact Young's modulus, Poisson's ratio. |
| In-cell macro- / micro-mechanical load frames | Mechanical tests for materials strength | Irradiated compact tensile strength. |
| Indenter/nano-indenter for active material | Small scale instrumented hardness test device | Irradiated compact/particle hardness, young's modulus, yield strength. |

## 6.4. MOLTEN SALT FUEL TYPES

In recent years, Molten Salt Reactor (MSR) technology has garnered growing interest [55–57].

In an MSR, the molten salt fuel is continuously circulated through the core. The principal advantages of liquid fuel over solid-fuel-element systems are (1) a high negative temperature coefficient of reactivity, (2) a lack of radiation damage that can limit fuel burnup, (3) the possibility of continuous fission-product removal, (4) the avoidance of the expense of fabricating new fuel elements, and (5) the possibility of adding makeup fuel as needed, which precludes the need for providing excess reactivity [58]. The high negative temperature coefficient and the lack of excess reactivity make possible a reactor, without control rods, which can automatically adjust power in response to changes of the electrical load [58]. The continuous flow of fuel presents a challenge for modern neutron transport and depletion tools designed for analysis of solid-fuel systems where the fission products, actinides, and activated isotopes remain relatively immobile within a fuel rod or assembly [59].

A variety of MSR designs are being investigated, but the basic concepts are similar for all MSR designs, including: the molten salt is used as the coolant only, or is used as both fuel and coolant [60]. In the second case both single-fluid and dual-fluid designs are possible (i.e., in a dual-fluid design one molten salt could contain fissile $^{233}UF_4$ and the fertile salt could contain $ThF_4$) [60]. For reactor operation, the salt (or salts) flow between a critical core and a heat exchanger (or exchangers) that are outside of the core, where heat can be transferred to a steam or closed gas cycle [61]. In this case, the fuel salts consist of a mixture of; fissile material, solvent (diluent), fissile oxidation prevention material, and fission products. Various salt compositions are included in the very large design space for liquid-fuelled MSRs (fluoride and chloride salt mixtures), fertile and fissile materials (thorium, uranium, and plutonium), neutron spectra (fast,

thermal, and intermediate), fuel cycle scenarios (full recycle, partial recycle, and once-through), and fuel salt processing choices (fission gas sparging and rare earth element separations) [58].

Like other advanced reactor concepts, the MSR faces significant challenges in the area of fuel and material qualification due to a combination of high temperature operation, a corrosive environment and intense neutron irradiation. As a result, each MSR design concept is anticipated to have varying testing requirements including a need to examine the fuel salts and related structures following irradiation. Gaps in the knowledge of molten salt behaviour and related examination and testing capabilities has spurred the development of experimental techniques which could provide a better understanding of in-core behaviour of and resulting changes to molten salts.

### 6.4.1. Corrosion effects on core components

Corrosion studies covering a wide range of reactor vessel and other structural materials including stainless, Ni based alloys, fuel cladding, and moderators – SiC graphite and MAX phases [62–66]). Electron microscopy techniques are widely used for corrosion (SEM/EDS [62–67], TEM and FIB [64, 67–69] make up most of the electron-based techniques, but more advanced methods such as 4D scanning TEM (4D STEM) [67] have been utilized.

There are also a variety of elemental/chemical analysis techniques, primarily taking the form of various spectroscopic techniques such as X-ray absorption fine structure (XAFS) spectroscopy and EPMA [62], Raman spectroscopy [61,71], LEAP/APT [69], IR Spectroscopy [69], X-ray photoelectron spectroscopy (XPS) and Electron-Spin Resonance Spectroscopy [65]. Spectrometry in the form of Glow-Discharge MS [65], SIMS [69], and XRD [66,69] have also been used to identify phases and chemistry of samples. Newton et al. [70] used the open circuit potential (OCP) measurements to assess the impact of U and Zr on the redox potential of chloride molten salts.

### 6.4.2. Evolution of salt with irradiation

The analysis of molten salts as they evolve during an irradiation is another field of study that covers a wide range of topics and techniques. Only a small number of recent papers with a focusing on the evolution of salts themselves were found (discussed below); a more in-depth literature review that examines PIE activities associated with molten salt evolution during/following irradiation may be warranted.

Kral and co-workers [72] used high-purity germanium (HPGe) detectors to assess the build-up of activation in a NaCl salt using an accelerator-driven system focused on a neutron spallation target. Although this study did not look at fuel-bearing salts, the principles are applicable. Zhou et al. [73] also used high-purity germanium (HPGe) detectors to assess FP build-up in irradiated U and Th bearing fluoride salts as part of a study looking at evaporation in irradiated salts. Inductively coupled mass spectrometry was used to further characterise evaporated and condensed salts.

Ramos-Ballesteros et al. [74] used two spectroscopy techniques (diffuse reflectance spectrometry and electron paramagnetic resonance spectroscopy) to assess defects in chloride salts that were introduced via gamma irradiation. Hania and co-workers [75] provide plans for a PIE study of Th bearing fluoride salts in graphite crucibles, including the use of differential scanning calorimetry, mass spectrometry, electron microscopy, XRD and light optical microscopy to analyse the salts and graphite cubicles.

Martin and co-workers [76] used several methods to discern the viscosity of molten salts, including a laser flash thermal conductivity measurement and DSC to analyse the thermal properties of the salts. Mancey [77] published a comprehensive review of molten-salt loops planned for materials testing. Tosolin [78] provided an extensive summary of methods and references concerning the synthesis of actinide salts of interest for the MSR systems, which generally employ halide salts with low coordination numbers to limit oxidation potential in the primary loop.

### 6.4.3. Characterization equipment for irradiated molten salts

Due to the reactivity of salts with moisture and oxygen, PIE of irradiated molten salts nominally requires an inert atmosphere and adequate radiation shielding. INL is developing a Molten Salt Thermo-Physical Examination Capability (MSTEC) infrastructure which includes a shielded cell with an inert argon atmosphere and characterization equipment for measurement of thermal physical properties critical to MSR modelling, design and operation. MSTEC is designed with the equipment necessary for synthesizing customized fuel salt compositions [79]. PIE analysis is unable to provide conclusive data on many salt aspects, such as effective thermal properties, as these will be affected by the continuous bubbling and solution precipitation within the salt. Shielded facilities with the capability of heating the salt above the melting point are required to obtain additional thermal physical data. Computational techniques can facilitate prediction of thermal physical properties over a broader range of temperature and chemical compositions than what can be realistically achieved experimentally. Properties important for fuel/coolant salt selection, reactor design, and computational modelling are listed in Table 7 [79].

TABLE 7. THERMAL-FLUID PHENOMENA REQUIRED FOR MSR MATERIALS STUDIES

| PROPERTY | APPLICATION | EXPERIMENTAL TECHNNIQUE |
|---|---|---|
| Corrosion rate Specification Redox Potentials | Structural material Salt chemistry | Electrochemistry |
| Density | Thermal hydraulics Neutronics | Neutron radiography Dilatometry Densitometer Pycnometer |
| Heat capacity | Heat transfer Energy transfer | DSC |
| Thermal conductivity | Heat transfer Energy transfer | Variable gap Transient hot wire 3-Omega Laser flash |
| Thermal expansion | Heat transfer Energy transfer Velocity Liquid composition and distribution | Laser flash |
| Radiation stability | Liquid composition and distribution Used fuel storage | DSC |
| Viscosity | Thermal hydraulics Temperature distribution Power distribution | Dynamic neutron radiography Viscometer Rheometer |

TABLE 7. THERMAL-FLUID PHENOMENA REQUIRED FOR MSR MATERIALS STUDIES (CONT.)

| PROPERTY | APPLICATION | EXPERIMENTAL TECHNNIQUE |
|---|---|---|
| Volatility | Temperature distribution<br>Power distribution<br>Liquid composition and distribution<br>Gas transport and composition | Thermo-gravimeter<br>GC-Mass Spec "Skimmer" |

A densitometer may be used to measure the density of molten salts, and a pycnometer may be used to determine the true volume and true density of solids and powders. Viscosity testing on molten salts will play an important role in the characterization of salt materials for advanced reactor concept applications, including how the salts flow through the system at ambient temperatures and under transition temperature conditions such as freezing and thawing, which are critical factors in determining a salt's suitability and long-term viability. In such cases a rheometer can be used. A proven method for accurate determination of the specific heat capacity of molten salts is calorimetry using a DSC. A DSC measuring cell consists of a furnace and sensor with designated positions for the sample and reference pans. A thermal mechanical analyzer (TMA) can apply stresses such as compression, tension, flexure, or torsion and can change both temperature and stress with time. This system is comprised of a furnace, thermocouples, stress sensors, and special sample holders depending on the sample size and type. INL has developed these instruments for molten salt characterization in MSTEC hot cells [79].

Ultrasonic-testing (UT) techniques could provide a valuable NDE assessments of the loop components following irradiation. The technique is expected to be employed to assess plating and corrosion effects. It can also be used for localized freezing/thawing evaluations during PIE. Material characterization (metallography), using electron microscopy or electrochemical measurements, would also be used to support any corrosion evaluations.

Fibre-optic-based measurements during PIE can be used to characterize a salt's optical properties. Pyrometers can be used to evaluate radiative-heat transfer, while laser-based spectroscopy methods can be used for evaluation of bulk salt properties. Optical spectroscopy may be employed to characterize the different salt species present at the final burnup state (this will not account for precipitating and volatile species produced during irradiation) [80].

An instrumentation framework for MSRs was issued in 2018 by ORNL [79] and reviews the Molten-Salt Reactor Experiment (MSRE) reactor operating experience, with an overview of the specialized instrumentation necessary to operate and maintain MSR. The framework focuses on identifying MSR measurement technology gaps and provides recommendations regarding R&D and related demonstration activities to close the gaps. The authors claimed that modern MSR designs can rely on instrumentation demonstrated during MSR development and did not identify any fundamental technology gaps that would prevent MSR operation and maintenance. However, it was noted that improved instrumentation technology combined with modern process modelling and simulation could significantly improve reliability and decrease the operating costs of future MSR. Hence, the conclusions regarding the scientific framework focus heavily on application of instrumentation in highly radioactive environments that are not

be easily accessible. A similar conclusion is drawn when PIE test procedures are assessed for molten salt fuel types. The observations and conclusions from the framework are listed below [81]:

— Most instrumentation for MSR operations does not come into direct contact with the molten salt;
— Measurements used to determine the reactor heat balance occur on the balance-of-plant side of the primary heat exchanger;
— High dose rates in containment prohibit human entry for calibration and maintenance, potentially impacting the integration of automated instrumentation technologies as well as automation of maintenance activities into the reactor design;
— Technology for reliable online fuel salt sample acquisition is at a low technology readiness level (TRL);
— Reliable methods and instrumentation are necessary for inventory tracking of radionuclides and requires development for safeguards and non-proliferation assurances;
— Flow measurement systems constitute the largest technology hurdles remaining to enable deployment of robust systems;
— High temperature, radiation-tolerant, commercial-grade instrumentation from other industrial processes may be used for molten salt reactor applications.

### 6.4.4. MSR structural testing requirements

While reactor structural materials are outside the scope of this analysis in general, in the vast majority of molten salt heat transport system designs there is no fuel cladding. The FP barriers are the system piping and core structural materials. Material selection and qualification is an important consideration for the deployment of MSRs. Corrosion of alloys in molten salts is driven by four main factors, including: the salt constituents, salt impurities, temperature gradients, and the presence of dissimilar materials.

Busby et al. [82] reviewed candidate materials for MSRs with emphasis on mechanical properties, including time-independent properties, creep rupture, fatigue and thermal stability, along with material product form and weldability. Hastelloy N, Incoloy 800H, stainless steels 304 and 316, and Haynes 230 and 242 were included in the review; these metals were considered during historical or current MSR concept designs. Incoloy 800H and 304 SS and 316 SS are considered to be qualified as Class A materials in ASME BPVC[13] Section III, Division 5, and can be used for the construction of Class A components in high-temperature reactors such as MSRs. Some of these materials are not compatible with molten salt environments and may incorporate Hastelloy N cladding and liners. In the long term, materials suitable for high operating temperatures or high creep strength will be needed for MSR designs, considering the significant pressure difference between the molten salt and the gaseous phase in the secondary heat exchangers. Busby et al. [82] indicated a variety of alloys known as Hastelloy N variants; however, a robust qualification process is required to identify the ideal materials suitable for the various environments. Therefore, ongoing research on structural materials is recommended to continue in the following categories:

— Hastelloy type alloys.

---

[13] American Society for Mechanical Engineers Boiler and Pressure Vessel Code.

- Qualifying Hastelloy materials with greater radiation-tolerance would have the following benefits;
- Control embrittlement, possibly with additions of Ti, Nb, and/or Hf;
- Control tellurium-based cracking, possibly with Cr addition (migration needs to be evaluated to verify);
- Extend operating temperature to 700°C.

— Other metallic materials need to be evaluated.

— Nominal operating temperature of 700°C require evaluation.

— Greater knowledge of degradation phenomena is required.

— Interactions at material-salt interface require further evaluation.

— In-situ characterization of interfaces are required.

— Corrosion tests in a realistic environment are required.

*6.4.4.1.    Phenomena identification and ranking table (PIRT) guidance on PIE approach for molten salt*

The phenomena identification and ranking table (PIRT), which is a tool to assess current knowledge levels or predictive capabilities of models, providing direction to a focused R&D program to support safety analysis and licensing, can be used as a guidance for PIE approach for MSR fuel. A summary list of all phenomena and final rankings was prepared by Hummel et al. [83]. Phenomena ranked 'highly important' (H) but with 'low knowledge' (≤2) are summarized in Table 8 [83] for the flowing fuel salt reactor concept, and Table 9 [83] for the fixed fuel salt reactor concept.

TABLE 8. HIGH-IMPORTANCE/LOW-KNOWLEDGE PHENOMENA FOR FLOWING FUEL SALT REATOR CONCEPTS

| Phenomena Title | Component | Importance Rank | Knowledge Rank |
|---|---|---|---|
| Chemical specification | - | H | 2 |
| Reaction of salts with oxygen-containing species | - | H | 1 |
| Volatilization | Fission products | H | 1 |
|  | Actinides | H | 1 |
| Radionuclide transport through the salt | - | H | 2 |
| Neutral convection heat transfer | Molten salt | H | 2 |
| Natural convection mass transport | Molten salt | H | 2 |
| Steam generation | Energetic (steam explosion) | H | 2 |

TABLE 9. HIGH-IMPORTANCE/LOW-KNOWLEDGE PHENOMENA FOR FIXED FUEL SALT
REATOR CONCEPTS

| Phenomena Title | Component | Importance Rank | Knowledge Rank |
|---|---|---|---|
| Chemical specification | - | H | 1 |
| Fuel salt-coolant salt interaction | - | H | 2 |
| Volatilization | Fission products | H | 1 |
| | Actinides | H | 1 |
| Radionuclide transport through the salt | - | H | 2 |
| Neutral convection heat transfer | Molten salt | H | 2 |
| Steam generation | Energetic (steam explosion) | H | 2 |

Based on the PIRT analysis results for a severe accident condition in an MSR-type SMR, the phenomena below are considered highly important to the accident progression or consequence but are poorly understood phenomena, or subject to significant uncertainty in their prediction. Regarding severe-accident-related R&D studies, the following phenomena are considered the highest-priority to support safety analyses and licensing of MSR-type SMRs [83].

### 6.4.4.2. Chemical speciation of elements in the salt

In addition to the stock light elements and actinides, FPs, corrosion products, and activation products will all be present in the salt as one or more chemical species. This chemical speciation affects the physical and transport properties of these elements as well as their ability to deposit on or react with the heat transport system and containment surfaces. Data from the MSRE under normal operating conditions are limited [84,85]. The use of fluoride salts other than FLiBe, or the use of chloride salts, significantly diminishes the knowledge base with respect to speciation effects.

### 6.4.4.3. Reaction of fuel salts with oxygen-containing species

Formation of FPs and actinide oxyhalides and oxide chemical species during this process will affect the volatility and solubility of actinides and FPs. Data on oxide precipitation from fluoride salts in the MSRE are limited [86], although there has been some recent work on FLiBe salts [87]. The use of a chloride-based fuel salt diluent further diminishes the knowledge base.

### 6.4.4.4. Fuel salt–coolant salt interaction

In the event of a leak or breach in a fluid boundary (such as a heat exchanger tube or a fuel pin), a coolant salt may mix with the fuel salt, depending on the reactor design. The coolant salt will affect the release of fission products and actinides from the fuel salt by dilution and by changes in chemical speciation. While uncertainty exists in the precise salt compositions, the chemical

64

compatibility between salts in adjacent loops of the heat transport system will undoubtedly require examination during reactor design, as it was for the MSRE [86].

### 6.4.4.5. *Volatilization of fission products and actinides*

Mass transport of the vapour away from the condensed-phase surface and reactions of gaseous chemical species will allow more volatilization from the condensed phase. Studies have focused on the volatilization of actinides from salt mixtures mostly in the presence of $F_2$ and at higher temperatures than in postulated accident scenarios [88,89]. FP-containing water pools located remote of the molten salt may be at a much lower initial pH than containment pools; the lower pH may lead to higher fractional iodine volatility [90]. The followings need to be taken into account:

— Radionuclide transport through salt
This phenomenon encompasses the transport, including diffusion and interfacial mass transfer, of radionuclide species through the fuel salt and coolant salt to the gas plena above. The best source of information to date is the MSRE, in which different volatilization behaviours between stable fluorides, noble metals, and noble gases were identified [85]. Some work has occurred since then [91], although few studies have been dedicated to this topic;

— Natural convection heat and mass transfer in molten salt
In natural convection, buoyancy-driven flow occurs due to temperature and concentration gradients and the force of gravity. Failure to remove decay heat would lead to elevated temperatures that allow the release of radionuclides through increased volatility and thus increased potential for structural failures. Predictions of natural convection in molten salts are subject to significant uncertainty due to the limited knowledge of irradiated molten salt properties (for example, viscosity, heat capacity, and thermal conductivity);

— Energetic steam generation
If water contacts the molten salt, the water will vaporize or boil to produce steam. Two types of steam-generating interaction may occur. The non-energetic type involves pressure build-up that can provide a gradual driving force for radiological releases from the confinement. The energetic type is typically a fast-acting process involving sudden contact between molten salt and water that results in a 'steam explosion'. Steam explosions have been a subject of concern in MSR safety [92,93]. Experiments have shown that a vapour explosion could occur when molten salt is poured into water [94]. Accident-condition FP release tests were completed at CNL. Six samples of molten salt material (F-Na-K-U, F-Na-K-Th, and F-Cl-Na-K-U) were prepared from samples of irradiated $UO_2$ and $ThO_2$ fuels. The tests in the experiment were intended to explore the behaviour of FP in molten salt mixtures under inert and oxidizing conditions. The powdered oxide fuel samples were converted to molten salt mixtures by heating to ~850 K with $KHF_2$ and either NaF or NaCl, then further heated to 1270 K and subjected to a flow of argon, steam or air for approximately 4000 s in Fig. 27). The tests were performed as part of the GBI7 hot-cell experiment [95], primarily intended to measure grain boundary inventories (GBI) of noble gases in solid fuels. The furnace (Figs 27 and 28) was a horizontal tube furnace with molybdenum di-silicide heating elements and an out-of-cell temperature controller. The furnace was mounted on tracks to facilitate unloading and loading furnace tube assemblies and positioning of the sample location in the line of sight of the direct viewing γ-spectrometer (Fig. 27). For the molten salt tests, the furnace tubes were made of 2" Schedule 10 Hastelloy N pipe with Type 316 stainless steel (SS) endcaps welded to the tube (Fig. 28).
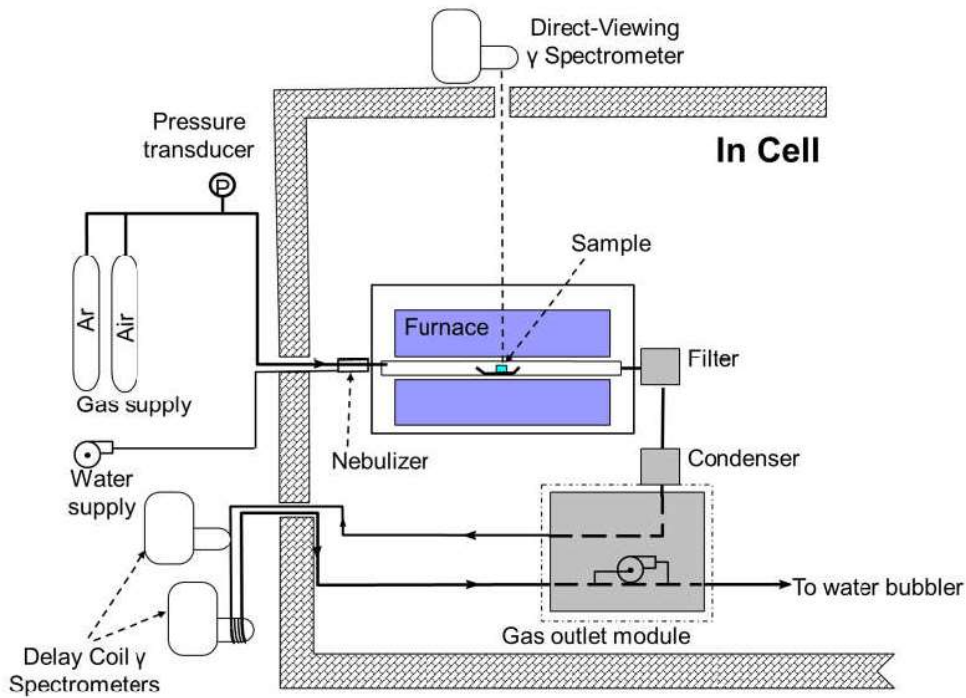
*FIG. 27. Schematic of overall FP release experiment setup (courtesy of CNL)*
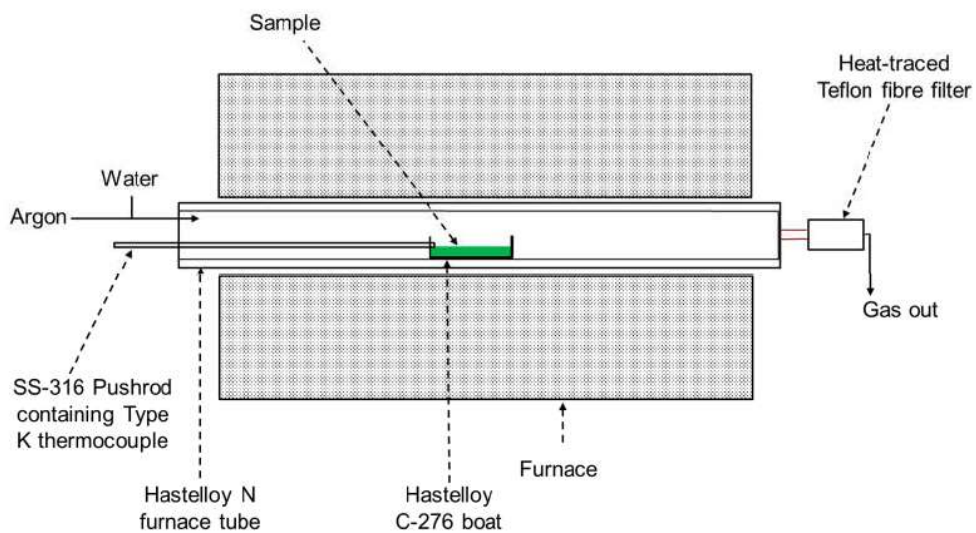


*FIG. 28. Schematic of Hot cell furnace apparatus used in CNL experiment (courtesy of CNL)*

### 6.4.5. Summary of PIE Techniques for Molten Salt Fuel

Table 10 [96] provides a summary of the techniques identified above.

TABLE 10. SUMMARY OF MSR DUWL PIE TECHNIQUES

| Technique | Brief Description | Characteristic or Feature Measured |
|---|---|---|
| Calorimetric cells | Calorimetric cells can be designed for in-pile measurements in static configurations. Accurate measurement will rely on the isolation of different parasitic effects. | • Heat capacity at final burnup<br>• Phase diagrams of salt mixtures<br>• Onset temperatures<br>• Liquidus temperatures<br>• Enthalpies of fusion and crystallization<br>• Evolution of thermophysical properties with burnup |
| Viscometer | Capillary efflux, rotational, or oscillating cup viscometers can be used to measure molten salts viscosity. | • Salt viscosity at a given burnup and temperature<br>• Evolution of thermophysical properties with temperature |
| Pycnometer | Pycnometer uses a balance to measure the density in reference to a working fluid like water or mercury. | • Salt density |
| Dilatometer | Dilatometry offers several advantages since it can be performed in a sealed system, and none of the instrumentation contacts the salt. | • Salt density and volume changes<br>• Thermal Expansion (push-rod dilatometer) |
| Laser flash analysis | Non-contact, non-destructive method to measure the thermal diffusivity of molten salt at high temperature. | • Thermal conductivity at final burnup<br>• Thermal diffusivity<br>• Evolution of thermophysical properties with burnup |
| Thermo-Gravimetric analysis differential scanning calorimetry (TGA-DSC) | TGA indicates the weight changes or mass loss in the sample material as a function of temperature or time during each measurement. | • Heat capacity, melting point, and heat of fusion of the eutectic salts at different temperatures |
| Neutron radiography | Neutron radiography is a non-destructive imaging method that reveals the internal structure of a sample by subjecting it to a neutron beam. | • Thermal hydraulic properties such as density and viscosity measurements |

TABLE 10. SUMMARY OF MSR DUWL PIE TECHNIQUES (CONT.)

| Technique | Brief Description | Characteristic or Feature Measured |
|---|---|---|
| Raman spectroscopy | Raman spectroscopy is one such analytical technique that provides information regarding molten salt content, dissolved analyte coordination and speciation. | • Structure and bonding of species in molten salt mixtures<br>• Oxidation states of lanthanides, and actinides<br>• Identify and quantify tritium in polyatomic forms, such as $T_2$ and TF<br>• Detection and quantification of $I_2$ within the gas phase (Variations in binary/ternary phase diagrams) |
| Laser-induced breakdown spectroscopy (LIBS) | Powerful emission-based optical technique. This optical spectroscopy technique has potential for U and Th analysis, especially in view of the hazardous environment and remote application required in the molten Salt reactor system. | • Measure salt composition and U concentration<br>• Fission product detection |
| Electrochemical monitoring and control | Redox potential control methodologies include gas sparging, contacting the salt with a reducing metal, and adding soluble salt redox buffers to the salt. | • Reduction-oxidation potential measurement<br>• Fission product source term<br>• Measuring diffusion and activity coefficients<br>• Material corrosion at high burnup |
| Differential thermal analysis (DTA) | Differential thermal analysis is the measurement of the difference in temperature between a sample and a reference as heat is applied to the system. This method is sensitive to endothermic and exothermic processes including phase transitions, dehydration, decomposition, redox, or solid-state reactions. | • Phase change temperature<br>• Evolution of thermophysical properties with burnup and salt mixture changes |
| Ultrasonic test (UT) | Ultrasonic testing systems can be developed for fluid density and viscosity measurement. Ultrasonic testing can also be used for structural material defect analysis and corrosion monitoring. | • Element plating on structure<br>• Material corrosion, Localized freezing/thawing<br>• Component degradation |
| Rheometer | Rheological behaviours of the molten salt mixtures with different suspended solid particles. | • Viscosity and rheology of irradiated salt |

TABLE 10. SUMMARY OF MSR DUWL PIE TECHNIQUES (CONT.)

| Technique | Brief Description | Characteristic or Feature Measured |
|---|---|---|
| Gamma spectrometer | HPGe remote detectors can be used for gamma spectrometry of fuel molten salt. | • Behaviour of fission products<br>• Activities of radioactive nuclides<br>• Production and behaviour of activation products |
| Knudsen cell effusion test | This technique involves placing a condensed sample in a Knudsen cell, a small enclosure. Samples will be subjected to a temperature ramp to complete evaporation. | • Fractional fission gas release<br>• Formation of exotic salt compounds<br>• High-temperature stability of fission products in the irradiated salt<br>• Salt boiling point and vapour Pressure |
| Diffuse reflectance spectrometry | This method utilizes visible and near-infrared light to trace substances in their real matrix or after certain chemical transformations of the target substance. | • Long-lived transients and diffusion-promoted aggregates<br>• Dissolved ions in irradiated salt |
| Inductively coupled plasma – optical emission spectroscopy (ICP-OES) | ICP-OES is a universal approach for measuring the trace elemental impurities present in actinide-rich materials. | • Component demonstration and corrosion products<br>• Precipitation and plating of noble metals, actinides, and other salt compounds |
| X-Ray absorption spectroscopy | The experiment is usually performed at synchrotron radiation facilities, which provide intense and tuneable X-Ray beams. | • Chemical speciation and local atomic structure in various molten salts<br>• Speciation of metals and radiation-induced reactions in molten salt<br>• Physical and chemical properties of molten salts and corrosion mechanisms |

## 6.5. METAL-CLAD SOLID FUEL TYPES

Several SMR designs are based around existing LWR technology but scaled down in power generation to conform to SMR power output criteria. This includes fuel and the cladding materials typically utilizing ceramic $UO_2$ pellets and clad in a Zr alloy. Hence existing PIE techniques typically used to examine LWR or PHWR (e.g., CANDU) ceramic fuels may be applied with some modifications to similar but smaller-scale reactor technologies.

### 6.5.1. Fuel handling

The receipt and storage of multiple fuel rods or fuel assemblies in a hot cell may prove difficult; transportation mechanisms (i.e., flasks) need to be able to accommodate a full-sized LWR assembly (or about 25 fuel rods); this also ensures hot cell are not limited to smaller assemblies

that may limit their usefulness. This includes NDE tooling and sectioning capabilities to perform PIE on boiling water reactor channel boxes. Tooling required to safely extract individual fuel rods into a hot cell from a flask needs to be developed to facilitate transfer of novel fuel or fuel assemblies (for example, smaller reactor cores can be entirely disassembled in a hot cell).

### 6.5.2. Non-destructive testing

Development of gamma scanning systems capable of scanning a full-length LWR fuel rods is recommended. Frequency Scanning Eddy-Current Technique (FSECT) on or ultrasonic testing (UT) of full-length fuel rods is also a useful PIE capability for the purpose of crud and oxide analyses or defect detection. Neutron radiography is also a useful technique for defect detection, including identification of primary and secondary hydriding defects.

### 6.5.3. Mechanical testing

Although comprehensive mechanical testing capabilities may exist at a laboratory, usually some gaps exist due to radiological and contamination risks associated with handling of irradiated fuels. Hot cell ring tensile testing on rings of Zr cladding (or PHWR fuel sheath) is a capability that could be considered for implementation. Separate toolsets and potentially new in-cell load frame may be necessary to handle fuel contaminated tensile and fatigue test specimens. In-cell biaxial cladding burst testing is also a useful PIE capability that can be applied to LWR and PHWR fuel cladding.

With regards to storage, transportation and long-term disposal of ceramic LWR- and PHWR-type type advanced fuel designs, additional equipment development and testing is a capability that requires further development, including:

— Irradiated fuel impact testing for integrity during transportation and handling;
— Irradiated fuel impact particulate collection and analysis for long term dry storage applications;
— Irradiated fuel 3-point and 4-point bend tests for integrity during transportation and handling;
— Irradiated fuel ring compression tests to study postulated transportation accidents;
— High-temperature mechanical testing (400-600 °C, depending on scenario) to address fuel cooling concerns during storage.

### 6.5.4. Thermal characteristics testing

If advanced fuels are to be used that require fuel thermal conductivity measurements, although some laboratories have the capability to perform these measurements on un-irradiated fuel, this capability for irradiated fuel would require development, or assistance from laboratories with this capability.

### 6.5.5. Summary of PIE techniques for metallic-clad ceramic fuel

Table 11 provides a summary of the techniques identified in the previous discussion of metallic-clad ceramic fuel.

TABLE 11. SUMMARY OF METALLIC-CLAD CERAMIC FUEL PIE
TECHNIQUES

| Technique | Brief Description | Characteristic or Feature Measured |
|---|---|---|
| Visual Inspection | Use of high-resolution cameras to the condition of the outer surface of the fuel cladding | Dimensional measurement (qualitative), general condition of fuel, defect detection |
| Profilometry | Contact profilometry of the outer surface of fuel | Dimensional measurement (quantitative) |
| Gamma Scanning | Pass the fuel in front of the collimator of a gamma spectrometer | The gamma emission profile of the fuel. Quantities and distribution of fission product isotopes |
| Fission gas collection, gas volume determination, internal void volume determination | Using a fission gas collection system, puncture and extract the fill gas and released fission gas from the system. Repressurize and extract fill gas to determine internal void volume. | Determine fission gas content, fission gas volume, % fission gas release, internal void volume of rod |
| Hot vacuum mass extraction spectrometry | Heating metallic samples under vacuum to extract hydrogen/deuterium | Quantity of hydrogen/deuterium in a metallic sample |
| Immersion density | Section and de-clad a fuel sample, weigh, immerse in fluid | Density |
| Metallography / Ceramography | Cutting, grinding, polishing samples in transverse and longitudinal configurations | <ul><li>Inside diameter/outside diameter oxide thickness,</li><li>Crud or coating presence/thickness,</li><li>defect detection,</li><li>hydride orientation and distribution in cladding,</li><li>fission product distribution in fuel,</li><li>grain morphology in cladding and fuel</li></ul> |
| SEM | Sectioning and sample preparation of fuel pin to observe the cross-section under SEM | <ul><li>Crud microchemistry analysis</li><li>oxidation and corrosion analysis</li><li>hydride orientation and distribution in cladding,</li><li>fission product distribution in fuel</li><li>grain morphology in cladding and fuel</li></ul> |

TABLE 11. SUMMARY OF METALLIC-CLAD CERAMIC FUEL PIE
TECHNIQUES (CONT.)

| Technique | Brief Description | Characteristic or Feature Measured |
|---|---|---|
| FIB lift-out | It uses a focused ion beam to do repeated and sequential milling and imaging, which can be used for 3D reconstruction. It can be also used to lift out a lamella and thin it to electron transparent thickness. | • 3D internal structure<br>• grain morphology in cladding and fuel |
| TEM | Electron diffraction and nano-scale chemical analysis of FIB lamella lifted out from the region of interest determined under SEM | • crystal structure of nano-scale fission product precipitates, oxide and hydride<br>• microchemistry analysis<br>• nano-sized defects analysis caused by irradiation and corrosion |
| In-cell macro- / micro-mechanical load frames | Mechanical tests for materials strength | • Irradiated compact tensile strength |
| Indenter/nano-indenter for active material | Small scale instrumented hardness test device | • Irradiated compact/particle hardness, Young's modulus, yield strength |

## 6.6. METALLIC FUEL TYPES

At least one SMR design being considered in North America plans to utilize a metallic fuel type. Therefore, the assessment of PIE capabilities for metallic fuel is of importance. One SMR design includes stainless steel-clad U-10%Zr fuel. U-Zr oxidizes rapidly in air which requires destructive PIE techniques be conducted in an inert atmosphere, similarly to molten salt fuels.

Metal fuels (including currently existing U-Si and U-Mo based fuels employed as research reactor fuel), initially developed for fast reactors, have higher fissile densities than other fuel types and provide higher reactor core performance such as higher breeding ratio and lower fissile inventories. Among many fuel alloys, U-10Zr (wt.%) and U-Pu-10Zr were considered to have the best overall performance.

Metallic fuel exhibits a characteristic behaviour under neutron irradiation different from other fuel types (such as ceramic pellet-type fuels). A metal fuel pin or slug tends to have better fission gas retention[14], and potentially a higher rate of gas swelling during early stages of irradiation. This may induce greater fuel-cladding mechanical interaction (FCMI) and fuel cladding or fuel particle-fuel core matrix chemical interaction. Metallic fuels tend to have a higher creep rate which may lead to increased deformation of the fuel slug. Thirdly, the fuel alloy may undergo phase transformation during irradiation, which can result in fuel constituent

---

[14] As metallic fuel once given opportunity to swell (only to about 1.5% burnup without constraint), there are interconnection of porosities in the fuel and fission gas release may proceed at a high release rate.

redistribution and excessive swelling, altering the mechanical and thermal properties of the fuel. As such, fuel dimensional stability, structural defects of fuel cladding or fuel-matrix interactions, FP distribution and analysis, microstructure and elemental analysis are typical PIE activities associated with metallic fuels. The techniques used for PIE can be divided into four categories: dimensional measurement (and fuel rod or fuel core densities), optical microstructure and microchemistry analysis, FP analysis and thermal properties measurement.

### 6.6.1. Dimensional/structural measurement

Neutron radiography is a non-destructive imaging method that reveals details about the internal structure of a sample by subjecting it to a neutron beam. Application of neutron radiography on irradiated U-Pu-Zr and U-Zr fuels were reported in a few publications [18,97–101]. The quantitative data generated by neutron radiography is the axial growth of the fuel slug. Digital image processing was used to extract axial growth information [99]. In addition, large defects and density changes in the fuel slug were also revealed by neutron radiography.

Profilometry of fuel cladding is performed (i.e., diametral measurement of fuel pin or plates as a function of the axial position), given that FCMI caused by fuel swelling is a performance concern at high fuel burnup [97]. Two types of profilometry techniques have been reported in the literature [18]. One is the element contact profilometer such as via LVDTs, where diameter measurements are collected with ±0.0005 cm accuracy [97,98]. The other is laser profilometry, which measures any diameter in the range from 2.5 to 25 mm with an accuracy of ±0.0025 mm [18,101]. In addition, the capability to profile metallic plate-type fuels has been developed and can be used to assess fuel plate swelling [102].

X-Ray radiography is not as widely used as neutron radiography for metallic fuels due to limited penetration. Gras [103] explored the potential of applying X-Ray radiography to metallic fuel PIE and found that this technique can produce a clear picture of the cladding and fuel-cladding interface.

### 6.6.2. Microstructure and microchemistry analysis

Metallography of metallic fuel under optical microscopes is also a widely used PIE techniques, providing an overview of the irradiated microstructure of fuel pins with a spatial resolution down to approximately 1 μm. Radial cross-sections at different axial positions of fuel pins and longitudinal cross-sections are typically prepared to investigate the evolution of microstructure with the axial and radial temperature distribution and with increasing burnup.

SEM is a powerful tool for PIE of metallic fuels [104–107]; through application of various detection equipment the SEM can provide in-depth information about a material's elemental composition and morphology. Backscatter-electron (BSE) imaging has been used to image the phase distribution, FP precipitates and porosity in a fuel, and corrosion degradation. Electron-dispersive X-ray (EDX) mapping, 2D line scans, and point spectrum analysis have been used to investigate elemental distribution within a fuel core, including radial variation in Zr, Pu, and U, and FP precipitates.

TEM analysis including EDX and electron-diffraction techniques was performed on a FIB lift-out of a neutron-irradiated U-10%Zr fuel sample [104]. This study included a detailed phase identification (matrix phases and nano-scale precipitates) within irradiated annular U-10Zr fuel by TEM electron diffraction pattern indexing guided by composition analysis from scanning TEM energy dispersive X-ray spectroscopy (STEM-EDS) mapping. Interaction of fission

atoms and vacancies with the phase interfaces were also investigated and provide a deeper understanding of the bubble growth and swelling behaviour under irradiation.

Synchrotron X-Ray micro-computed tomography (μ-CT) has been utilized to analyze the three-dimensional morphology of the microstructure of irradiated U–10%Zr nuclear fuel [108]. The 3D porosity of a small region ($\sim8 \times 10^5$ μm$^3$) located in the intermediate fuel redistribution zone was removed using a FIB, was determined to be 7.2%. A detailed 3D phase morphology (four distinctive phases are identified) and 3D-void morphology were obtained through absorption contrast and propagation-based phase contrast enhanced μ-CT techniques. These provided a greater volume-based understanding of the void growth and microstructure evolution under neutron irradiation.

### 6.6.3. Fission product analysis

Standard gamma spectrometry scans of pin type fuel consist of an axial scan to examine axial redistribution of fission products in the fuel after irradiation. Relative burnup based on certain chemically stable radionuclides is also often derived from axial gamma spectrometry scans. Radial distribution of gamma emitting radionuclides in the fuel can be obtained by scanning horizontally across a fuel pin at several different angles. The collected spectra are analyzed, and radionuclide-specific data is combined using a back-filtered inverse Radon transformation to create a two-dimensional activity intensity map of the scanned region [100].

In addition to the typical axial gamma spectrometry scans, it is possible to rotate the PGS from a horizontal to a vertical orientation. In this orientation over several angles spectra can be collected and the tomography reconstructed to provide a two-dimensional FP distribution representation at a given axial location. This technique is referred to as gamma emission computed tomography (GECT), first developed at INL [109].

The fission product monitor residual heavy atom is a method of fuel burnup determination using the measured mass of a specific FP in the fuel, the cumulative fission yield of that specific FP, and the total mass of actinides present in the sample. One of the main limitations in achieving increased burnup in metallic U-Zr nuclear fuel is fuel-cladding chemical interaction (FCCI), where the migration of the FP lanthanides from the fuel to the periphery is one of the major contributors to FCCI. A 'liquid-like' transport mechanism proposes the lanthanide transport is aided by liquid caesium and liquid sodium in the pores of the fuel and at the fuel periphery.

### 6.6.4. Thermal properties measurement

Laser flash analysis (LFA) is a technique with high accuracy and repeatability in measuring bulk thermal diffusivity of various nuclear fuel types [110–112]. In this technique, a laser pulse is applied to one surface of the sample while the temperature rise is recorded on the opposite surface. This technique can also be used to measure the conductivity of the matrix as a function of temperature.

Phase diagrams represent the interaction between two components across the range of mixtures based on thermodynamics. Differential scanning calorimeter (DSC) is an experimental method used in phase diagram determination. In DSC, the difference in the heat flow rate compared to a reference sample and the heat flow rate compared to a test sample is measured, keeping both samples at the same temperature. This difference is measured while the samples are undergoing a temperature profile [113].

A Thermal conductivity microscope (TCM) is an instrument that uses focused laser beams to simultaneously determine thermal conductivity (k) and thermal diffusivity (D). Typically, only D values can be obtained using thermal wave methods, with conductivity requiring additional measurement techniques to determine density and heat capacity values. However, the TCM is unique in that it can simultaneously measure both k and D values using a technique called modulated thermos-reflectance. This measurement approach involves measuring the temperature field spatial profile of samples excited by an amplitude modulated, continuous-wave laser beam. A thin gold film is applied to the samples to ensure strong optical absorption and to establish a second boundary condition that introduces an expression containing the substrate thermal conductivity. Measurements using the TCM can be performed on metallic fuels samples in a radial pattern along the sample [114].

### 6.6.5.  Summary of PIE Techniques for Metallic Fuel

Table 12 summarizes the PIE techniques previously identified for metallic fuel types.

TABLE 12. SUMMARY OF METALLIC FUEL PIE TECHNIQUES

| Technique | Brief Description | Characteristic or Feature Measured |
|---|---|---|
| Neutron Radiography | A non-destructive imaging method that reveals the internal structure of a sample by subjecting it to a neutron beam. | <ul><li>Fuel slug axial growth.</li><li>Morphology of the fuel slug and fuel cladding (projection view internal structure).</li></ul> |
| Profilometry | Measure the fuel pin diameter as a function of the axial position. | Radial swelling of the fuel cladding as a function of the axial position. |
| X-Ray radiography or computed tomography | Non-destructively create a 2D projection view or 3D view of the internal structure of fuel cladding and interface of fuel and cladding. | <ul><li>Outer diameters of the fuel cladding and fuel slug.</li><li>Image of the top and bottom end of the fuel slug.</li></ul> |
| Metallography | Sectioning and sample preparation of fuel pin to observe the cross-section under an optical microscope. | <ul><li>Fuel radial swelling.</li><li>Microstructure observation such as Fuel radial variation of phase constituent, porosity, large precipitates.</li><li>FCMI and FCCI.</li><li>Structural defects, such as cracking and large cavity.</li></ul> |
| SEM | Sectioning and sample preparation of fuel pin to observe the cross-section under SEM. | <ul><li>Microstructure observation at higher resolutions, such as Fuel radial variation of phase constituent, porosity, sub-micron scale precipitates.</li><li>FCMI and FCCI.</li><li>Structural defects, such as cracking and corrosion of cladding.</li><li>Elemental composition analysis of matrix phase and precipitates.</li><li>Elemental composition line scan and 2D mapping</li></ul> |

TABLE 12. SUMMARY OF METALLIC FUEL PIE TECHNIQUES (CONT.)

| Technique | Brief Description | Characteristic or Feature Measured |
|---|---|---|
| FIB lift-out | It uses a focused ion beam to do repeated and sequential milling and imaging, which can be used for 3D reconstruction. It can be also used to lift out a lamella and thin it to electron transparent thickness. | • 3D tomography of constituent phases and pores.<br>• Prepare thin lamellae for TEM investigation. |
| TEM | Electron diffraction and nano-scale chemical analysis of FIB lamella lifted out from the region of interest determined under SEM. | • Phase identification of phase constituent and precipitates.<br>• Chemical composition of constituent phases and precipitates.<br>• Elemental segregation at interface and boundaries. |
| Synchrotron XCT | Non-destructively 3D tomography on a small volume sample cut from neutron-irradiated fuel slug using FIB. | • Quantitative 3D information of porosity.<br>• 3D morphology of constituent phases and pores. |
| Gamma spectrometry | Analysis of dissolved solid samples of irradiated fuel. | • To determine fuel burnup, and isotopic content. |
| Gamma scanning | Standard gamma spectroscopy scans of pin type fuel consist of an axial scan of the fuel pin to investigate the axial redistribution of fission products in the fuel after irradiation. | • Variation of burnup along axial direction of rod.<br>• Axial movement of fission products, especially Cs. |
| Gamma emission computed tomography (GECT) | Based on rotating the precision gamma scanner from a horizontal to a vertical orientation and performing a series of rotations over several angles. | • 2D distribution of fission products.<br>• Fission product migration. |
| Mass Spectrometry | Mass spectrometry techniques such as thermal ionization mass spectrometry (TIMS), SIMS, time of flight mass spectrometry, inductively coupled plasma mass spectrometry (ICP-MS) are commonly used to measure isotopic composition. | • Destruction of actinides and minor actinides.<br>• Burnup calculations.<br>• Element distribution maps.<br>• Isotopic composition, including radiometric counting.<br>• Fission gas analysis. |
| Atom probe tomography (APT) | APT has established itself to be an effective technique for elucidating 3D chemical composition in materials at nanoscale for a wide range of structural materials used for nuclear application. | • Mass spectra and element distribution maps.<br>• Isotopic quantification.<br>• Analyzing local burnup.<br>• Characterize the microstructural changes and chemical analysis on fission products. |
| Laser flash analysis (LFA) | In this technique, a laser pulse is applied to one surface of the sample while the temperature rise is recorded on the opposite surface. | • Thermal diffusivity of lanthanides.<br>• Thermal conductivity of matrix. |
| Differential scanning | In DSC, the difference in the heat flow rate to a reference sample and the heat flow rate to a testing | • Temperature dependence of neodymium in liquid caesium.<br>• Lanthanide transport in the U-Zr |

TABLE 12. SUMMARY OF METALLIC FUEL PIE TECHNIQUES (CONT.)

| Technique | Brief Description | Characteristic or Feature Measured |
|---|---|---|
| calorimetry (DSC) | sample, to keep both samples at the same temperature, is measured. | fuel.<br>• Alloy phase transformations.<br>• Heat capacity measurements. |
| Thermal conductivity microscope (TCM) | This is an instrument that uses tightly focused laser beams to simultaneously determine thermal conductivity (k) and thermal diffusivity (D). | • Phase dependent thermal conductivity.<br>• Thermo-reflectance measurements.<br>• Local thermal conductivity values. |
| In-cell tension and compression testing | Mechanical tests for materials strength. | • Irradiated fuel slug or cladding's Young's modulus, Poisson's ratio. |
| In-cell macro / micro mechanical load frames | Mechanical tests for materials strength. | • Irradiated fuel slug or cladding's Tensile Strength. |
| Indenter/nano-indenter for active material | Small scale instrumented hardness test device. | • Irradiated fuel pin's hardness, Young's modulus, yield strength. |

# 7. GAP ASSESSMENT METHODOLOGIES IN PIE TECHNIQUES FOR ADVANCED REACTOR FUELS

## 7.1. BACKGROUND

In assessing PIE developments over the last decade, alongside the most common advanced/future reactor designs, it has become apparent that there exist a number of capability gaps (or challenges) that are associated with the progression of PIE in support of the advanced reactor fuels and materials of the future. These challenges or 'gaps' are as follows:

— Unique sample preparation challenges associated with novel materials, some of which may only be available in small quantities;
— Lack of standardization for many new or advancing PIE techniques, for sub-size and novel materials;
— Availability of materials to conduct or refine Advanced PIE methodologies;
— Acceptance of a standard set of PIE for molten salts.

It is also acknowledged that establishing commonality and sharing PIE approaches / methodologies may ease some of the frequently experienced operational constraints of 'core' PIE equipment and facilities.

Meaningful collaboration (Section 8) will help to address these gaps and support existing and new PIE facilities in better anticipating future PIE demands to support the fuel lifecycle of advanced reactor materials. This situation is more desirable under the circumstance that materials test reactors or irradiation facilities are aged and their number is decreasing. All irradiation services may rely on a few facilities with open access for international cooperation. Therefore, available irradiation facilities can be takin into account as one of the contributing challenges/gaps relevant to PIE work, which is not within the scope of this publication.

## 7.2. IDENTIFYING AND ADDRESSING PIE GAPS

In order to properly address the gaps discussed in this section, it is recognized that 'fuel technology-agnostic' hot cell PIE capabilities are likely to be significant, based on their ability to characterize multiple material types. One example of this is hot cell optical microscopy, discussed in Section 4.1. In most cases with these technologies, some modifications may be required to the equipment or sample preparation methods in order to examine new material types. Existing and new PIE facilities may then determine and evolve capabilities in line with the development of advanced reactors.

The listed PIE techniques for advanced reactor fuels and materials (discussed in Sections 6.3 through 6.6) may not be available at any single laboratory. Because some of these techniques are also still in development, and national nuclear programmes may have different drivers across Member States, it is also possible these identified techniques are at different stages of development (known as technology readiness levels (TRLs) [115]; see Table 13). These TRLs can be useful in determining deployment or development timeframes in support of research programmes.

TABLE 13. TECHNOLOGY READINESS LEVELS

| Relative Level of Development | Technical Readiness Level | Description | Example |
|---|---|---|---|
| System operation | TRL 9 | Actual system operated over the full range of expected conditions. | A final form system operating with the full range of waste processing. |
| System commissioning | TRL 8 | Actual system completed and qualified through test and demonstration. | Hot commissioning a system. |
| | TRL 7 | Full-scale, similar (prototypical) system demonstrated in a relevant environment. | Cold commissioning a system with a range of simulants and/or real inactive waste processing. |
| Technology demonstration | TRL 6 | Engineering/pilot-scale, similar (prototypical) system validation in a relevant environment. | Testing an engineering scale model well beyond lab scale testing. |
| Technology development | TRL 5 | Laboratory scale, similar system validation in relevant environment. Basic components integrate such that configuration is similar to final form. | Testing a high-fidelity system in a simulated environment and/or with real waste and simulants. |
| | TRL 4 | Component and/or system validation in laboratory environment. Basic components are integrated to establish how the pieces will work together. | Integration of "ad hoc" hardware in a laboratory and testing with a range of simulants. |
| Research to prove feasibility | TRL 3 | Analytical and experimental critical function and/or characteristic proof of concept. Active research and development is initiated. | Analytical and laboratory scale testing to physically validate predictions. Components are not yet integrated or representative. Testing may use simulants. |
| | TRL 2 | Technology concept and/or application formulated. Invention begins. Applications are speculative and there may be no proof or detailed analysis to support the assumption. | Analytical studies. |
| Basic technology research | | | |
| | TRL 1 | Basic principles observed and reported. Scientific research begins to translate to applied science and development. | Paper study of a technology's basic properties. |

## 7.3. CONSIDERATIONS FOR PIE TECHNIQUE DEVELOPMENT

There are a number of factors key to determining which PIE techniques represent the most advantageous investment for a nuclear laboratory based on a Member State's perceived needs to support respective nuclear industries in the short to long-term future. For hot cell PIE techniques that are desired but not available without some or full development, the desired PIE techniques may be assigned a ranking based on the following criteria (scoring examples are shown in corresponding tables):

— Perceived need (see Section 7.3.1) and technology readiness levels (see Section 7.3.2);
— Degree to which the PIE technique is technology agnostic (see Section 7.3.3) or diverse application of a PIE technique (see Section 7.3.4);
— Time to deployment of the PIE technique (see Section 7.3.5);
— Approximate cost to fully commission, operate and maintain the PIE equipment (see Section 7.3.6);
— Availability and appropriate type of collaboration agreement or commercial sub-contract (considering intellectual property and other export controls) (see Section 7.3.7).

### 7.3.1. Effect of perceived need

Table 14 provides an example of scoring the effect of perceived need.

TABLE 14. EXAMPLE OF SCORING THE EFFECT OF PERCEIVED NEED

| Score | Timeframe |
|---|---|
| 5 | Potential customer requires capability within 2 yrs |
| 4 | 3-5 yrs |
| 3 | 6-10 yrs |
| 2 | 11-20 yrs |
| 1 | >20 yrs |
| 0 | No perceived customer need |

### 7.3.2. Effect of technical readiness level (TRL)

Table 15 provides an example of scoring the effect of TRL.

TABLE 15. EXAMPLE OF SCORING THE EFFECT OF TECHNICAL READINESS LEVEL

| Score | Readiness Level |
|---|---|
| 5 | TRL 8-9: All demonstrations completed, ready or deployed in commercial setting. |
| 4 | TRL 6-7: Prototype tested in simulated environment, ready for operational environment demonstration. |
| 3 | TRL 4-5: Component validation in lab or simulated environment. |
| 2 | TRL 2-3: Invention to support concept, active research still required. |
| 1 | TRL 1: Basic concept exists. |

### 7.3.3. Effect of technology agnostic

This variable considers how many fuels a specific PIE technique can be applied to. The wider the spread, the greater the chances of being used, the greater the value of the technique. Table 16 provides an example of scoring the effect of technology agnostic.

TABLE 16. EXAMPLE OF SCORING THE EFFECT OF TECHNOLOGY AGNOSTIC

| Score | Number of Fuel Types That a PIE Technique is Applicable To |
|-------|-----------------------------------------------------------|
| 5 | All known fuel types |
| 4 | --- |
| 3 | More than one type |
| 2 | --- |
| 1 | One specific fuel type |

### 7.3.4. Effect of diverse application of a technology

A technique provides more benefit if it can provide measurement of more than one characteristic. Table 17 provide an example of scoring the effect of the diverse application of a technology.

TABLE 17. EXAMPLE OF SCORING THE EFFECT OF THE DIVERSE APPLICATION OF A PIE TECHNIQUE

| Score | Availability |
|-------|--------------|
| 5 | Measures five (5) or more characteristics |
| 4 | Measures four (4) characteristics |
| 3 | Measures three (3) characteristics |
| 2 | Measures two (2) characteristics |
| 1 | Measures one (1) characteristic |

### 7.3.5. Effect of delivery time

Delivery time is the total elapsed time from start to a commissioned process is in place. Table 18 provides an example of scoring the effect of delivery time.

TABLE 18. EXAMPLE OF SCORING THE EFFECT OF DELIVERY TIME

| Score | Timeframe |
|-------|-----------|
| 5 | 1-2 yrs |
| 4 | 3-5 yrs |
| 3 | 6-10 yrs |
| 2 | 11-15 yrs |
| 1 | 16-20 yrs |
| 0 | >20 yrs |

### 7.3.6. Effect of cost

Cost is all of the associated expenses for putting the technique into operation, either on site, or through established collaboration or sub-contract. Table 19 provides an example of scoring the effect of cost.

TABLE 19. EXAMPLE OF SCORING FOR COST

| Score | Cost to develop |
|---|---|
| 5 | $0k< Cost <$100k |
| 4 | $100k< Cost <$500k |
| 3 | $500k< Cost <$1M |
| 2 | $1M< Cost <$5M |
| 1 | Cost >$5M |

### 7.3.7. Effect of availability for collaboration

Considerations such as equipment demand/availability, the need for verification and validation of data using similar instrumentation and sample preparation methods need to be considered. It is possible that through efficient and regularly used transportation processes between laboratories, the availability of similar equipment can be better exploited. For example, if an active FIB and SEM are not available for extensive maintenance at one laboratory, samples could be shipped to another laboratory with similar capabilities. Table 20 provides an example of scoring the effect of cost.

TABLE 20. EXAMPLE OF SCORING FOR AVAILABILITY FOR COLLABORATION

| Score | Availability |
|---|---|
| 5 | No external facilities capable or developing the technique, no commercial contractors. |
| 4 | |
| 3 | Little interest, but one external facility willing to develop capability in collaboration or on commercial basis. |
| 2 | |
| 1 | Multiple external facilities willing to develop capability in collaboration or on commercial basis. |
| 0 | Known external facility capable of the technique and willing to collaborate or on commercial basis, other facilities willing to develop it. |

### 7.4. SCORING FOR PRIORITIZATION

All leads to each criterion in Section 7.3 are scored on a scale of one to five as described in Tables 13 through 20. However, some of the criteria have more significance in deciding whether there is value in investing in a particular technique. As such, each score has a multiplier based on its relative importance. The most significant criterion is the perceived need. If there is no need for a technique, then there is no reason to invest in it at the present time. The next most significant criterion is the cost of implementation. Funds are finite, therefore the more one technique costs to establish, the fewer techniques a laboratory may be able to establish, so the lower the score. Table 21 shows a typical scoring table.

TABLE 21. EXAMPLE OF SCORING FOR PRIORITIZATION

| Criterion | Base Score | Multiplier | Maximum Score |
|---|---|---|---|
| Perceived need | | | |
| Cost | | | |
| Delivery time | | | |
| Availability for collaboration/sub-contract | | | |
| Number of characteristics that can be measured | | | |
| Degree to which the technique is technology agnostic | | | |
| Technical readiness level | | | |
| Total maximum score | | | |

# 8. INTERNATIONAL COLLABORATION

## 8.1. THE DRIVERS AND BENEFITS OF COLLABORATION IN DEVELOPMENT AND USE OF ADVANCED PIE TECHNIQUES

There are four major drivers identified to justify the need to pursue strategic collaborations between nuclear laboratories and other industry partners.

**Driver #1 – Growing demand for PIE services due to advanced reactor development**

The concurrent development of many advanced reactor designs that use varying fuel types and structural materials, all require performance data to support their construction and expected operation, are expected to strain existing PIE resources. This will lead to longer wait times for frequently used or unique PIE toolsets, and lead to delays to safety and licensing approvals for new reactor designs. Meanwhile, current-generation reactor fleets developing ATF concepts, in addition to life-extension PIE programs, will also require PIE and further affect hot cell resource loading. The continual development of isotope production and other fuel re-processing technologies are also expected to create additional work for PIE facilities.

Collaborations between multiple laboratories could help to reduce resource burden in hot cell facilities, alleviate equipment availability concerns, and expand access to a greater number of PIE techniques for use during a comprehensive fuel PIE campaign. Not every nuclear laboratory may have all of the necessary PIE capabilities for a concise examination of every fuel type. Effective collaborations could therefore accelerate development of PIE techniques, allow for more effective prioritization of actions to fill gaps regarding fuel PIE capabilities, improve reliability of the data through cross-laboratory verification and validation exercises, and thus address a fuel qualification inquiry from nuclear regulators in a timelier manner, and create alternate paths to obtaining the required fuel or material performance data.

**Driver #2: Knowledge and workforce development to maintain PIE expertise**

The development of multiple advanced SMR (and MMR) concepts will require substantial investment and training of skilled hot cell resources to support the expected throughput of current and future PIE hot cell facilities.

Collaboration in advanced fuel PIE provides an opportunity for critical knowledge transfer between collaborative organizations across member states that have a mutual interest in developing a specific advanced fuel reactor technology and help to train new cohorts of skilled fuels and materials fuel engineers/scientists and hot cell technicians.

**Driver #3: The Need for harmonization of sample preparation techniques for non-ASTM Standardized tests**

To ensure consistent and reliable PIE results are obtained at different facilities for non-ASTM standardized tests such as subsized tensile tests, compact tension tests, shear punch tests. The harmonization of sample preparation techniques among nuclear laboratories was recommended. Collaborations can be used as a means of improving and standardizing small/sub-sized sample preparation processes and verifying fuel PIE results through verification and validation exercises (e.g., round-robin testing). Similar sample preparation methods are expected to help achieve similar datasets and mutually agreed-upon interpretation of results.

**Driver #4: Limited access to irradiated fuels and materials for advanced reactors**

Access to irradiated Fuels and Materials for advanced reactors is limited and difficult to obtain and can delay fuel development and qualification. Through cross-laboratory collaborations and sharing of irradiated material archive and library, in consultation with the fuel fabricator and/or SMR operator, irradiated test samples can be obtained in sufficient quantity to allow for shipment of multiple samples to and from laboratories for the required examinations, as well as for testing and commissioning of both new PIE techniques and related sample preparation methods.

## 8.2. CHALLENGES ASSOCIATED WITH COLLABORATION

### 8.2.1. Technical challenges and prioritization

There are technical challenges associated with developing effective collaborations. Ensuring that collaborations in advanced fuel PIE are structured towards a common technical interest is a key challenge. For example, the wish to demonstrate and deploy the same reactor type in two or more member states provides justification for collaboration between PIE facilities, to maximize facility use and expedite development of useful PIE techniques that can be applied to most fuel.

Consensus between multiple laboratories on what fuel performance parameters are of greatest importance and priority for the regulator, can influence the direction of PIE technique development and for each fuel type and the scope of collaboration between nuclear laboratories.

There are also technical challenges associated with advanced reactor fuel type sample preparation methods for some laboratories, related to both the need for further development and refinement of sample preparation techniques, but also the standardization of the techniques.

### 8.2.2. Logistics/planning challenges

Staffing challenges with very busy staff, difficulties in scheduling the training time and cross-training opportunities, could hamper efficient collaboration efforts.

Planning of a comprehensive set of examinations where the work occurs at two or more laboratories can become complex and time consuming.

RAM shipping logistics challenges associated with small sample transport are expected to present challenges initially, as sample preparation, characterization, packaging, route selection and regulatory approvals are prepared. Reasons for transporting fuel/cladding samples to external PIE facilities can be to alleviate resource loading (including during extended equipment maintenance periods), obtain similar data for verification and validation purposes, or to utilize PIE techniques unique to an external laboratory.

Intellectual property controls (e.g., non-disclosure agreements), export control approvals of tangible and intangible information by the regulator and/or other government entities will be required prior to shipping any physical material, or controlled information, between member states, adding to the complexity of a PIE project with multiple member states.

## 8.3. COLLABORATION METHODS

As new SMRs and advanced reactors are developed, the performance parameters inherent to each advanced fuel type will determine the PIE capabilities required to assess these fuel performance parameters. Knowing what techniques are required and what laboratory has the techniques available for use can result in the development of a cross-laboratory 'PIE roadmap', where specific PIE techniques can be employed for advanced fuel and material characterization.

As new hot cell facilities are constructed, and existing facilities refurbished and/or upgraded, additional skilled resources will require development of expertise to meet the near- and long-term future demand on PIE facilities as irradiation testing and PIE programs come to fruition.

The drivers for collaboration between multiple nuclear laboratories listed in Section 8.1 present the main justifications for engaging in collaborative PIE on advanced reactors fuels and materials. The ranking of the importance and need for specific PIE techniques, in collaboration with other laboratories, can streamline subsequent knowledge and technique gaps, allowing for a more strategic implementation of new/developing PIE toolsets and sample preparation techniques.

In the interest of ensuring efficient hot cell throughput, effective knowledge transfer during development of PIE techniques, and developing the necessary techniques to adequately assess the performance of multiple fuel types, it is recommended that strategic collaborations between two or more nuclear laboratories are developed in support of SMR technologies of mutual interest. Such collaborations can ensure that:

— The required capabilities for any given fuel type are at a high technical readiness level (i.e., are operable, or require only minor modifications to become operable) and knowledge/equipment gaps can be identified;
— The tools are regularly maintained and ready for use to maximize availability;
— The toolsets, or resulting PIE data, can be accessed by external customers, where all intellectual property can be controlled as required.

In the subsequent sections, potential methods to facilitate collaborations among laboratories are described, based on discussions at TM 2021.

### 8.3.1. International Centers based on Research Reactors

Participants in TM 2021 and the follow-up Consultancy Meeting in November 2021 discussed to become part of the IAEA initiative on International Centres based on Research Reactors (ICERR[15]) which aims to facilitate Member States gain timely access to relevant nuclear infrastructure (e.g., facilities, resources) based on research reactors and their ancillary facilities including PIE facilities. The participants felt that the ICERR can allow Member States' access to existing facilities for training or research purpose via bilateral cooperation between laboratories.

---

[15] Refer to: https://www.iaea.org/about/partnerships/international-centres-based-on-research-reactors-icerrs.

### 8.3.2. HOTLAB database

IAEA's PIE database (see footnote 2) provides catalogue information on existing PIE facilities (current it includes information on 42 hot labs from 22 countries). This PIE database has been developed in cooperation with HOTLAB, and updated information are directly provided by HOTLAB members. This PIE database is a good tool to obtain overall information on available hot laboratories.

Each facility data include:

— General & cell characteristics;
— Acceptance information (condition);
— Available NDE, DE and other techniques;
— Availability of rod re-fabrication & instrumentation;
— Available storage and conditioning capabilities;
— Reference publications.


### 8.3.3. Coordinated research project

The TM 2021 meeting participants suggested to initiate an IAEA's CRP that will focus on the standardization of sub-sized fuel and material sample preparation methods for PIE and advanced characterization of novel fuels and structural materials for SMRs and other advanced reactor applications.

This CRP is intended to strengthen Member States' ability to obtain experimental data by expanding their PIE and other advanced characterization capabilities through multi-laboratory collaborations. Specific goals to be achieved are:

— To develop a 'PIE roadmap' for a given fuel and/or structural material type such as TRISO, SiC, graphite, new or existing alloys that incorporates advanced characterization techniques and harmonizes preparation, testing, and characterization methods across collaborating laboratories;
— To execute the round-robin PIE exercise for a given fuel and/or structural material type that includes both non-destructive examination (NDE) and destructive examination (DE);
— To demonstrate and look for efficiencies associated with transport of small /subsized samples to and from collaborating laboratories.


To facilitate the development of advanced PIE techniques and reduce difficulties with transportation of radioactive samples and related high dose rates, it is recommended that methods for preparing small/subsized samples be standardized in nuclear laboratories for specific PIE toolsets.

### 8.3.4. Irradiated material archive and library

The Nuclear Science User Facility (NSUF[16]) manages the Nuclear Fuels and Materials Library (NFML[17]), a collection of specialized information and material specimens from past and ongoing irradiation test campaigns, real-world components retrieved from decommissioned power reactors, and donations from other sources. Everything in the NFML is available to the nuclear research community, either through a peer-reviewed proposal process or through direct programmatic request. The NFML initiative maximizes the value of previous and ongoing materials and nuclear fuels irradiation test campaigns. Similarly, the UK also maintains an irradiated material archive where irradiated materials can be made available to the international research community for research purpose.

---

[16] Refer to: https://nsuf.inl.gov/.
[17] Refer to: https://nsuf.inl.gov/Page/fuels_materials_library.

# REFERENCES

[1]     INTERNATIONAL ATOMIC ENERGY AGENCY, Post-Irradiation Examination, and In-Pile Measurement Techniques for Water Reactor Fuels, IAEA-TECDOC-CD-1635, IAEA, Vienna (2010).

[2]     INTERNATIONAL ATOMIC ENERGY AGENCY, Hot Cell Post-Irradiation Examination and Poolside Inspection of Nuclear Fuel, IAEA-TECDOC-1673, IAEA, Vienna (2011).

[3]     INTERNATIONAL ATOMIC ENERGY AGENCY, Quality and Reliability Aspects in Nuclear Power Reactor Fuel Engineering – Guidance and Best Practices to Improve Nuclear Fuel Reliability and Performance in Water Cooled Reactors, Nuclear Energy series No. NF-G-2.1 (Rev.1), in press.

[4]     SYKES, M.L., EDWARDS, I.A., THOMAS, K.M., Metal carbonyl decomposition in the advanced gas cooled reactor, Carbon, **31** (1993) pp. 467–472.

[5]     HORSLEY, G.W., CAIRNS, J.A., The inhibition of carbon deposition on stainless steel by prior selective oxidation, App. Surface Science, **18** (1984) pp. 273–286.

[6]     HAYNES, T., BALL, J.A., SHEA, J.H., WENMAN, M.R., Modelling pellet-clad mechanical interaction during extended reduced power operation in bonded nuclear fuel, J. Nuclear Materials, **465** (2015) pp. 280–292.

[7]     MACHADO, J., et al. "An ultrasonic probe for NDT inspection of fuel assembly used in nuclear power plant reactors", Proceedings of the 15th World Conference on Non-Destructive Testing, Rome, 2000.

[8]     ROSENKRANTZ, E., et al., Ultrasonic measurement of gas pressure and composition for nuclear fuel rods, nuclear instruments and methods in physics research section a: accelerators, spectrometers, detectors and associated equipment, **603** (2009) pp. 504–509.

[9]     DAW, J., et al., Design Requirements for Ultrasonic Deformation Sensor for TREAT Experiments, INL, Idaho Falls (2018).

[10]    ARMSTRONG., J, et al., "Developments in post-irradiation examination hot cell equipment on CANDU fuel at Chalk River Laboratories (CNL)", Proceedings of the 14th International Conference on CANDU Fuel, Ontario, Canada, 2019 July.

[11]    CORBETT, S., "Review of defect root-cause post-irradiation examination (PIE) of PHWR fuels at CNL, and related developments in PIE at CNL to support defect root-cause examinations for PHWR utilities", Presented at the Technical Meeting on Fuel Failures in Normal Operation of Water Reactors: Experience, Causes and Mitigation, IAEA, 2020 December.

[12]    GÄBLER, S., HEUER, H., HEINRICH, G., Measuring and imaging permittivity of insulators using high-frequency eddy-current devices, IEEE Transactions on Instrumentation and Measurement, **64** (2015) pp. 2227–2238.

[13]     SAHAKYAN, A., Koel, A., RANG, T., Non-destructive eddy current measurements for silicon carbide heterostructure analysis, WIT Transactions on Engineering Sciences, **116** (2017) pp. 49–60.

[14]     HEUER, H., Characterization of Ceramic Matrix Composites Using Eddy Current Techniques, Annual report 2016/17, pp.32, Frauhofer Institute for ceramic Technologies and Systems (IKTS) (2017).

[15]     AMERICAN SOCIETY FOR TESTING AND MATERIALS, Standard Practice for Measuring Coating Thickness by Magnetic-Field or Eddy-Current (Electromagnetic) Testing Methods, ASTM-E376-11, ASTM (2017).

[16]     HARP, J.M., CAPPIA, F., CAPRIOTTI, L., Post-Irradiation Examination of the ATF-1 Experiments – 2018 Status, INL, Idaho Falls (2018).

[17]     CAPPIA, F., Post-Irradiation Examinations of the ATF Experiments – 2020 Status, INL, Idaho Falls (2021).

[18]     PORTER, D.L., TSAI, H., Full-length U-xPu-10Zr (x = 0, 8, 19 wt.%) fast reactor fuel test in FFTF, J. Nucl. Mater., **427** (2012) pp. 46–57.

[19]     DEGUELDRE, C.A., The Analysis of Nuclear Materials and Their Environments, ISBN 978-3-319-58004-3 (ISBN 978-3-319-58006-7 E-Book), Springer International Publishing AG (2017).

[20]     INTERNATIONAL ATOMIC ENERGY AGENCY, Advances in Small Modular Reactor Technology Developments, A Supplement to IAEA Advanced Reactor Information System (ARIS), 2020 Edition, Vienna (2020).

[21]     DEMKOWICZ, P.A., LIU, B**.,** HUNN, J.D., Coated particle fuel: historical perspectives and current progress, J. Nucl. Mater., **515** (2019) pp. 434–450.

[22]     PRICE, M.S.T., The Dragon project origins, achievements and legacies, Nucl. Eng. Des., **251** (2012) pp. 60–69.

[23]     BARNES, C.M., AGR-1 Fuel Product Specification and Characterization Guidance, INL, Idaho Falls (2006).

[24]     ELECTRIC POWER RESEARCH INSTITUTE, Uranium Oxycarbide (UCO) Tristructural Isotropic (TRISO) Coated Particle Fuel Performance, Topical Report EPRI-AR-1 (NP), EPRI, Palo Alto, CA (2019).

[25]     HUNN, J. D. et al., Detection and analysis of particles with failed sic in agr-1 fuel compacts, Nucl. Eng. Des., **306** (2016) pp. 36–46.

[26]     FUKUDA, K. et al., Research and development of HTTR coated particle fuel, J. Nucl. Sci. Technol., **28** (1991) pp. 570–581.

[27]     DEMKOWICZ, P. A. et al., The fuel accident condition simulator (FACS) furnace system for high temperature performance testing of VHTR fuel, Nucl. Eng. Des., **251** (2012) pp. 164–172.

[28]    MORRIS, R. N., BALDWIN, C. A., DEMKOWICZ, P. A., HUNN, J. D., REBER, E. L., "Performance of AGR-1 high-temperature reactor fuel during post-irradiation heating tests, Nucl. Eng. Des., **306** (2016) pp. 24–35.

[29]    COLLIN, B. P., PETTI, D. A., DEMKOWICZ, P. A., MAKI, J. T., Comparison of fission product release predictions using PARFUME with results from the AGR-1 safety tests, Nucl. Eng. Des., **301** (2016) pp. 378–390.

[30]    DEMKOWICZ, P. A., REBER, E. L., SCATES, D. M., SCOTT, L., COLLIN, B. P., First high temperature safety tests of AGR-1 TRISO fuel with the fuel accident condition simulator (FACS) furnace, J. Nucl. Mater., **464** (2015) pp. 320–330.

[31]    MORRIS, R. N., HUNN, J. D., BALDWIN, C. A., MONTGOMERY, F. C., GERCZAK, T. J., DEMKOWICZ, P. A., Initial results from safety testing of US AGR-2 irradiation test fuel, Nucl. Eng. Des., **329** (2018) pp. 124–133.

[32]    DEMKOWICZ, P. A., HUNN, J. D., PETTI, D. A., MORRIS, R. N., Key results from irradiation and post-irradiation examination of AGR-1 UCO TRISO fuel, Nucl. Eng. Des., **329** (2018) pp. 102–109.

[33]    BALDWIN, C. A., HUNN, J. D., MORRIS, R. N., MONTGOMERY, F. C., SILVA, C. M., DEMKOWICZ, P. A., First elevated-temperature performance testing of coated particle fuel compacts from the AGR-1 irradiation experiment, Nucl. Eng. Des., **271**, (2014) pp. 131–141.

[34]    HUNN, J. D., MORRIS, R. N., BALDWIN, C. A., BURNS, Z. M., MONTGOMERY, F. C., SKITT, D. J., Safety Testing of AGR-2 UCO Compacts 6-4-2 and 2-3-1, ORNL, Oak Ridge (2017).

[35]    HUNN, J. D. et al., Safety Testing and Post-Safety Test Examination of AGR-2 UCO Compact 2-3-2 and AGR-2 UO$_2$ Compact 3-4-1, ORNL, Oak Ridge (2018).

[36]    KIM, B.G., YEO, S., JEONG, K.C., KIM, Y.K., LEE, Y.W., CHO, M.S., The first irradiation testing and PIE or TRISO-coated particle fuel in Korea, Nucl. Eng. Des., **329** (2018) pp. 34–45.

[37]    MORRIS, R.N., BALDWIN, C. A., COLLINS, J.L., The Core Conduction Cooldown Test Facility: Current Status and Issues, ORNL, Oak Ridge (1992).

[38]    HUNN, J. D., MORRIS, R. N., BALDWIN, C. A., MONTGOMERY, F. C., GERCZAK, T. J., PIE on Safety-Tested AGR-1 Compact 4-2-2, ORNL, Oak Ridge (2015).

[39]    BROWN, N.R., A review of in-pile fuel safety tests of TRISO fuel forms and future testing opportunities in non-HTGR applications, J. Nucl. Mater., **534** (2020) 152139.

[40]    PLOGER, S., DEMKOWICZ, P., HUNN, J., MORRIS, R., "Microscopic analysis of irradiated AGR-1 coated particle fuel compacts," 2012, [Online]. Available: https://www.osti.gov/biblio/1064045.

[41]    US DEPARTMENT OF ENERGY, Ceramographic Examinations of Irradiated AGR-1 Fuel Compacts, Idaho Falls (2012).

[42]     RICE, F.J., STEMPIEN, J.D., DEMKOWICZ, P.A., Ceramography of irradiated TRISO fuel from the AGR-2 experiment, Nucl. Eng. Des., **329** (2018) pp. 73–81.

[43]     UETA, S. et al., "Study on plutonium burner high temperature gas-cooled reactor in Japan – Introduction scenario, reactor safety and fabrication tests of the 3S-TRISO fuel, Nucl. Eng. Des., **357** (2020) 110419.

[44]     GERCZAK, T. J., SEIBERT, R., HUNN, J.D., "Role of microstructure on CO corrosion of SiC layer in $UO_2$-TRISO fuel, J. Nucl. Mater., **537** (2020) 152185.

[45]     BARI, K., OSARINMWIAN, C., LÓPEZ-HONORATO, E., ABRAM, T.J., Characterization of the porosity in TRISO coated fuel particles and its effect on the relative thermal diffusivity, Nucl. Eng. Des., **265** (2013) pp. 668–674.

[46]     GERCZAK, T.J. et al., Analysis of fission product distribution and composition in the TRISO layers of AGR-2 fuel, Nucl. Eng. Des.. **364** (2020) 110656.

[47]     ARREGUI-MENA J.D., SEIBERT, R.L., GERCZAK, T.J., Characterization of PyC/SiC interfaces with FIB-SEM tomography, J. Nucl. Mater., **545**, (2021) 152736.

[48]     LILLO, T. M., VAN ROOYEN, I. J., Influence of SiC grain boundary character on fission product transport in irradiated TRISO fuel, J. Nucl. Mater., **473** (2016) pp. 83–92.

[49]     VAN ROOYEN, I.J., JANNEY, D. E., MILLER, B.D., DEMKOWICZ, P.A., RIESTERER, J., Electron microscopic evaluation and fission product identification of irradiated TRISO coated particles from the AGR-1 experiment: a preliminary review, J. Nuc. Eng. and Design, **271** (2014) pp. 114-122.

[50]     MINATO, K., FUKUDA, K., SEKINO, H., ISHIKAWA, A., OEDA, E., Deterioration of ZrC-coated fuel particle caused by failure of pyrolytic carbon layer, J. Nucl. Mater., **252** (1998) pp. 13–21.

[51]     HUNN, J.D. et al., Initial examination of fuel compacts and TRISO particles from the US AGR-2 irradiation test, Nucl. Eng. Des., **329** (2018) pp. 89–101.

[52]     FU, Z., VAN ROOYEN, I.J., M.BACHHAV, M., YANG, Y., Microstructure and fission products in the UCO kernel of an AGR-1 TRISO fuel particle after post irradiation safety testing, J. Nucl. Mater., **528** (2020) 151884.

[53]     DEVIDA, C., BETTI, M., PEERANI, P., TOSCANO, E.H., GOLL, W., "Quantitative Burnup Determination: A Comparison of Different Experimental Methods", 2005, doi: https://doi.org/.

[54]     HARTWELL, J.K., SCATES, M., Design and Expected Performance of the AGR-1 Fission Product Monitoring System (FPMS), INL, Idaho Falls, (2005). Doi: 10.2172/911217.

[55]     HANIA, P.R., et al., Irradiation of thorium-bearing molten fluoride salt in graphite crucibles, Nucl. Eng. Des., **375** (2021) p. 111094.

[56]    SERP, J., et al., The molten salt reactor (MSR) in Generation IV: overview and perspectives, Prog. Nucl. Energy, **77** (2014) pp. 308–319.

[57]    MERLE-LUCOTTE, E., HEUER, D., ALLIBERT, M, GHETTA, V., LE BRUN, C., "Materials issues for Generation IV systems", Introduction to the Physics of Molten Salt Reactors BT, pp. 501–521 (2008). Electronic ISSN 1874-6535, Print ISSN 1874-6500.

[58]    ENGEL, J R., BAUMAN, H.F., DEARING, J.F., GRIMES, W.R., MCCOY, H.E.J., "Development status and potential program for development of proliferation-resistant molten-salt reactors", 1979, Accessed: Dec. 17, 2020. [Online]. Available: http://inis.iaea.

[59]    BETZLER, B.R., POWERS, J.J., WORRALL, A., Molten salt reactor neutronics and fuel cycle modeling and simulation with SCALE, Ann. Nucl. Energy, **101** (2017) pp. 489–503.

[60]    LEBLANC, D., Molten salt reactors: a new beginning for an old idea, Nucl. Eng. Des., **240** (2010) pp. 1644–1656.

[61]    RILEY, B.J., MCFARLANE, J., DELCUL, G.D.,, VIENNA, J.D., CONTESCU, C.I.,, FORSBERG, C.W., Molten salt reactor waste and effluent management strategies: a review, Nucl. Eng. Des., **345** (2019) pp. 94–109.

[62]    EZELL, N.D.B., RAIMAN, S.S., KURLEY, J.M., MCDUFFEE, J., Neutron irradiation of alloy N and 316L stainless steel in contact with a molten chloride salt, Nucl. Eng. Technol., **53** (2021) pp. 920–926.

[63]    DIANNE BULL EZELL, N., MCDUFFEE, J., RAIMAN, S., BRYANT, D., SCHMIDLIN, J., Examination of corrosion development in a chloride salt irradiation experiment, Trans. Am. Nucl. Soc., **120** (2019) pp. 319–321.

[64]    LI, J., et al., Corrosion behavior of ion-irradiated SiC in FliNaK molten salt, Corros. Sci., **163** (2020) 108229.

[65]    YANG, X., et al., Role of helium ion irradiation in the corrosion of CVD−SiC in molten Lif−Naf−KF salt, Corros. Sci., **182** (2021) 109287.

[66]    MAGNUS, C., COOPER, D. JANTZEN, C., LAMBERT, H., ABRAM, T., RAINFORTH, M., Synthesis and high temperature corrosion behaviour of nearly monolithic $Ti_3AlC_2$ max phase in molten chloride salt, Corros. Sci., **182** (2021) 109193.

[67]    YANG, Y., et al., Advanced electron microscopy characterization of intergranular corrosion in Ni-20Cr alloy under molten salt environment, Microsc. Microanal., **26** (2020) pp. 180–182.

[68]    LEI, G., LI, C., JIANG, Z., HUANG, H., Irradiation accelerated fluoride molten salt corrosion of nickel-based UNS N10003 alloy revealed by x-ray absorptionfine structure, Corros. Sci., **165** (2020) 108408.

[69]     BAKAI, A.S., Combined effect of molten fluoride salt and irradiation on Ni-based alloys, NATO Sci. Peace Secur. Ser. B Phys. Biophys. (2008) pp. 537–557.

[70]     NEWTON, M.L., HAMILTON, D.E., SIMPSON, M.F., Methods of redox control and measurement in molten NaCl-CaCl$_2$ -Ucl$_3$, ECS Meet. Abstr., vol. MA2020-02, no. **59** (2020) pp. 2913–2913.

[71]     BETZLER, B.R., et al., Fuel cycle and neutronic performance of a spectral shift molten salt reactor design, Ann. Nucl. Energy, **119** (2018) pp. 396–410.

[72]     KRAL, D., et al., "Measurement of activation products in chloride salts irradiated by spallation neutrons", Proc. – 2020 21st Int. Sci. Conf. Electr. Power Eng. EPE 2020, 2020.

[73]     ZHOU, J., et al., Evaporation behavior of 2LiF–BeF$_2$ –ZrF$_4$ molten salt with irradiated nuclear fuel ," RSC Adv., **11** (2021) pp. 26284–26290.

[74]     RAMOS-BALLESTEROS, A., et al., Gamma radiation-induced defects in KCl, MgCl$_2$, and ZnCl$_2$ salts at room temperature, Phys. Chem. Chem. Phys., **23** (2021) pp. 10384-10394.

[75]     HANIA, P.R., et al., Irradiation of thorium-bearing molten fluoride salt in graphite crucibles, Nucl. Eng. Des., **375** (2021) 111094.

[76]     MARTIN, A., EZELL, N., RUSSELL, N., GALLAGHER, R., Thermophysical Property Measurements of Molten Salts: Perspectives on Fuel and Irradiated Salts, 2021. Doi: 10.13182/t123-32940.

[77]     MANCEY, D.S., Global Review of Facilities Used to Test Materials in Molten Salts for the Purpose of Supporting Molten Salt Reactor Development, CNL Report No. 153-120200-440-013 (2020).

[78]     TOSOLIN, A., Literature Review on the Preparation of Actinide Halides of Interest for the Molten Salt Reactor, CNL Report No. 153-124000-440-019 (2020).

[79]     KARLSSON, T.Y., et al., Demonstrate Characterization Equipment to Be Used on Irradiated Molten Salts in MSTEC, United States (2021). [Online]. Available: https://www.osti.gov/biblio/1814713.

[80]     ABOU JAOUDE, A., STERBENTZ, J.W., PALMER, J., CALDERONI, P., "Evaluation of a Versatile Experimental Salt Irradiation Loop (VESIL) inside the Advanced Test Reactor", United States, 2019. Doi: 10.2172/1511048.

[81]     NEAL, P., Review of Molten Salt Loop Instrumentation in Literature, CNL Report No. 153-120200-290-000 (2021).

[82]     BUSBY, J., et al., Technical Gap Assessment for Materials and Component Integrity Issues for Molten Salt Reactors, ORNL, Oak Ridge (2019).

[83]     HUMMEL, D.W., et al., "Results of a phenomena identification and ranking table (PIRT) exercise for a severe accident in a small modular high-temperature gas-cooled reactor, CNL Nucl. Rev., **8** (2019) pp. 159–169. doi: 10.12943/CNR.2019.00.

[84]     GRIMES, W.R., Molten-salt reactor chemistry, Nucl. Appl. Technol., **8** (1970), pp. 137–155.

[85]     COMPERE, E.L., KIRSLIS, S.S., BOHLMANN, E.G., BLANKENSHIP, F.F., GRIMES, W.R., Fission product behavior in the Molten Salt Reactor Experiment, ORNL, Oak Ridge (1975). Doi: 10.2172/4077644.

[86]     GRIMES, W.R., Molten-salt reactor chemistry, Nucl. Appl. Technol., **8** (1970) pp. 137–155.

[87]     PENG, H., HUANG, W., XIE, L., LI, Q., Solubility and precipitation investigations of $UO_2$ in $LiF-BeF_2$ molten salt, J. Nucl. Mater., **531** (2020) 152004.

[88]     LINDAUER, R.B., Processing of the MSRE Flush and Fuel Salts, ORNL, Oak Ridge (1969). Doi: 10.2172/4781475.

[89]     Chemical Engineering Division Research Highlights, May –December 1968, Lemont, 1969. Doi: 10.2172/4793442.

[90]     CLEMENT, B. et al., State of the Art Report on Iodine Chemistry, OECD-NEA. [Online]. Available at: http://inis.iaea.org/search/search.aspx?orig_q=RN:44035206 .

[91]     YAMAWAKI, M., ARITA, Y., FUKUMOTO, K FUJIMURA, R., Evaluation study of source term for severe accident analysis of molten salt reactors, J. Plasma Fusion Res. Ser., **11** (2015) pp. 113–119.

[92]     FLETCHER, D.F., Steam explosion triggering: a review of theoretical and experimental investigations, Nucl. Eng. Des., **155** (1995) pp. 27–36.

[93]     LIPSETT, S.G., Explosions from molten materials and water, Fire Technol., **2** (1966) pp. 118–126.

[94]     HOHMANN, H., KOTTOWSKI, H., SCHINS, H., HENRY, R.E., Experimental Investigations of Spontaneous and Triggered Vapour Explosions in the Molten Salt/Water System, United States, 1983. [Online]. Available: http://inis.iaea.org/search/search.aspx?orig_q.

[95]     DICKSON, R.S., PEPLINSKIE, R.T., GAUTHIER, M.D., "Release of fission products from CANDU fuel in air environment: leading the renaissance", Proc. The 10th international conference on CANDU fuel,, p. 133, 2018. [Online]. Available: http://inis.iaea.org/search/search.aspx?orig_q=RN:41031954.

[96]     HOLCOMB, D.E., KISNER, R.A., CETINER, S.M., Instrumentation Framework for Molten Salt Reactors, United States, 2018. Doi: 10.2172/1462848.

[97]     CAPRIOTTI, L., HARP, J., Status PIE Report on Legacy EBR-II and FFTF Metallic Fuel Experiments, United States, 2019. [Online]. Available: https://www.osti.gov/biblio/1604754.

[98]     CARMACK, W.J., PORTER, D.L., CUMMINGS, D.G.,CHICHESTER, H.M., HAYES, S.L., WOOTAN, D.W., Examination of Legacy Metallic Fuel Pins (U-10Zr) Tested in FFTF, United States, 2020. Doi: 10.2172/1617195.

[99]    GRIBOK, A.V., PORTER, D.L., PAAREN, K.M., GALE, M.D., MIDDLEMAS, S.C., LYBECK, N.J., Automatic information extraction from neutron radiography imaging to estimate axial fuel expansion in EBR-II," J. Nucl. Mater., **557** (2021) 153250.

[100]   HARP, J.M., CHICHESTER, H.J.M., CAPRIOTTI, L., Post-irradiation examination results of several metallic fuel alloys and forms from low burnup AFC irradiations, J. Nucl. Mater., **509** (2018) pp. 377–391.

[101]   ADAM, M.F., "In-cell element laser profilometer at the hot fuel examination facility", in Conf. Remote Syst. Technol., Proc., vol. 26, 1978. [Online]. Available: https://www.osti.gov/biblio/6772482.

[102]   LEENAERS, A. et al., "LEONIDAS E-FUTURE: results of the destructive analyses of the U(Mo)-Al(Si) fuel plates", Proceedings from the European Research Reactor Conference, Prague, Czech Republic, 18-22 March 2012, pp. 90-107. Available: https://www.igorr.com/Documents/2012-PRAGUE/rrfm2012-transactions.pdf.

[103]   GRAS, C., STANLEY, S.J., Post-irradiation examination of a fuel pin using a microscopic x-ray system: measurement of carbon deposition and pin metrology, Ann. Nucl. Energy, **35** (2008) pp. 829–837.

[104]   YAO, T., et al., $\alpha$-U and $\omega$-Uzr$_2$ in neutron irradiated U-10Zr annular metallic fuel, J. Nucl. Mater., **542** (2020) 152536.

[105]   MARIANI, R.D., PORTER, D.L., O'HOLLERAN, T.P., HAYES, S.L., KENNEDY, J.R., Lanthanides in metallic nuclear fuels: their behavior and methods for their control, J. Nucl. Mater., **419** (2011) pp. 263–271.

[106]   HARP, J.M., PORTER, D.L., MILLER, B.D., TROWBRIDGE, T.L., CARMACK, W.J., Scanning electron microscopy examination of a fast flux test facility irradiated U-10Zr fuel cross section clad with HT-9, J. Nucl. Mater., **494** (2017) pp. 227–239.

[107]   HELMREICH, G.W. SEIBERT, R.L., Post-Irradiation Examination of Low Neutron Dose Metal Fuel Parallelepipeds, ORNL, Oak Ridge (2019). Doi: 10.2172/1557482.

[108]   THOMAS, J., et al., The application of synchrotron micro-computed tomography to characterize the three- dimensional microstructure in irradiated nuclear fuel, J. Nucl. Mater., **537** (2020) 152161.

[109]   HOFMAN, G.L., HAYES, S.L., PETRI, M.C., Temperature gradient driven constituent redistribution in U-Zr alloys, J. Nucl. Mater., **227** (1996), pp. 277–286.

[110]   WHITE, J.T., NELSON, A.T., DUNWOODY, J.T., BYLER, D.D., D. SAFARIK, J., MCCLELLAN, K.J., Thermophysical properties of U$_3$Si$_2$ to 1773K, J. Nucl. Mater., **464** (2015) pp. 275–280.

[111]   WHITE, J.T., NELSON, A.T., Thermal conductivity of UO$_{2+x}$ and U$_4$O$_{9-y}$, J. Nucl. Mater., **443** (2013) pp. 342–350.

[112]   JANNEY, D.E., PAPESCH, C.A., FCRD Advanced Reactor (Transmutation) Fuels Handbook, INL, Idaho Falls (2016). Doi: 10.2172/1374786.

[113]    ISLER, J.P., Interactions of Lanthanides and Liquid Alkali Metals for 'Liquid-Like' Lanthanide Transport in U-Zr Fuel, The Ohio State University (2017)..

[114]    ADKINS, C.A., PAVLOV, T.R., MIDDLEMAS, S.C., SCHLEY, R.S., MARSHALL, M.C., COLE, M.R., "Demonstrate Thermal Property Measurement on Irradiated Fuel in IMCL," United States, 2019. [Online]. Available: https://www.osti.gov/biblio/1605593.

[115]    US DEPARTMENT OF ENERGY, Technology Readiness Assessment Guide, DOE Report No.  DOE G 413.3-4A (2011).

# ANNEX I.

## ANNEX: CONTENTS OF SUPPLEMENTARY ELECTRONIC FILES

The supplementary electronic files for this publication can be found on the publication's individual web page at www.iaea.org/publications. These are presentation files provided at the Technical Meeting on Advances in Post-Irradiation Examination Techniques for Power-Reactor Irradiated Fuels and Innovative Fuels, virtually held on 21–27 July 2021. Each file is described with the title of the presentation and the name of its presenter below:

TABLE I-1. DESCRIPTION OF SUPPLEMENTARY ELECTRONIC FILES

| File No. | Description (presentation title and presentation provider) |
|---|---|
| 01 | A Brief Review of Post-Irradiation Examination at the Canadian Nuclear Laboratories, and Recent Advances in PIE to Support Innovative Fuel and Reactor Designs, presented by Nihan ONDER (CNL, Canada) |
| 02 | Multiscale Characterization Techniques: Towards the Understanding of the Irradiated Nuclear Fuel Microstructure, presented by Catherine SABATHIER (CEA, France) |
| 03 | Post Irradiation Examination Techniques for Thermal Reactor Fuels, presented by Prerna MISHRA (BARC, India) |
| 04 | Advances in PIE Techniques at UK Heavily Shielded Hot Cells on Sellafield Site, presented by Susan MORGAN (NNL, UK) |
| 05 | Transportation and Post Irradiation Examination of a CANDU Bundle from Cernavoda Nuclear Power Plant, presented by Madalin SAVU (RATEN-ICN, Romania) |
| 06 | Advanced Vacuum Sipping for Spent Fuel Classification, presented by Rodríguez ROBERTO (ENUSA, Spain) |
| 07 | Evaluating the Performance of KHRR Fuel Rod in TRR Reactor Using In-Pile and PIE Tests, presented by Abdullah RIAHI (AEOI, Islamic Republic of Iran) |
| 08 | The Need for PIE to Support the Synthesis and Modelling of Gadolinium and/or Erbium Additions to SMR 17x17 Fuel Assembly Pellets and/or Cladding, presented by Arturo BEVILACQVA (CNEA, Argentina) |
| 09 | Research on Radiation Damage Behaviour of Zirconium Alloy Cladding Materials Based on Accelerator and Multi-Scale Modelling, presented by Lu WU (National Power Institute of China, China) |
| 10 | Multi Frequency Eddy Current Measurements on Zircaloy Fuel Components, presented by Erik Tomas ANGLAND (Westinghouse, Sweden) |
| 11 | Hot Cells Tools and Methods for the Safety Assessment of Nuclear Fuels, presented by Dimitrios PAPAIOANNOU (JRC, EC) |
| 12 | Techniques to Study Mixed Nitride Uranium-Plutonium Fuel at RIAR JSC, presented by Evgenii MAKAROV (RIAR, Russian Federation |
| 13 | PIE Capabilities to Support the Development of Innovative Fuels at INL, presented by Peng XU (INL, USA) |
| 14 | High Burnup Structure Evolution from Grain Boundary, presented by Changqing TENG (Nuclear Power Institute of China, China) |

# LIST OF ABBREVIATIONS

| | |
|---|---|
| AGR | Advanced Gas Reactor |
| ANDES | ATR NDE System |
| ANL | Argonne National Laboratory |
| APS | Advanced Photon Source |
| APT | Atom probe tomography |
| ASTM | The American Society for Testing and Materials |
| ATF | Accident tolerant and advanced technology fuel |
| ATR | Advanced Test Reactor |
| BNL | Brookhaven National Laboratory |
| BSE | Backscattered electron |
| CCCTF | Core Conduction Cooldown Test Facility |
| CCD | Charge coupled device |
| CHNS analyzer | Carbon, hydrogen, nitride and surfer analyzer |
| CNL | Canadian Nuclear Laboratories |
| CRP | Coordinated research project |
| CT | Computed tomography, or Coulometric Titration |
| D | Thermal diffusivity |
| DBTT | Ductile-to-brittle transition temperature |
| DE | Destructive examination |
| DIC | Digital image correlation |
| DLBL | Deconsolidation-leach-burn-leach |
| DSC | Differential scanning calorimeter |
| DTA | Differential thermal analysis |
| EBSD | Electron backscatter diffraction |
| EC | Eddy current |
| EDC | Expansion-due-to-compression |

| | |
|---|---|
| EDS | Energy dispersive spectroscopy |
| EDX | Electron-dispersive X-ray |
| EELS | Electron energy loss spectroscopy |
| EGRFP | Expert Group of Reactor Fuel Performance of OECD-NEA |
| EPMA | Electron probe microanalyzer |
| FACS | Fuel Accident Condition Simulator |
| FCCI | Fuel-cladding chemical interaction |
| FCM | Fully ceramic microencapsulated |
| FCMI | Fuel-cladding mechanical interaction. |
| FIB | Focused ion beam |
| FIMA | Fissions per initial metal atom |
| FP | Fission product |
| FPMS | Fission Product Monitoring System |
| FSECT | Frequency scanning eddy-current technique |
| GASR | Gas Assay, Sample and Recharge |
| GBI | Grain boundary inventory |
| GECT | Gamma emission computed tomography |
| HALEU | High-assay low enriched uranium |
| HEPA | high-efficiency particulate air |
| HFEF | Hot Fuel Examination Facility |
| HFIR | High Flux Isotope Reactor |
| HPGe | High-purity germanium |
| HTGR | High-temperature gas-cooled reactor |
| HVE | Hot Vacuum Extraction |
| ICERR | International Centres based on Research Reactors |
| ICP | Inductively coupled plasma |

| | |
|---|---|
| IGMA | Irradiated-microsphere gamma analyzer |
| IMCL | Irradiated Materials Characterization Laboratory |
| IMGA | Irradiated Microsphere Gamma Analyzer |
| INL | Idaho Nuclear Laboratory |
| IPyC | Inner pyrolytic carbon layer |
| IR | infrared (IR) cells |
| JMTR | Japan Material Testing Reactor |
| k | Thermal conductivity |
| LA | Laser ablation |
| LALO | Large area lift-outs |
| LANSCE | Los Alamos Neutron Science Center |
| LEAP | Local electrode atom probe |
| LFA | laser flash analyzer |
| LIBS | Laser induced breakdown spectroscopy |
| LMFR | Liquid metal-cooled fast reactor |
| LVDT | Linear Variable Differential Transformer |
| LWR | Light water reactor |
| MMR | Micro modular reactor |
| MS | Mass spectrometry. |
| MSR | Molten salt-cooled reactor |
| MSRE | Molten-Salt Reactor Experiment |
| MSTEC | Molten Salt Thermo-Physical Examination Capability |
| NDE | Non-destructive examination |
| NFML | Nuclear Fuels and Materials Library |
| NNL | National Nuclear Laboratory |
| NRAD | Neutron Radiography Reactor |
| NSUF | Nuclear Science User Facility |

| OCP | Open circuit potential |
|-----|------------------------|
| OECD-NEA | the Organization for Economic Cooperation and Development – Nuclear Energy Agency |
| OES | Optical emission spectroscopy |
| OGL | Oarai Gas Loop |
| OPG | Ontario Power Generation |
| OPyC | Outer pyrolytic carbon layer |
| ORNL | Oak Ridge National Laboratory |
| PAS | Positron annihilation spectroscopy |
| PGS | Precision Gamma Scanner |
| PHWR | Pressurized heavy water reactor |
| PIE | Post-irradiation examination |
| PIRT | phenomena identification and ranking table |
| RC | Ring compression |
| RT | Room temperature |
| R/B | Release/Birth ratio |
| SCC | Stress corrosion cracking |
| SE | Secondary electron |
| SEM | Scanning electron microscopy |
| SIMS | Secondary ion mass spectrometry |
| SMR | Small modular reactor |
| SNS | Spallation Neutron Source |
| SS | Stainless steel |
| SSMT | Small scale mechanical testing |
| STEM | Scanning transmission electron microscope |
| TC | Thermal conductivity |
| TCM | TC microscope |

| | |
|---|---|
| TEM | Transmission electron microscopy |
| TGA | Thermogravimetric analysis |
| TIMS | Thermal ionization mass spectrometry |
| TM | Technical Meeting |
| TMA | Thermal mechanical analyzer |
| TOF | Time-of-flight |
| TRISO | Tri-structural isotropic |
| TRL | Technology readiness level |
| T-FE | Schottky-type field emission |
| UT | Ultrasonic test |
| XAFS spectroscopy | X-ray absorption fine structure spectroscopy |
| XCT | X-ray CT |
| XPS | X-ray photoelectron spectroscopy |
| XRD | X-ray diffraction |
| XRM | X-ray microscopy |
| WCR | Water cooled reactor |
| WDS | Wavelength dispersive X-ray spectroscopy |
| 2D | Two-dimensional |
| 3D | Three-dimensional |

# CONTRIBUTORS TO DRAFTING AND REVIEW

| | |
|---|---|
| Bagheripoor, M. | Canadian Nuclear Laboratories (CNL), Canada |
| Corbett, S. | Canadian Nuclear Laboratories (CNL), Canada |
| Goncharenko, Y. | RIAR JSC, Russian Federation |
| Harrison, N. | Canadian Nuclear Laboratories (CNL), Canada |
| Jones, C. | CNL (consultant), Canada |
| Mo, K. | Argonne National Laboratory (ANL), USA |
| Morgan, S. | National Nuclear Laboratory (NNL), UK |
| Onder, N. | Canadian Nuclear Laboratories (CNL), Canada |
| Sim, K. | International Atomic Energy Agency |
| Sears, D. | International Atomic Energy Agency |
| Swainson, I. | International Atomic Energy Agency |
| Yu, H. | Canadian Nuclear Laboratories (CNL), Canada |
| Xu, P. | Idaho National Laboratory (INL), USA |
| Yacout, A. | Argonne National Laboratory (ANL), USA |
| Ye, B. | Argonne National Laboratory (ANL), USA |

**Technical Meeting**

Vienna, 21–27 July 2021

**Consultancy Meetings**

Vienna, 15–16 November 2021

Vienna, 9–11 February 2022

# ORDERING LOCALLY

IAEA priced publications may be purchased from the sources listed below or from major local booksellers.

Orders for unpriced publications should be made directly to the IAEA. The contact details are given at the end of this list.

## NORTH AMERICA

**Bernan / Rowman & Littlefield**

15250 NBN Way, Blue Ridge Summit, PA 17214, USA
Telephone: +1 800 462 6420 • Fax: +1 800 338 4550

Email: orders@rowman.com • Web site: www.rowman.com/bernan

## REST OF WORLD

Please contact your preferred local supplier, or our lead distributor:

**Eurospan Group**

Gray's Inn House
127 Clerkenwell Road
London EC1R 5DB
United Kingdom

**Trade orders and enquiries:**

Telephone: +44 (0)176 760 4972 • Fax: +44 (0)176 760 1640
Email: eurospan@turpin-distribution.com

**Individual orders:**

www.eurospanbookstore.com/iaea

**For further information:**

Telephone: +44 (0)207 240 0856 • Fax: +44 (0)207 379 0609
Email: info@eurospangroup.com • Web site: www.eurospangroup.com

**Orders for both priced and unpriced publications may be addressed directly to:**

Marketing and Sales Unit
International Atomic Energy Agency
Vienna International Centre, PO Box 100, 1400 Vienna, Austria
Telephone: +43 1 2600 22529 or 22530 • Fax: +43 1 26007 22529
Email: sales.publications@iaea.org • Web site: www.iaea.org/publications

International Atomic Energy Agency
Vienna